

---

# EVALUATION OF SURROGATE ENDPOINTS BASED ON META-ANALYSIS WITH SURROGATE INDICES

---

A PREPRINT

✉ Florian Stijven\*<sup>1</sup> and ✉ Peter B. Gilbert<sup>2, 3, 4</sup>

<sup>1</sup>I-BioStat, KU Leuven, Leuven, Belgium

<sup>2</sup>Vaccine and Infectious Disease Division, Fred Hutchinson Cancer Research Center, Seattle, WA, USA

<sup>3</sup>Public Health Sciences Division, Fred Hutchinson Cancer Research Center, Seattle, WA, USA

<sup>4</sup>Department of Biostatistics, University of Washington, Seattle, WA, USA

September 3, 2025

## ABSTRACT

We introduce in this paper an extension of the meta-analytic (MA) framework for evaluating surrogate endpoints. While the MA framework is regarded as the gold standard for surrogate endpoint evaluation, it is limited in its ability to handle complex surrogates and does not take into account possible differences in the distribution of baseline covariates across trials. By contrast, in the context of data fusion, the surrogate-index (SI) framework accommodates complex surrogates and allows for complex relationships between baseline covariates, surrogates, and clinical endpoints. However, the SI framework is not a surrogate evaluation framework and relies on strong identifying assumptions. To address the MA framework's limitations, we propose an extension that incorporates ideas from the SI framework. We first formalize the data-generating mechanism underlying the MA framework, providing a transparent description of the untestable assumptions required for valid inferences in any evaluation of trial-level surrogacy—assumptions often left implicit in the MA framework. While this formalization is meaningful in its own right, it is also required for our main contribution: We propose to estimate a specific transformation of the baseline covariates and the surrogate, the so-called surrogate index. This estimated transformation serves as a new potential univariate surrogate and is optimal in a trial-level surrogacy sense under certain conditions. We show that, under weak additional conditions, this new univariate surrogate can be evaluated as a trial-level surrogate as if the transformation were known a priori.

This approach enables the evaluation of the trial-level surrogacy of complex surrogates and can be implemented using standard software. We illustrate this approach with a set of COVID-19 vaccine trials where antibody markers are assessed as potential trial-level surrogate endpoints.

**Keywords** Surrogate endpoints · Meta-analysis · Surrogate index · Data-adaptive target parameter · COVID-19

## Contents

<b>1</b>	<b>Introduction</b>	<b>4</b>
<b>2</b>	<b>Individual-Patient Data in a Meta-Analysis</b>	<b>4</b>
2.1	Individual-Patient Data from a Single Trial . . . . .	5
2.2	Data from a Population of Trials . . . . .	5
2.2.1	Population of Trials . . . . .	5

---

\*florian.stijven@kuleuven.be

2.2.2	Trial-Level Treatment Effects . . . . .	7
2.3	Models . . . . .	7
2.4	Parameters and Estimands . . . . .	8
2.4.1	Full-Data Parameters . . . . .	8
2.4.2	Statistical Parameters . . . . .	9
<b>3</b>	<b>Meta-Analysis with an (Optimal) Transformed Surrogate</b>	<b>9</b>
3.1	Parameters and Estimands . . . . .	10
3.1.1	A Priori Selected $g$ . . . . .	10
3.1.2	Estimated $gN$ . . . . .	11
3.2	Plug-in Estimator . . . . .	12
<b>4</b>	<b>Inference for Data-Adaptive Parameters via Estimating Equations</b>	<b>12</b>
4.1	Notation . . . . .	12
4.2	General Data-Adaptive Target Parameters . . . . .	12
4.3	Data-Adaptive Target Parameters Defined Through Estimating Functions . . . . .	13
4.3.1	A General Theorem . . . . .	13
4.4	Plug-in Estimator for Data-Adaptive Target Parameter in MA Framework . . . . .	14
<b>5</b>	<b>Alternative Asymptotic Regime</b>	<b>15</b>
<b>6</b>	<b>Simulations</b>	<b>15</b>
<b>7</b>	<b>Application to COVID-19 trials</b>	<b>16</b>
7.1	Data Description . . . . .	16
7.2	Estimating the surrogate index $gN$ . . . . .	17
7.3	Trial-Level Treatment Effects . . . . .	18
7.4	Results . . . . .	18
7.4.1	Original Data . . . . .	18
7.4.2	Pseudo-Real Data . . . . .	20
<b>8</b>	<b>Conclusions</b>	<b>22</b>
<b>A</b>	<b>Surrogate Index</b>	<b>24</b>
A.1	Setting and Notation . . . . .	24
A.2	Identification . . . . .	25
A.3	Estimation . . . . .	26
A.4	Limitations . . . . .	26
<b>B</b>	<b>Canonical Parametric Meta-Analysis</b>	<b>26</b>
B.1	(Approximate) Observed-Data Likelihood . . . . .	26
B.2	Prediction of $\beta_0$ . . . . .	28
B.3	Bayesian Implementation . . . . .	29

<b>C</b>	<b>Plug-In Estimator and Efficiency</b>	<b>29</b>
C.1	Plug-In Estimator . . . . .	29
C.1.1	Estimating Function . . . . .	29
C.1.2	Finite-Sample Corrections . . . . .	30
C.1.3	Approximate Prediction Intervals . . . . .	30
C.2	Semi-Parametric Efficiency Analysis . . . . .	31
C.2.1	Results for General Multivariate Meta-Analysis . . . . .	31
C.2.2	Implications . . . . .	31
<b>D</b>	<b>Conditions of Theorem 2</b>	<b>32</b>
D.1	General Discussion . . . . .	32
D.2	Plug-in Estimator for Data-Adaptive Target Parameter in MA Framework . . . . .	32
D.3	Overfitting of the Surrogate Index Estimator . . . . .	34
<b>E</b>	<b>Alternative Asymptotic Regime</b>	<b>34</b>
E.1	Setting and Notation . . . . .	34
E.2	Alternative Assumptions . . . . .	35
E.3	Rate Conditions . . . . .	37
E.4	Practical Relevance . . . . .	38
<b>F</b>	<b>Proofs</b>	<b>39</b>
F.1	Proof of Lemma 3.1 . . . . .	39
F.2	Proof of Lemma E.1 . . . . .	40
F.3	Proof of Theorem 2 . . . . .	42
F.4	Proof of Lemma F.1 . . . . .	44
F.5	Proof of Lemma C.1 and Corollary 1 . . . . .	45
F.6	Proof of Lemma D.1 . . . . .	46
F.7	Proof of Lemma D.2 . . . . .	47
<b>G</b>	<b>Simulations</b>	<b>48</b>
G.1	Data-Generating Mechanism . . . . .	48
G.1.1	Proof-of-Concept Scenario . . . . .	48
G.1.2	Vaccine Scenario . . . . .	49
G.2	Results . . . . .	51
G.3	Verification of the Asymptotics and its Failure . . . . .	54
<b>H</b>	<b>Data Application</b>	<b>57</b>
H.1	Data Exploration . . . . .	58
H.2	Adjustment of Neutralization Titer to Circulating Strains . . . . .	59
H.3	Surrogate Index Estimators . . . . .	62
H.4	Additional Results . . . . .	63

H.4.1 Additional Non-Parametric Meta-Analysis Results . . . . .	63
H.4.2 Bayesian Meta-Analysis . . . . .	63

## 1 Introduction

In clinical trials, the primary endpoint is ideally a clinical endpoint, defined as an endpoint that “describes or reflects how an individual feels, functions, or survives” (FDA-NIH Biomarker Working Group, 2016). However, clinical endpoints are often costly, time-consuming, and difficult to measure, prompting trialists to use so-called surrogate endpoints as primary endpoints. Surrogate endpoints are biomarkers or intermediate outcomes that may substitute for clinical endpoints. While using a surrogate endpoint can increase a trial’s efficiency, it should be evaluated before it replaces a clinical endpoint. Prentice (1989) was the first to propose statistical criteria for evaluating surrogate endpoints. Since then, numerous approaches have been developed, including the proportion explained (Freedman et al., 1992), principal surrogacy (Frangakis & Rubin, 2002), the information-theoretic causal inference approach (Alonso et al., 2015), and the meta-analytic (MA) framework (Alonso et al., 2016; Buyse et al., 2000). Joffe and Greene (2009) provide an overview of these approaches and how they are related to each other. This report presents novel contributions to the MA framework for evaluating surrogate endpoints.

The meta-analytic framework is the gold standard for *evaluating* surrogate endpoints (Fleming & Powers, 2012; Institute of Medicine (US) Committee on Qualification of Biomarkers and Surrogate Endpoints in Chronic Disease, 2011; VanderWeele, 2013; Weir & Taylor, 2022). However, the canonical MA framework has important limitations: (i) it is generally restricted to the evaluation of univariate surrogates<sup>2</sup>, and (ii) it does not account for differences in the distribution of baseline covariates across trials<sup>3</sup>. This is inconsistent with clinical reality, where promising surrogates may be complex and baseline covariates may explain differences between trials.

By contrast—although not an approach for evaluating surrogate endpoints—the surrogate-index (SI) framework (Athey et al., 2019; Gilbert et al., 2024) accommodates complex surrogates and allows for complex relations between (i) the baseline covariates and the surrogate and (ii) the clinical endpoint. The objective in the SI framework is inference about the treatment effect on the clinical endpoint in a clinical trial where the clinical endpoint was not observed, but where a surrogate endpoint was observed. Athey et al. (2019) show that this is possible under additional identifying assumptions if there is an observational data set where, in addition to the baseline covariates and the surrogate endpoint, the clinical endpoint was measured. However, these identifying assumptions are very strong: for instance, the surrogate should be a perfect surrogate. We will apply ideas from the SI framework to the MA framework.

In this paper, we make two contributions to the MA framework for evaluating surrogate endpoints. First, we formalize the data-generating mechanism that leads to a transparent description of the untestable assumptions required for valid inferences in any application of the MA framework. Second, we introduce a novel approach for evaluating complex surrogates in the MA framework. This approach moreover allows for the inclusion of baseline covariates, which “corrects” for possible differences in the distribution of baseline covariates across trials, and can therefore lead to very different results as compared to the canonical MA framework, even when the surrogate is a “simple” univariate endpoint. The implementation of our approach is straightforward and can be done with standard software.

The remainder of this paper is structured as follows: First, we introduce the data-generating mechanism underlying the MA framework in Section 2 together with a general discussion of relevant models and parameters. In Section 3, we introduce parameters, and corresponding identifying assumptions, that are relevant for evaluating surrogates in the MA framework. Some of these parameters are data-adaptive; therefore, we discuss inference about general data-adaptive parameters in Section 4. Section 5 describes how the identifying assumptions can be relaxed by switching to another asymptotic regime and Section 6 summarizes the results of simulations. The proposed approach is applied to a set of COVID-19 vaccine trials in Section 7 where antibody markers are evaluated as potential trial-level surrogates for symptomatic infection. We end with some concluding remarks in Section 8.

## 2 Individual-Patient Data in a Meta-Analysis

In this section, we formalize the data-generating mechanism underlying the MA framework for evaluating surrogate endpoints. This data-generating mechanism is applicable to the canonical MA framework but is more general and formal than what is typically presented (e.g. Alonso et al., 2016; Buyse et al., 2000). This degree of generality is not

<sup>2</sup>Although there is some work on multivariate surrogates—see, e.g., Alonso et al. (2004) and Gabriel et al. (2019)—such methods can only be applied for low-dimensional surrogates (e.g., bi- or trivariate surrogates) or when additional structure can be imposed on the multivariate surrogate (e.g., repeated measurements).

<sup>3</sup>An exception is Rosin et al. (2025), although they do not build on the existing MA framework and target different estimands.

required for the canonical MA framework but is necessary for the novel approach proposed in this paper. We first introduce the data-generating mechanism for the individual-patient data from a single trial and then extend this to a population of trials. We then discuss models and target parameters from a general perspective.

We assume that all mappings introduced in this section are measurable with respect to the relevant measurable space. In some contexts, we refer to these mappings as random variables or random elements.

## 2.1 Individual-Patient Data from a Single Trial

We assume there exists a set of trials  $\mathbb{T}$ , which contains all possible trials in the area of interest. We use the notation  $T \in \mathbb{T}$  to refer to a single trial from this set. The object  $T$  contains all information about the corresponding trial, some of which is observable (e.g., trial protocol, treatment class, and sample size) and some of which is unobservable (e.g., the true observed-data distribution in that trial). In any trial  $T \in \mathbb{T}$ , the observable random variables are:

- $X$ : A set of baseline covariates with support  $\mathcal{X}$ .
- $Z$ : The treatment assignment, a binary random variable with support  $\mathcal{Z} = \{0, 1\}$  where  $Z = 1$  indicates experimental treatment and  $Z = 0$  indicates control treatment. While the control and experimental treatments may differ across trials, we do assume that there always is an unambiguous control and experimental treatment.
- $S$ : The surrogate endpoint, a random variable with support  $\mathcal{S}$ . In what follows, we keep  $\mathcal{S}$  general to allow for complex surrogates.
- $Y$ : The clinical endpoint, a random variable with support  $\mathcal{Y} \subseteq \mathbb{R}$ .

**Example 1** (set of trials  $\mathbb{T}$ ). In the data application in Section 7, the set of trials  $\mathbb{T}$  is the set of all phase 3 COVID-19 vaccine trials that could have been conducted in 2020–2021.

We let  $\mathcal{M}^*$  be a model<sup>4</sup> for the distribution of the observed data  $(X, Z, S, Y)$  in any  $T \in \mathbb{T}$ . We assume simple randomization in each trial throughout this report; hence,  $\mathcal{M}^*$  is a semi-parametric model: the only restriction is that  $X \perp Z$  for all distributions in  $\mathcal{M}^*$ . Hence, this model is the same for all trials in  $\mathbb{T}$ . We let  $\mathcal{P} : \mathbb{T} \rightarrow \mathcal{M}^*$  be a mapping from the set of possible trials to a *within-trial* observed-data distribution where  $P^T := \mathcal{P}(T)$ .

The trial’s sample size is information contained in the object  $T$ . Hence, we let  $n : \mathbb{T} \rightarrow \mathbb{N}$  be the mapping that extracts the sample size from  $T$ . Given that trial  $T$  is included in the meta-analysis, the observed data for trial  $T$  are  $n(T)$  i.i.d. samples from  $P^T$ . The corresponding empirical within-trial distribution is denoted by  $P_n^T \in \mathcal{M}_{NP}^*$ , where  $\mathcal{M}_{NP}^*$  is a non-parametric model for the distribution of  $(X, Z, S, Y)$  that contains all possible empirical distributions. Note that, for a fixed trial  $T$ ,  $\mathcal{P}(T)$  and  $n(T)$  are non-random elements in, respectively,  $\mathcal{M}^*$  and  $\mathbb{N}$ . In contrast, for the same trial,  $P_n^T$  is a random element in  $\mathcal{M}_{NP}^*$  whose distribution is determined by  $P^T$  and  $n(T)$ .

## 2.2 Data from a Population of Trials

In the MA framework, we have individual-patient data on  $(X, Z, S, Y)$  from  $N$  clinical trials. A clinical trial is treated as the unit of analysis in this framework; hence,  $T$  is treated as a random element. We now describe the data-generating mechanism where trials are sampled from a population of trials.

### 2.2.1 Population of Trials

The observed data are sampled hierarchically in the MA framework (as also visualized in Figure 1):

1. Trials are distributed according to the *full-data* distribution  $P^F \in \mathcal{M}^F$  where  $\mathcal{M}^F$  is a model for the distribution of trials, which is left unspecified. From now on, we consider  $T$  as a random element distributed according to  $P^F$ .

We further assume that the  $N$  available trials are i.i.d. sampled from  $P^F$  and denote the  $j$ ’th sampled trial by  $T_j$ .

2. In what follows, we are only interested in particular characteristics of the trials  $T$ , or in other words, particular mappings from  $\mathbb{T}$  (e.g.,  $\mathcal{P}$  and  $n$ , as introduced before). Because we now treat  $T$  as a random element with distribution  $P^F$ ,  $P^T := \mathcal{P}(T)$  and  $n := n(T)$  are also random elements whose distribution is determined by  $P^F$ .

<sup>4</sup>A model  $\mathcal{M}^*$  is defined as a collection of distributions for the observed data  $(X, Z, S, Y)$ . A non-parametric model includes essentially all possible distributions. A semi-parametric model restricts the model more (e.g., excluding distributions for which  $X \perp Z$  does not hold), but is still infinite dimensional. A parametric model is finite dimensional.

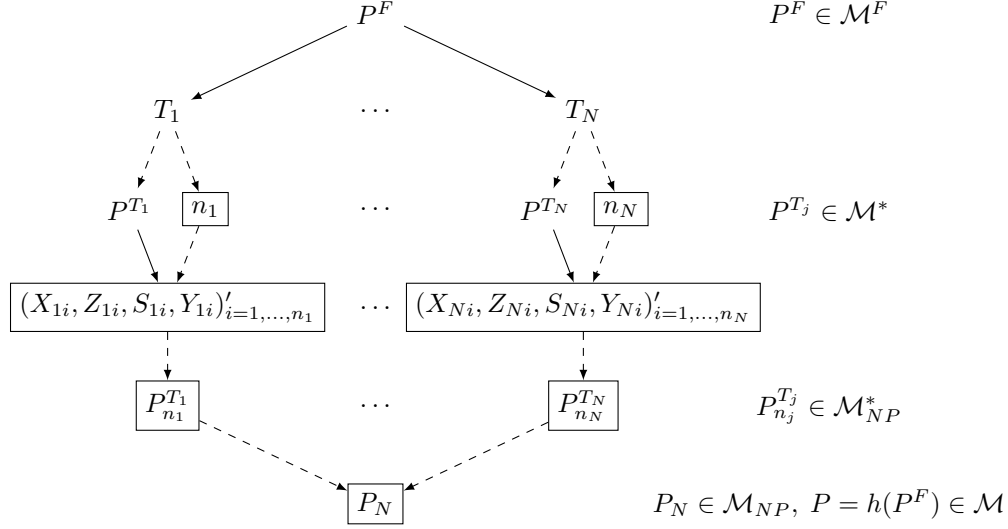


Figure 1: Data-generating mechanism underlying the meta-analytic framework. Dashed arrows represent mappings. Full arrows represent sampling. Objects surrounded by a rectangle represent the observed data.  $\mathcal{M}^F$ : full-data model;  $\mathcal{M}^*$ : within-trial model;  $\mathcal{M}_{NP}^*$ : non-parametric within-trial model;  $\mathcal{M}$ : observed-data model;  $\mathcal{M}_{NP}$ : non-parametric observed-data model.

For the  $j$ 'th sampled trial, we let  $P^{T_j}$  and  $n_j$  be the within-trial observed-data distribution and sample size, respectively.

3. While  $n$  is an observable random variable,  $P^T$  is not observable; we only observe the empirical distribution  $P_n^T$ .

We again add subscript  $j$  to refer to the  $j$ 'th trial:  $P_{n_j}^{T_j}$  is the observed empirical distribution in the  $j$ 'th trial. We further denote the observed data for patient  $i$  in trial  $j$  as  $(X_{ji}, Z_{ji}, S_{ji}, Y_{ji})'$ .

Putting everything together, the observed-data distribution is denoted by  $P \in \mathcal{M}$  where  $\mathcal{M}$  is a model for the distribution of the observed trial-level data  $(n, P_n^T) \in \mathbb{N} \times \mathcal{M}_{NP}^*$ . Furthermore, the observed-data distribution  $P$  is determined by the full-data distribution  $P^F$ . This is represented by the mapping  $h : \mathcal{M}^F \rightarrow \mathcal{M}$  where  $h(P^F)$  is the observed-data distribution implied by  $P^F$ .

We assume that the observed data  $\{(n_1, P_{n_1}^{T_1}), \dots, (n_N, P_{n_N}^{T_N})\}$  are  $N$  i.i.d. samples from  $P_0 := h(P_0^F)$  where the subscript 0 refers to the true distribution. In addition, we let  $P_N \in \mathcal{M}_{NP}$  be the empirical measure based on the observed trial-level data:

$$P_N(A) := \frac{1}{N} \sum_{j=1}^N \mathbb{1} \left\{ (n_j, P_{n_j}^{T_j}) \in A \right\} \text{ for } A \subseteq \mathbb{N} \times \mathcal{M}_{NP}^*.$$

**Remark 1** (random trial  $T$ ). For the methods presented later on, the trial random element  $T$  is superfluous because the observed data and the target parameters only depend on  $T$  through  $P^T$  and  $n$ . However, the random element  $T$  is useful for thinking about the data-generating mechanism and its i.i.d. assumption and, in our opinion, facilitates criticism of the meta-analysis. This is important because all ensuing inferences rely on the plausibility of the observed trials being an i.i.d. sample from a certain population of trials.

**Example 2** (i.i.d. sampling of trials). In the data application in Section 7, the full-data distribution  $P^F$  is the distribution of all possible phase 3 COVID-19 vaccine trials that could have been conducted in 2020–2021. The notion of such a distribution is arguably vague, but is required for inferences in the MA framework and determines for which future trials the surrogacy evaluation is valid: If we can show  $S$  to be a good trial-level surrogate in this population of trials, then this may justify using  $S$  as primary endpoint in future trials that are sampled from  $P^F$ . However, such results cannot in principle be extended to new trials for which this common-population assumption does not hold (e.g., vaccine trials with vaccines with very different mechanisms of action).

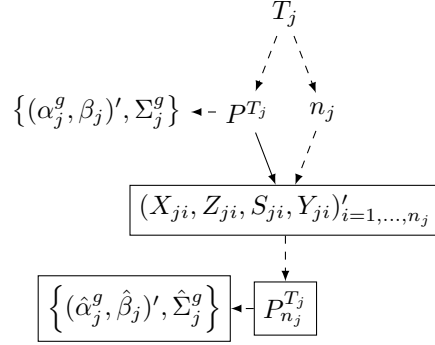


Figure 2: True and estimated treatment effects as functionals of the true and empirical within-trial distributions, respectively. Dashed arrows represent mappings. Full arrows represent sampling. Objects surrounded by a rectangle represent the observed data.

### 2.2.2 Trial-Level Treatment Effects

Two random variables are of special interest in a meta-analysis: the (unobserved) true trial-level treatment effects and the (observed) estimated trial-level treatment effects. Figure 2 illustrates how these two variables fit into the data-generating mechanism. We extend the canonical MA framework by considering treatment effects on  $g(X, S)$  for an arbitrary real-valued function  $g : \mathcal{X} \times \mathcal{S} \rightarrow \mathbb{R}$ . The canonical MA framework is a special case where  $g(X, S) = S$ . Below, we introduce functionals and variables indexed by  $g$ ; we omit the index  $g$  when referring to  $g(X, S) = S$ . For now, we impose no restrictions on  $g$  and refer to  $g(X, S)$  as the transformed surrogate for an arbitrary function  $g$ . Later on, we will consider specific functions  $g$  for which we will use different notations.

**True Treatment Effects** We let  $\alpha^g : \mathcal{M}^* \rightarrow \mathbb{R}$  and  $\beta : \mathcal{M}^* \rightarrow \mathbb{R}$  be functionals that map the within-trial distribution  $P^T$  to the true treatment effects on the transformed surrogate and the clinical endpoint, respectively. In what follows, we will consider functionals of the following form, which only depend on conditional first moments of the within-trial distribution:

$$\alpha^g = f_\alpha [E_{P^T} \{g(X, S) \mid Z = 1\}, E_{P^T} \{g(X, S) \mid Z = 0\}] \text{ and } \beta = f_\beta [E_{P^T} \{Y \mid Z = 1\}, E_{P^T} \{Y \mid Z = 0\}], \quad (1)$$

where  $f_\alpha, f_\beta : \mathbb{R}^2 \rightarrow \mathbb{R}$  are contrast functions and  $E_{P^T}$  is the expectation under within-trial distribution  $P^T$ .

Further on, we will interchangeably use  $\alpha^g$  and  $\beta$  to refer to the above functionals or to the corresponding random variables  $\alpha^g := \alpha^g(P^T)$  and  $\beta := \beta(P^T)$  for  $T \sim P^F$ . Note that these random variables are not observable.

**Estimated Treatment Effects** We let  $\hat{\alpha}^g : \mathcal{M}_{NP}^* \rightarrow \mathbb{R}$  and  $\hat{\beta} : \mathcal{M}_{NP}^* \rightarrow \mathbb{R}$  be functionals that map the empirical within-trial distribution  $P_n^T$  to the estimated treatment effects on the transformed surrogate and clinical endpoint, respectively. As before, we interchangeably use  $\hat{\alpha}^g$  and  $\hat{\beta}$  to refer to the functionals or to the corresponding random variables  $\hat{\alpha}^g := \hat{\alpha}^g(P_n^T)$  and  $\hat{\beta} := \hat{\beta}(P_n^T)$  for  $(n, P_n^T) \sim P$ . Note that these random variables are observable.

A related mapping is  $\hat{\Sigma}^g : \mathbb{N} \times \mathcal{M}_{NP}^* \rightarrow \mathbb{R}^{2 \times 2}$  which maps the empirical within-trial distribution to the estimated covariance matrix of the root- $n$  standardized estimated treatment effects on the transformed surrogate and the clinical endpoint. As before, we interchangeably use  $\hat{\Sigma}^g$  to refer to the mapping or to the corresponding random element  $\hat{\Sigma}^g := \hat{\Sigma}^g(n, P_n^T)$  for  $(n, P_n^T) \sim P$ . Note that this random element is also observable, but that this is the *estimated* covariance matrix and not the true covariance matrix, which we denote by  $\Sigma^g : \mathbb{N} \times \mathcal{M}^* \rightarrow \mathbb{R}^{2 \times 2}$  and define as

$$\Sigma^g(n, P^T) := n \cdot \text{Var}_{P^T, n} (\hat{\alpha}^g, \hat{\beta}),$$

where  $\text{Var}_{P^T, n}$  is the variance under sampling  $n$  i.i.d. samples from  $P^T$ . The distinction between  $\hat{\Sigma}^g$  and  $\Sigma^g$  will become important later on.

## 2.3 Models

In the canonical MA framework, the observed-data model  $\mathcal{M}$  is often parametric; the parameter of interest then simply is a function of the model parameters.

**Example 3.** Consider a setting without baseline covariates. One could assume that the data in each trial are bivariate normal:

$$(S_{ji}, Y_{ji})' \mid Z_{ji} = z \sim \mathcal{N}(\boldsymbol{\mu}_j^z, C_j),$$

where  $\boldsymbol{\mu}_j^z$  is the trial-specific mean vector for treatment  $z$  and  $C_j$  is the trial-specific covariance matrix, which is assumed to not depend on treatment. The within-trial model  $\mathcal{M}^*$  is parametric here. One could further make parametric assumptions about the distribution of the trial-specific parameters, for example,

$$\begin{pmatrix} \boldsymbol{\mu}_j^0 \\ \boldsymbol{\mu}_j^1 \end{pmatrix} \sim \mathcal{N}(\boldsymbol{\theta}, D) \quad \text{and} \quad C_j = C.$$

If we treat the distribution of  $n$  as known, the model  $\mathcal{M}$  would be a parametric model with parameters  $\boldsymbol{\theta}$ ,  $D$ , and  $C$ . In fact, this is a linear mixed model where  $\boldsymbol{\mu}_j^0$  and  $\boldsymbol{\mu}_j^1$  are random effects that are assumed to be multivariate normal with mean  $\boldsymbol{\theta}$  and covariance  $D$ . This model has been proposed for evaluating surrogate endpoints (Alonso et al., 2016; Buysse et al., 2000). The distribution of  $(\alpha, \beta)'$ , defined as mean differences, follows immediately as

$$\begin{pmatrix} \alpha_j \\ \beta_j \end{pmatrix} = \boldsymbol{\mu}_j^1 - \boldsymbol{\mu}_j^0 \sim N(A\boldsymbol{\theta}, ADA^\top).$$

for  $A$  an appropriate contrast matrix.

In two-stage meta-analyses, the within-trial model  $\mathcal{M}^*$  is often semi- or non-parametric and parametric assumptions are only made about the distribution of the trial-level parameters, as in the next example.

**Example 4.** Burzykowski et al. (2001) assume that  $\mathcal{M}^*$  is a semi-parametric Cox proportional hazards model. Let  $(\hat{\alpha}_j, \hat{\beta}_j)'$  be the estimated hazard ratios with corresponding estimated covariance matrix  $\hat{\Sigma}_j$  (e.g., obtained through the sandwich estimator). Burzykowski et al. (2001) further assume that the true trial-level hazard ratios  $(\alpha_j, \beta_j)'$  are bivariate normal:

$$\begin{pmatrix} \alpha_j \\ \beta_j \end{pmatrix} \sim N(\boldsymbol{\theta}, D).$$

The parameters  $\boldsymbol{\theta}$  and  $D$  are not identified from the observed data without additional assumptions, however. Burzykowski et al. (2001), therefore, assume that the sampling distribution  $(\hat{\alpha}_j - \alpha_j, \hat{\beta}_j - \beta_j)'$  in a given trial  $j$  is bivariate normal with mean zero and covariance matrix  $\Sigma_j$ , where additionally  $\hat{\Sigma}_j = \Sigma_j$ .

In Example 3, the target parameters are identified seemingly without making identifying assumptions, whereas in Example 4, the target parameters are only identified under additional identifying assumptions that relate  $(\hat{\alpha}_j, \hat{\beta}_j)'$  to  $(\alpha_j, \beta_j)'$ . This is because (untestable) identifying and (testable) modelling assumptions are mixed in the former example. In what follows, we will work under a non-parametric observed-data model  $\mathcal{M}$  unless stated otherwise. Hence, we will not make any testable assumptions, but we will need to make untestable<sup>5</sup> identifying assumptions to identify certain target parameters. This is formalized next.

## 2.4 Parameters and Estimands

As in the causal-inference and missing-data literature, we distinguish between full-data parameters as functionals of the full-data distribution, and statistical parameters as functionals of the observed-data distribution (Hernán & Robins, 2023). The values obtained by evaluating these functionals in the true distribution ( $P_0^F$  and  $P_0$ , respectively) are called estimands. Full-data parameters are of primary interest but are not identified with the observed data. Therefore, untestable identifying assumptions are needed to equate statistical parameters with full-data parameters. After making these identifying assumptions, estimation of the full-data parameters becomes a statistical problem.

We discuss general parameters next. The specific parameters targeted by our methods will be introduced in the next section.

### 2.4.1 Full-Data Parameters

A full-data parameter is represented by the following mapping:

$$\Psi^F : \mathcal{M}^F \rightarrow \mathbb{R}^p. \quad (2)$$

<sup>5</sup>Although these assumptions cannot be tested with the observed data, it will become clear that some identifying assumptions can be argued to hold (approximately) using known properties of certain estimators. This is somewhat similar to the no confounding assumption in randomized trials: the assumption is not testable but can be argued to hold based on the study design.

Oftentimes in meta-analyses, the full-data parameters only depend on the full-data distribution  $P^F$  through its implied distribution of the trial-level treatment effects. For instance, the variance of  $\beta$  is a measure of between-trial heterogeneity:

$$\Psi^F(P^F) = E_{P^F} \{\beta - E_{P^F}(\beta)\}^2. \quad (3)$$

Note that the above parameter is well defined under a non-parametric full-data model whenever  $E_{P^F}\beta^2 < \infty$ . Other parameters may only be defined under parametric assumptions, as illustrated in the next example.

**Example 5.** Continuing with the linear mixed model from Example 3, a full-data parameter could be the parameters of the random effects distribution:  $\Psi^F(P^F) = (\theta', \text{vec}(D)')'$ , where  $\text{vec}(\cdot)$  is the vectorization operator. Note that  $\theta$  and  $D$  are implicitly functionals of  $P^F$ . The mapping  $\Psi^F$  is only well defined under the parametric full-data model  $\mathcal{M}^F$  that satisfies the linear mixed model assumptions.

### 2.4.2 Statistical Parameters

A statistical parameter is represented by the following mapping:

$$\Psi : \mathcal{M} \rightarrow \mathbb{R}^p.$$

Most statistical parameters are only meaningful if they equal a relevant full-data parameter. This will only be true, however, under identifying assumptions (i.e., restrictions on the full-data model  $\mathcal{M}^F$ ). More specifically, we say that the full-data parameter  $\Psi^F$  is identified by the observed-data distribution if there exists a statistical parameter such that  $\Psi^F(P^F) = \Psi(h(P^F))$  for all  $P^F \in \mathcal{M}^F$ . Continuing with the full-data parameter in (3), we let  $\hat{\sigma}_{\hat{\beta}}$  be the element of  $\hat{\Sigma}^g$  corresponding to  $\hat{\beta}$ . Then, the following statistical parameter:

$$\Psi(P) = E_P \left( \hat{\beta} - E_P(\hat{\beta}) \right)^2 - E_P \left( n^{-1} \hat{\sigma}_{\hat{\beta}}^2 \right) \quad (4)$$

identifies the full-data parameter if the following identifying assumptions hold for all  $P^F \in \mathcal{M}^F$ :

$$E_{P^F} \beta = E_{h(P^F)} \hat{\beta} \quad \text{and} \quad E_{P^F} (\hat{\beta} - \beta)^2 = E_{h(P^F)} \left( n^{-1} \hat{\sigma}_{\hat{\beta}}^2 \right),$$

which follows from adding and subtracting  $\beta$  inside the first expectation in (4).

## 3 Meta-Analysis with an (Optimal) Transformed Surrogate

The main measure of surrogacy in the canonical MA framework is the (squared) Pearson correlation between the treatment effects on the surrogate and clinical endpoint:  $\alpha$  and  $\beta$ , respectively (see, e.g., Buyse et al., 2008; Sargent et al., 2005; Weir & Taylor, 2022). This is the so-called *trial-level correlation*, as it is based on trial-level treatment effects, which quantifies the so-called *trial-level surrogacy*.

In the previous section, we introduced the treatment effect on the transformed surrogate,  $\alpha^g$ , for an arbitrary function  $g$ . One could define the optimal function in terms of trial-level surrogacy as the function that maximizes the correlation between  $\alpha^g$  and  $\beta$ :  $g_{opt} := \arg \max_g \text{Corr}(\alpha^g, \beta)$  where  $\text{Corr}(\alpha^g, \beta)$  is the Pearson correlation between  $\alpha^g$  and  $\beta$ . However, implementing this is not practically feasible because the number of independent trials is usually very small (e.g., there are six independent trials in our application) and, hence, overfitting will occur. An alternative approach to finding a (near-)optimal  $g$  is needed.

As mentioned in the introduction, Athey et al. (2019) proposed a method that allows for inference about the treatment effect on  $Y$  in a given trial where only  $(X, Z, S)'$  were observed. This method relies on two key identifying assumptions, which we will informally translate to the MA framework: (i) surrogacy and (ii) comparability. We only present these assumptions and the corresponding identification arguments informally because they serve as a justification of our choice for an "optimal"  $g$ , but our approach remains valid (but may no longer be optimal) under violations of surrogacy and comparability.

**Assumption 3.1** (surrogacy). Under the within-trial distribution  $P^T$  in any trial  $T \in \mathbb{T}$ , the clinical endpoint  $Y$  is conditionally independent of the treatment assignment  $Z$  given the baseline covariates  $X$  and the surrogate  $S$ :

$$Y \perp Z \mid X, S \quad \text{for} \quad (X, Z, S, Y) \sim P^T.$$

**Assumption 3.2** (comparability). Let  $g_0(x, s) := E_{P_0^F} \{w(x, s; T) E_{P^T}(Y \mid X = x, S = s)\}$  be the (weighted) conditional expectation of  $Y$  given  $X$  and  $S$  where  $w(x, s; T)$  is an arbitrary trial-level weight function such that

$E_{P_0^F} \{w(x, s; T)\} = 1$  for all  $(x, s) \in \mathcal{X} \times \mathcal{S}$ . We term  $g_0$  the *surrogate index*.<sup>6</sup> The comparability assumption requires that  $E_{P^T}(Y | X = x, S = s)$  does not depend on  $T \in \mathbb{T}$ , which in turn implies that, for any trial  $T \in \mathbb{T}$ ,

$$E_{P^T}(Y | X = x, S = s) = g_0(x, s) \quad \forall (x, s) \text{ in the support of } P^T.$$

Under these two assumptions, the mean of  $Y$  under treatment  $z$  in an arbitrary trial  $T$  can be identified from the distribution of  $g_0(S, X)$  in the same trial:

$$\begin{aligned} E_{P^T} \{Y | Z = z\} &= E_{P^T} \{E_{P^T}(Y | X, Z = z, S) | Z = z\} && \text{(iterated expectation)} \\ &= E_{P^T} \{E_{P^T}(Y | X, S) | Z = z\} && \text{(surrogacy)} \\ &= E_{P^T} \{g_0(X, S) | Z = z\} && \text{(comparability)} \end{aligned}$$

If surrogacy and comparability hold,  $g_0$  is the optimal function in the sense that  $\text{Corr}(\alpha^{g_0}, \beta) = 1$  for treatment effect measures that only depend on the first conditional moments as in (1). Even if surrogacy and comparability do not hold—which is expected in most applications— $g_0(S, X)$  is well defined and is expected to be a good summary of  $(X, S)$  as long as surrogacy and comparability hold approximately. The key difference between  $g_{opt}$  defined before and  $g_0$ , however, is that  $g_0$  can be estimated by regressing  $Y$  onto  $X$  and  $S$  by pooling the individual-patient data from all trials (e.g., using off-the-shelf machine learning software). Overfitting will be less of an issue because the number of patient-level observations is much larger than the number of trials. Although some caution regarding overfitting is warranted, as further discussed in Appendix D.3.

In the remainder of this section, we first discuss full-data and statistical parameters, and corresponding identifying assumptions. We then discuss inference about these parameters when (i)  $g$  is known a priori and (ii) when  $g$  was estimated with the meta-analytic data.

### 3.1 Parameters and Estimands

For every  $g$ , the parameters of interest are features of the distribution of  $(\alpha^g, \beta)'$ . Since this distribution is indexed by  $g$ , the parameters are themselves also indexed by  $g$  and the question arises which parameter is most relevant. We divide the set of parameters into three classes according to the nature of  $g$ : First,  $g$  may be selected a priori (e.g., derived based on subject matter knowledge or estimated using external data). We discuss this as a starting point for the more difficult data-adaptive parameters. Second, one may be interested in the surrogacy when using the unknown surrogate index  $g_0$ . We will not target this parameter because (i) inference about parameters indexed by  $g_0$  is only possible under strong restrictions on the rate at which the *estimated surrogate index*, denoted by  $g_N$ , converges to  $g_0$  and (ii) the practical relevance of this parameter is questionable since  $g_0$  will remain unknown (even if  $g_N$  converges sufficiently fast to  $g_0$ ). Third, one may be interested in the surrogacy when using an estimated  $g_N$ . We prefer this parameter over the previous one because (i) inference is possible under weaker conditions and (ii)  $g_N$  is estimated from the data and, hence, known.

#### 3.1.1 A Priori Selected $g$

**Full-Data Parameters** The canonical MA framework is based on a bivariate normal model for the distribution of  $(\alpha^g, \beta)'$  for  $g(X, S) = S$ . Although such a parametric model is implausible, it could hold in principle for a single  $g$ . This cannot be extended to the current setting because that would require the distribution of  $(\alpha^g, \beta)'$  to be bivariate normal for any  $g$  in a set of possible functions  $\mathcal{G}$ . This is not possible if  $\mathcal{G}$  is sufficiently large<sup>7</sup>. Hence, the full-data parameter cannot rely on parametric assumptions about the distribution of  $(\alpha^g, \beta)'$ . The bivariate normal model used in the canonical MA framework is nonetheless convenient as the model parameters (i.e., the mean and covariance of a bivariate normal distribution) have a simple interpretation.

We follow the strategy of Vansteelandt and Dukes (2022) by defining the full-data parameters such that they reduce to the bivariate normal model parameters if the parametric assumptions hold but they should remain interpretable if the parametric assumptions do not hold. This leads to the following full-data parameters for a given  $g$ :

$$\begin{pmatrix} \Psi_1^{F,g}(P^F) \\ \Psi_2^{F,g}(P^F) \end{pmatrix} = \begin{pmatrix} E_{P^F} \alpha^g \\ E_{P^F} \beta \end{pmatrix} \quad \text{and} \quad \begin{pmatrix} \Psi_3^{F,g}(P^F) & \Psi_5^{F,g}(P^F) \\ \Psi_4^{F,g}(P^F) & \Psi_6^{F,g}(P^F) \end{pmatrix} = \text{Var}_{P^F} \left\{ \begin{pmatrix} \alpha^g \\ \beta \end{pmatrix} \right\}, \quad (5)$$

<sup>6</sup>The definition of  $g_0$  resembles the surrogate index as defined by Athey et al. (2019). However, Athey et al. (2019) define the surrogate index differently and in a setting with only two data sources. Under their surrogacy and comparability assumptions, our definition matches theirs.

<sup>7</sup>Assume normality holds with  $g_1(X, S) = S$  where  $S_{ji} = -0.5c_j$  if  $Z_{ji} = 0$  and  $S_{ji} = c_j$  if  $Z_{ji} = 1$ ; hence,  $\alpha_j^{g_1} = 1.5c_j$  when using mean contrasts. Further let  $c_j$  be normally distributed. Now consider  $g_2(X, S) = S^2$  where we now have that  $\alpha_j^{g_2} = 0.75c_j^2$  which cannot be normally distributed as it is non-negative.

where we let  $\Psi^{F,g}(P^F) = (\Psi_1^{F,g}(P^F), \dots, \Psi_5^{F,g}(P^F))'$ . Note that we are mainly interested in the trial-level correlation between  $\alpha^g$  and  $\beta$ . However, it is more convenient to work with the above target parameters because they are very simple functionals of the full-data distribution and the trial-level correlation is a function of these parameters anyhow.

**Statistical Parameters and Identifying Assumptions** Since we do not observe  $(\alpha^g, \beta)'$  directly, the full-data parameters are not identifiable without identifying assumptions. Under the following two identifying assumptions, the full-data parameters are identified with the observed-data distribution.

**Assumption 3.3** (unbiased estimation of trial-level treatment effects). Let  $\mathcal{G}$  be a set of real-valued functions on  $\mathcal{X} \times \mathcal{S}$ . Then, for all  $T \in \mathbb{T}$ , we have that

$$\forall g \in \mathcal{G} : E_{P^{T,n}} \left\{ (\hat{\alpha}^g, \hat{\beta})' \right\} = (\alpha^g(P^T), \beta(P^T))',$$

where  $E_{P^{T,n}}$  is the expectation over the empirical distributions  $P_n^T$  generated by sampling  $n = n(T)$  i.i.d. observations from  $P^T$ .

**Assumption 3.4** (unbiased estimation of within-trial sampling variability). Let  $\mathcal{G}$  be a set of real-valued functions on  $\mathcal{X} \times \mathcal{S}$ . Then, for all  $T \in \mathbb{T}$ , we have that

$$\forall g \in \mathcal{G} : E_{P^{T,n}}(\hat{\Sigma}^g) = \Sigma^g(n, P^T),$$

where  $E_{P^{T,n}}$  is the expectation over the empirical distributions  $P_n^T$  generated by sampling  $n = n(T)$  i.i.d. observations from  $P^T$ .

Note that these assumptions are stated for a set of possible transformations  $\mathcal{G}$ . When we are interested in only one specific transformation  $g$ , we can replace  $\mathcal{G}$  with  $\{g\}$ . Later on when the transformation will be estimated, these assumptions will be required to hold for  $\mathcal{G}$  being a large class of functions. These assumptions will only hold approximately in practice; we relax these assumptions, therefore, in Section 5 by switching to an alternative asymptotic regime.

Under the above assumptions, the full-data parameters are identified with the following simple statistical parameters.

**Lemma 3.1.** Define the statistical parameter  $\Psi^g := (\Psi_1^g, \dots, \Psi_5^g)'$  as follows:

$$\begin{pmatrix} \Psi_1^g(P) \\ \Psi_2^g(P) \end{pmatrix} = \begin{pmatrix} E_P \hat{\alpha}^g \\ E_P \hat{\beta} \end{pmatrix} \quad \text{and} \quad \begin{pmatrix} \Psi_3^g(P) & \Psi_2^g(P) \\ \Psi_5^g(P) & \Psi_4^g(P) \end{pmatrix} = \text{Var}_P \left\{ \begin{pmatrix} \hat{\alpha}^g \\ \hat{\beta} \end{pmatrix} \right\} - E_P \left( n^{-1} \hat{\Sigma}^g \right), \quad (6)$$

where  $P \in \mathcal{M}$  is an observed-data distribution. Under Assumptions 3.3 and 3.4, the full-data parameter (5) is identified in the sense that  $\Psi^{F,g}(P^F) = \Psi^g(h(P^F))$  for all  $P^F \in \mathcal{M}^F$  and  $g \in \mathcal{G}$  where  $h$  is the mapping from the full-data distribution to the implied observed-data distribution, as defined in Section 2.2.1.

This and all following lemmas and theorems are proved in Appendix F.

**Remark 2** (asymptotic efficiency). Assumptions 3.3 and 3.4 impose restrictions on the full-data model  $\mathcal{M}^F$ . These assumptions restrict the implied observed-data model  $\mathcal{M} = \{P = h(P^F) : P^F \in \mathcal{M}^F\}$ . However, the implied observed-data model remains locally non-parametric under weak regularity conditions. Hence, there is only one regular asymptotically linear estimator, which is consequently also efficient (Kennedy, 2017). Further details are provided in Appendix C.2.

### 3.1.2 Estimated $g_N$

So far, we have extended the canonical MA framework by introducing a non-parametric full-data parameter and a corresponding statistical parameter that identifies the former under straightforward identifying assumptions. These parameters are indexed by  $g \in \mathcal{G}$ , and as argued before, the surrogate index  $g_0$  is a good choice for  $g$ . The next step is to estimate the surrogate index and substitute that estimate for  $g$ . If the surrogate index would have been estimated on an independent data set, we could treat it as an a priori selected  $g$  and use the parameters defined in the previous subsection, which are not data adaptive. However, when the surrogate index is estimated using the meta-analytic data  $P_N$ , the target parameters become data-adaptive. These parameters are indexed by the estimated surrogate index  $g_N$ :  $\Psi^{F,g_N}$  and  $\Psi^{g_N}$ .

**Remark 3** (data-adaptive target parameters and cross-fitting). In the current application,  $g_N$  is an estimated regression function that indexes the target parameter. We will impose Donsker conditions on this estimator. This limits the complexity of the allowed surrogate index estimators for valid inference, even though many machine learning methods can still be used. In the non-parametric literature, cross-fitting is a popular approach to avoid Donsker conditions (see, e.g., Chernozhukov et al., 2018). Methods for inference about data-adaptive target parameters that use cross-fitting exist (see, e.g., van der Laan and Luedtke (2015, Section 7)), but target different types of data-adaptive parameters than the ones considered here. We, therefore, do not consider cross-fitting in this paper.

### 3.2 Plug-in Estimator

We consider the plug-in estimator for the (non-data-adaptive) statistical parameter  $\Psi^g$  in (6), denoted by  $\hat{\Psi}^g(P) = (\hat{\Psi}_1^g(P), \dots, \hat{\Psi}_5^g(P))'$  for  $P \in \mathcal{M}_{NP}$ . We consider the same estimator for the data-adaptive parameter  $\Psi^{g_N}$  by simply replacing  $g$  with  $g_N$ . This estimator, evaluated in the empirical distribution  $P_N$ , has the following closed-form expression:

$$\begin{pmatrix} \hat{\Psi}_1^g(P_N) \\ \hat{\Psi}_2^g(P_N) \end{pmatrix} = \begin{pmatrix} P_N \hat{\alpha}^g \\ P_N \hat{\beta} \end{pmatrix} \quad \text{and} \quad \begin{pmatrix} \hat{\Psi}_3^g(P_N) \\ \hat{\Psi}_4^g(P_N) \\ \hat{\Psi}_5^g(P_N) \end{pmatrix} = \text{Var}_{P_N} \left\{ \begin{pmatrix} \hat{\alpha}^g \\ \hat{\beta} \end{pmatrix} \right\} - P_N \left( n^{-1} \hat{\Sigma}^g \right). \quad (7)$$

This is a Z-estimator with no nuisance parameters that solves  $P_N \phi_{\theta}^g = \mathbf{0}$  where  $\phi_{\theta}^g : \mathbb{N} \times \mathcal{M}_{NP}^* \rightarrow \mathbb{R}^5$  is the estimating function indexed by the parameter of interest  $\theta$ . The plug-in estimator and properties of the corresponding estimating functions are further described in Appendix C. In Section 4, we present general results for inference about data-adaptive parameters defined as the solution to estimating equations of this form (i.e., defined as the solution of an estimating equation with no nuisance parameters).

**Remark 4** (estimates outside of the allowed range). The plug-in estimator for the variance matrix is simply the estimated variance of  $(\hat{\alpha}^g, \hat{\beta})'$  minus the average of the estimated within-trial variance matrices. A corresponding estimate may not be positive semi-definite; this is more likely to happen when  $N$  is small and the variance of  $(\alpha^g, \beta)'$  is small relative to the within-trial sampling variability.

## 4 Inference for Data-Adaptive Parameters via Estimating Equations

In this section, we discuss inference about data-adaptive target parameters. We first introduce general notation that is not specific to the MA framework (because the theoretical results are not specific to the MA framework). Second, we discuss known results for general data-adaptive target parameters and complement these results with a new theorem that provides conditions under which asymptotically valid inference is possible about data-adaptive target parameters that can be defined as the root of an estimating function with no nuisance parameters. Finally, we discuss the implications for the MA framework and the estimated surrogate index.

### 4.1 Notation

We will use the following notation throughout this section, which mostly follows the notation introduced in Section 2.2.1 but deviates in some aspects. Let  $\mathcal{M}$  be the model for the observed-data distribution. The true data-generating distribution is denoted by  $P_0 \in \mathcal{M}$ . We assume that the observed data are i.i.d. sampled from  $P_0$  where  $O \in \Omega$  denotes the random element distributed according to  $P_0$ . The corresponding empirical distribution of the observed data is denoted by  $P_N \in \mathcal{M}_{NP}$  where  $\mathcal{M}_{NP}$  is a non-parametric model containing all empirical distributions. We use the following notation for expectations with respect to these distributions, where  $f$  is any integrable real-valued function on  $\Omega$ :  $P_0 f := \int_{\Omega} f(o) dP_0(o)$  and  $P_N f := \int_{\Omega} f(o) dP_N(o)$ . Convergence in distribution is denoted by  $\xrightarrow{d}$ .

We let  $g \in \mathbb{D}$  be an element that indexes the statistical parameter  $\Psi^g : \mathcal{M} \rightarrow \mathbb{R}^p$ , where  $\mathbb{D}$  is a metric space with metric  $d$ . The statistical parameter is defined as the root of  $\theta \mapsto \Phi^g(\theta) := P \phi_{\theta}^g$  where  $\phi_{\theta}^g : \Omega \rightarrow \mathbb{R}^p$  is an estimating function. We denote the corresponding plug-in estimator by  $\hat{\Psi}^g(P_N)$ , which is defined as the (approximate<sup>8</sup>) root of  $\theta \mapsto \hat{\Phi}_N^g(\theta) := P_N \phi_{\theta}^g$ . We further let  $g_N$  be a random element in  $\mathbb{D}$  that depends on the observed data (i.e.,  $g_N$  is a function of  $P_N$ ); the corresponding data-adaptive target parameter is denoted by  $\Psi^{g_N}$ .

Furthermore, unless mentioned otherwise,  $\|x\|_2$  denotes the Euclidean norm of the vector  $x$ . The  $p \times p$  matrix of first-order partial derivatives of  $\Phi^g(\theta)$  with respect to  $\theta$  is denoted by  $\dot{\Phi}^g(\theta)$ .

### 4.2 General Data-Adaptive Target Parameters

The parameter  $\Psi^{g_N}(P)$  is data-adaptive because it is indexed by  $P_N$  through  $g_N$ . Theorem 3 from Hubbard et al. (2016), reproduced below with slight changes in notation, shows when and how asymptotically valid inferences are possible for general data-adaptive target parameters.

**Theorem 1.** Assume  $\hat{\Psi}^g(P_N)$  is an asymptotically linear estimator of  $\Psi^g(P_0)$  at  $P_0$  with influence function  $IC^g(P_0) : \Omega \rightarrow \mathbb{R}$  uniformly in the choice of the parameter  $g$  in the following sense:

$$\hat{\Psi}^{g_N}(P_N) - \Psi^{g_N}(P_0) = (P_N - P_0) IC^{g_N}(P_0) + R_N$$

<sup>8</sup>It will generally be sufficient that  $P_N \Phi^g(\theta) = o_P(N^{1/2})$  for  $\theta = \hat{\Psi}^g(P_N)$ .

where  $R_N = o_P(N^{-1/2})$ . In addition, assume  $P_0 \{IC^{g_N}(P_0) - IC^{g_0}(P_0)\}^2 = o_P(1)$  and  $IC^{g_N}(P_0)$  is an element of a  $P_0$ -Donsker class with probability tending to 1. Then,

$$\hat{\Psi}^{g_N}(P_N) - \Psi^{g_N}(P_0) = (P_N - P_0)IC^{g_0}(P_0) + o_P(N^{-1/2}) \quad (8)$$

and thus  $N^{1/2} \left\{ \hat{\Psi}^{g_N}(P_N) - \Psi^{g_N}(P_0) \right\}$  is asymptotically normally distributed with mean zero and variance  $\sigma^2 = P_0 IC^{g_0}(P_0)^2$ .

For every specific application with data-adaptive target parameters, one has to show that the conditions of this theorem hold. This is easy for data-adaptive target parameters that are means of a data-adaptively determined function of the data; however, verifying these conditions is difficult for more general data-adaptive target parameters. In the next subsection, we specialize Theorem 1 to the setting where the data-adaptive target parameter can be defined as the solution to an estimating equation without nuisance parameters. The value of the more specialized theorem is that the corresponding conditions are easier to verify in practice and that it contains a bootstrap result.

### 4.3 Data-Adaptive Target Parameters Defined Through Estimating Functions

#### 4.3.1 A General Theorem

Before presenting the specialized version of Theorem 1, we introduce some additional concepts and notation that are needed to state a bootstrap result. We let  $\tilde{P}_N$  be the empirical distribution of the bootstrap sample defined as  $\tilde{P}_N := \frac{1}{N} \sum_{i=1}^N W_i \cdot \delta_{O_i}$  where  $\delta_{O_i}$  is the Dirac measure at  $O_i$  and  $W_i$  is the bootstrap weight. For the multiplier bootstrap, the bootstrap weights  $W_i$  are i.i.d. random variables with mean  $0 < \mu < \infty$  and variance  $0 < \tau^2 < \infty$  such that  $\frac{\mu}{\tau^2} = 1$ , and with  $\|W\|_{2,1} < \infty^9$ . For the multinomial bootstrap, the bootstrap weights are obtained by sampling from a multinomial distribution with  $N$  trials and  $N$  categories, where the probability of each category is  $1/N$ . For both the multiplier and multinomial bootstrap, the bootstrap weights are independent of the observed data  $O_1, \dots, O_N$ .

For the bootstrap result, we use an alternative definition of weak convergence to define convergence of the conditional laws of bootstraps (see, e.g., Kosorok (2008, Section 2.2.3) for more details). Briefly, let  $(\mathbb{E}, e)$  be a metric space with metric  $e$  and let  $\check{X}_N$  be a sequence of bootstrapped processes in  $\mathbb{E}$  with random weights  $W$ . For some tight process  $X$  in  $\mathbb{E}$ , we use the notation  $\check{X}_N \xrightarrow[W]{P} X$  to mean that

$$\sup_{h \in BL_1} \left| E_W h(\check{X}_N) - E h(X) \right| \xrightarrow{P} 0 \text{ and } E_W h(\check{X}_N)^* - E h(\check{X}_N)_* \xrightarrow{P} 0,$$

where

- $BL_1$  is the set of Lipschitz functions on  $\mathbb{E}$  with Lipschitz constant 1 and with  $\|f\|_\infty \leq 1$
- $E_W h(\check{X}_N)$  is the expectation of  $h(\check{X}_N)$  with respect to the bootstrap weights  $W$  given the remaining data
- $h(\check{X}_N)^*$  and  $h(\check{X}_N)_*$  are the measurable majorants and minorants with respect to the joint data  $(O_1, \dots, O_N, W_1, \dots, W_N)$ .

We are now ready to state the theorem.

**Theorem 2.** Let  $\Theta \subset \mathbb{R}^p$  be open and define  $g \mapsto \theta_0^g$  such that  $\Phi^g(\theta_0^g) = 0$  for all  $g \in \mathcal{G} \subset \mathbb{D}$ . Further assume that  $g_N \in \mathcal{G}$  with probability tending to one as  $N \rightarrow \infty$ , where  $g_N$  depends on the observed data and  $(\mathbb{D}, d)$  is a metric space with metric  $d$ . Further assume there exists  $g^* \in \mathcal{G}$  such that  $d(g_N, g^*) = o_P(1)$  and define  $\rho \{(\theta_1, g_1), (\theta_2, g_2)\} := \|\theta_1 - \theta_2\|_2 + d(g_1, g_2)$  as a metric on  $\Theta \times \mathbb{D}$ .

Additionally assume the following conditions:

- (i)  $\Phi^g(\theta_N) \rightarrow 0$  implies that  $\theta_N \rightarrow \theta_0^g$  for all  $g \in \mathcal{G}$ .
- (ii)  $\{\phi_\theta^g : g \in \mathcal{G}, \theta \in \Theta\}$  is strong  $P_0$ -Glivenko–Cantelli.
- (iii)  $\exists \delta_1 > 0$  such that  $\{\phi_\theta^g : g \in \mathcal{G}, \|\theta - \theta_0^{g^*}\|_2 < \delta_1\}$  is  $P_0$ -Donsker and  $P_0 \|\phi_\theta^g - \phi_{\theta_0^{g^*}}^{g^*}\|_2^2 \rightarrow 0$  if  $\rho \{(\theta, g), (\theta_0^{g^*}, g^*)\} \rightarrow 0$ .

<sup>9</sup>The norm  $\|\cdot\|_{2,1}$  is defined as  $\int_0^\infty \sqrt{P(|W| > x)} dx$ .

- (iv)  $P_0 \|\phi_{\theta_0^*}^{g^*}\|_2^2 < \infty$  and  $\theta \mapsto \Phi^g(\theta)$  is differentiable in  $\|\theta - \theta_0^{g^*}\|_2 < \delta_2$  for some  $\delta_2 > 0$  for all  $g \in \mathcal{G}$  with the matrix of partial derivatives, denoted by  $\dot{\Phi}^g(\theta)$ , being invertible at  $\theta_0^{g^*}$  for  $g = g^*$ . Further assume that  $(\theta, g) \mapsto \dot{\Phi}^g(\theta)$  is continuous at  $(\theta_0^{g^*}, g^*)$  with respect to the metric  $\rho$ .
- (v)  $\hat{\theta}_N^{g_N}$  and  $\tilde{\theta}_N^{g_N}$  solve the empirical and bootstrapped estimating equations approximately:  $P_N \phi_{\hat{\theta}_N^{g_N}}^{g_N} = o_P(N^{-1/2})$  and  $\tilde{P}_N \phi_{\tilde{\theta}_N^{g_N}}^{g_N} = o_P(N^{-1/2})$ .
- (vi)  $g \mapsto \Phi^g(\theta)$  is Lipschitz continuous uniformly over  $\theta \in \Theta$ :  $\|\Phi^{g_1}(\theta) - \Phi^{g_2}(\theta)\|_2 \leq L \cdot d(g_1, g_2)$  for all  $g_1, g_2 \in \mathcal{G}$  and  $\theta \in \Theta$  for some  $L > 0$ .

Under conditions (i) to (vi), we have that

$$N^{1/2} \left( \hat{\theta}_N^{g_N} - \theta_0^{g_N} \right) \xrightarrow{d} Z \sim N(0, \Sigma_0^{g^*}) \text{ as } N \rightarrow \infty,$$

and

$$N^{1/2} \left( \tilde{\theta}_N^{g_N} - \hat{\theta}_N^{g_N} \right) \xrightarrow[W]{P} Z \sim N(0, \Sigma_0^{g^*}) \text{ as } N \rightarrow \infty,$$

where  $\Sigma_0^{g^*} = \left( \dot{\Phi}^{g^*}(\theta_0^{g^*}) \right)^{-1} P_0 \left( \phi_{\theta_0^{g^*}}^{g^*} \right)^{\otimes 2} \left( \dot{\Phi}^{g^*}(\theta_0^{g^*}) \right)^{-1}$ .

Note that Theorem 2 is based on Kosorok (2008, Theorem 10.16); the proof is also similar. The difference is that our Theorem 2 applies to data-adaptive target parameters. Conditions (i) to (v) above resemble conditions (A) to (E) in Kosorok (2008, Theorem 10.16) and are standard conditions for the consistency and asymptotic normality of Z-estimators; however, condition (vi) is new. The latter condition essentially requires that small changes in  $g$  only lead to small changes in the estimating function  $\theta \mapsto \Phi^g(\theta)$ . Conditions (i–vi) are discussed in more detail in Appendix D.

Theorem 2 shows that one can essentially ignore the fact that  $g_N$  depends on the data when targeting the data-adaptive parameter. However, while the sandwich estimator for  $\Sigma_0^{g^*}$  is consistent under weak conditions, this is not guaranteed under the conditions of Theorem 2. We can in any case use the bootstrap to obtain a consistent estimator of  $\Sigma_0^{g^*}$  or we can use the bootstrap distribution directly for constructing confidence intervals (e.g., percentile confidence intervals) for the data-adaptive parameter  $\Psi^{g_N}$ . Also note that  $g_N$  is not re-estimated in the bootstrap samples.

#### 4.4 Plug-in Estimator for Data-Adaptive Target Parameter in MA Framework

The conditions in Theorem 2 are difficult to verify for the statistical parameter (6) in the MA framework because of the non-standard data-generating mechanism where the observed data are random elements in  $\mathbb{N} \times \mathcal{M}_{NP}^*$ . We, therefore, propose a set of conditions in Appendix D.2 (further referred to as conditions (a–f)) specialized to this setting, which are sufficient for the conditions in Theorem 2. We discuss the key conditions from Appendix D.2 only briefly here. See Appendix D.2 for the full set of conditions and a more detailed discussion.

**Remark 5.** The general notation used in Theorem 2 relates to the notation introduced in Section 3 as follows: The observed data are the within-trial sample sizes and the corresponding empirical distribution functions,  $O = (n, P_n^T)$ , which are random elements in  $\Omega = \mathbb{N} \times \mathcal{M}_{NP}^*$ . The target parameter is indexed by the real-valued function  $g \in \mathcal{G}$  on  $\mathcal{X} \times \mathcal{S}$  where we assume that  $\mathbb{D} = l^\infty(\mathcal{X} \times \mathcal{S})$ , which is the class of bounded real-valued functions on  $\mathcal{X} \times \mathcal{S}$ . We use the metric induced by the supremum norm  $d(g, g') = \|g - g'\|_\infty$ .

Condition (a) requires that the estimated surrogate index  $g_N$  converges to a fixed function in the supremum norm.

- (a) There exists a  $g^* \in \mathcal{G}$  such that  $\|g_N - g^*\|_\infty \xrightarrow{P} 0$  and  $g_N \in \mathcal{G}$  with probability tending to one.

This is a very weak condition that should be satisfied for any reasonable regression method. However, it has important implications (related to overfitting and positivity violations) for finite samples as discussed in Appendix D.3.

Conditions (c–d) restrict the complexity of the trial-specific treatment effect estimators and the estimator for  $g_N$ :  $\hat{\alpha}^g$  should be smooth in  $g$  and  $\mathcal{G}$  should not be too complex. Conditions (c–d) can be shown using many strategies and are for instance satisfied when using parametric estimators for  $g_N$ . Otherwise, if we impose mild smoothness conditions on the estimator  $(n, P_n^T) \mapsto \hat{\alpha}^g(n, P_n^T)$ , conditions (c–d) are satisfied whenever  $\mathcal{G}$  is a  $P_{a,0}$ -Donsker class<sup>10</sup>. This allows one to use many machine learning methods to estimate  $g_N$ .

<sup>10</sup> $P_{a,0}$  is the distribution on  $\mathcal{X} \times \mathcal{S}$  induced by sampling  $(n, P_n^T)$  from  $P_0$  and then sampling a random value from  $P_n^T$ .

Conditions (b) and (e–f) are minor regularity conditions which are expected to hold in practically any realistic application.

Under the conditions (a–f) from Appendix D.2, the conditions of Theorem 2 are satisfied for the estimator (7) of the data-adaptive target parameter  $\Psi^{gN}(P_0)$  defined in (6). Hence,  $N^{1/2} \left( \hat{\Psi}^{gN}(P_N) - \Psi^{gN}(P_0) \right)$  is asymptotically normal with mean zero and a covariance matrix

$$\Sigma_0^{g*} = \left( \dot{\Phi}^{g*}(\theta_0^{g*}) \right)^{-1} P_0 \left( \phi_{\theta_0^{g*}}^{g*} \right)^{\otimes 2} \left( \dot{\Phi}^{g*}(\theta_0^{g*}) \right)^{-1}$$

which can be consistently estimated by the sandwich estimator:

$$\left( P_N \dot{\phi}_{\hat{\theta}_N^{gN}}^{gN} \right)^{-1} \cdot P_N \left( \phi_{\hat{\theta}_N^{gN}}^{gN} \right)^{\otimes 2} \cdot \left( P_N \dot{\phi}_{\hat{\theta}_N^{gN}}^{gN} \right)^{-1}, \quad (9)$$

where  $\hat{\theta}_N^{gN} := \hat{\Psi}^{gN}(P_N)$ . However, the sandwich estimator may not perform well in small samples. Luckily, the bootstrap is valid by Theorem 2 and corresponding confidence intervals may behave better in small samples. Because the number of independent trials  $N$  tends to be small in practice, the multinomial bootstrap will lead to a very discrete bootstrap distribution. We expect this to negatively influence finite-sample performance. Therefore, we opt for the Bayesian bootstrap instead (Rubin, 1981), which is a multiplier bootstrap with the weights  $W$  independently sampled from a unit exponential distribution.

## 5 Alternative Asymptotic Regime

In the data-generating mechanism introduced in Section 2.2, the trial-specific sample sizes  $n$  were functions of the trial  $T$  (i.e.,  $n : T \mapsto n(T)$ ). Hence, for each sampled trial  $T$ ,  $n$  is a constant even as the number of independent trials  $N$  increases. In this asymptotic regime, the estimator in (7) is consistent and asymptotically normal under Assumptions 3.3 and 3.4. These assumptions essentially only hold for estimators based on sample means, however. Furthermore, efficient estimators<sup>11</sup> are often preferred as they have smaller asymptotic variance than simple, but finite-sample unbiased, estimators. In other cases, simple estimators are not consistent, even in randomized trials (e.g., estimators of the mean difference in the presence of missing data under missing at random). In addition, even simple estimators for common treatment effect measures, like vaccine efficacy, are generally finite-sample biased.

In Appendix E, we modify the asymptotic regime by letting the trial-specific sample sizes be a function of the number of independent trials  $N$ . Specifically, we let  $n : N \mapsto n(N)$  where  $\lim_{N \rightarrow \infty} n(N) = \infty$ . In this alternative asymptotic regime, we relax Assumptions 3.3 and 3.4 to corresponding assumptions where the biases converge to zero at a certain rate. Given these rates, we determine the rates at which  $n$  should increase as a function of  $N$  for the results of the previous sections to remain valid. Intuitively, the faster the within-trial biases converge to zero, the slower the within-trial sample sizes are allowed to grow as a function of  $N$ .

We have not included the details of this alternative asymptotic regime in the main text for two reasons: First, the analysis approach does not change under this alternative asymptotic regime. Second, the rate at which the within-trial sample sizes should grow as a function of  $N$  has little practical relevance because the within-trial sample sizes are generally much larger than the number of independent trials  $N$  in practice. In Appendix E, we report on a small simulation study that illustrates this point.

## 6 Simulations

We conducted simulations to evaluate the finite-sample performance of the proposed methods. We consider two scenarios: a proof-of-concept scenario and a more realistic vaccine-trials scenario. The proof-of-concept scenario uses a simple data-generating mechanism that demonstrates the potential advantage of using the estimated surrogate index as potential surrogate. Here, the trial-level correlations for the estimated surrogate indices (i.e., the data-adaptive parameters) were much closer to 1 than the trial-level correlations for the untransformed surrogate endpoints; this is also reflected in the corresponding estimators and inferences. The vaccine-trials scenario has a more realistic data-generating mechanism. In the remainder of this section, we summarize the main findings of the simulations, focusing on the vaccine-trials scenario. The simulations are discussed in full detail in Appendix G.

<sup>11</sup>For instance, covariate-adjusted estimators based on parametric regression models (Van Lancker et al., 2024) or semi-parametrically efficient estimators like targeted maximum likelihood and debiased machine learning estimators (Chernozhukov et al., 2018; van der Laan & Rose, 2018).

In all simulations, two finite-sample adjustments are used. First, in (7), the variance of  $(\hat{\alpha}^g, \hat{\beta})$  is estimated by dividing by  $N - 1$  instead of  $N$ . Second, the sandwich estimator in (9) is adjusted by multiplying it with  $N/(N - 1)$  and confidence intervals based on the normal approximation and sandwich estimator are computed using the  $t$  distribution with  $N - 1$  degrees of freedom (instead of the normal distribution).

Confidence intervals constructed using the bootstrap (BCa) and the sandwich estimator showed reduced coverage in small-sample settings ( $N = 6$ ); however, coverage improves as the number of trials increases. For  $N = 12$  and  $N = 24$ , the sandwich confidence intervals had near-nominal coverage, while the BCa confidence intervals had slight undercoverage. For  $N = 6$ , the sandwich confidence intervals do not always have closer to nominal coverage than the BCa confidence intervals. These results indicate that there is no best method for constructing confidence intervals for  $N = 6$  and we, therefore, recommend to use different types of confidence intervals simultaneously to increase robustness of the conclusions. For larger sample sizes, sandwich confidence intervals should be preferred based on the simulations results. We nonetheless also recommend to use multiple types of confidence intervals for larger  $N$  as these simulations do not encompass all possible data-generating mechanisms.

We also studied confidence intervals based on a parametric Bayesian model in the simulations. This approach is generally asymptotically not valid for the data-adaptive target parameters defined in (6). However, this approach may be more stable in small samples and may, therefore, be preferred in practice. Furthermore, this approach is often used in practice, whereas the non-parametric estimator (7) is not. We found that the credible intervals based on the Bayesian model had good coverage in small samples, confirming the above intuitions.

The difficulties for valid inference in small samples does not seem to be related to the data-adaptive nature of the target parameter because the same difficulties were observed for estimating the trial-level correlations of the untransformed surrogate endpoints.

Appendix G also includes simulations that confirm the theoretical results regarding the alternative asymptotic regime, briefly discussed in Section 5 and elaborated on in Appendix E. These simulations indicate that one should not worry about violating the rate conditions in practice because most reasonable estimators are approximately unbiased in finite samples and  $n \gg N$  in most meta-analyses. If one of the latter two conditions is not satisfied (e.g., many small trials are included in the meta-analysis), inferences may be invalid.

## 7 Application to COVID-19 trials

### 7.1 Data Description

The surrogate-endpoint analysis included five Phase 3 COVID-19 vaccine trials: P3001 (Moderna), P3002 (AstraZeneca), P3003 (Janssen), P3004 (Novavax), and P3005 (Sanofi). The Sanofi trial consisted of two stages: stage 1 studied a monovalent vaccine and stage 2 studied a bivalent vaccine. These two stages, moreover, included a considerable number of non-naive subjects (i.e., subjects who have been previously infected). We, therefore, split the Sanofi trial into four separate trials: (i) stage 1, naive only; (ii) stage 1, non-naive only; (iii) stage 2, naive only; and (iv) stage 2, non-naive only. We further refer to the latter as the Sanofi trials, ignoring that they are strictly speaking trial subunits.

Two antibody markers have been measured in these trials as potential correlates of protection<sup>12</sup> (CoPs): (i) IgG binding antibody concentration against the D614 index strain Spike protein (IgG Spike) and (ii) 50% inhibitory dilution neutralizing antibody titer (nAb ID50) against the D614G reference strain. These markers were measured at different time points post-enrollment: 57 days for Moderna, 57 days for AstraZeneca, 29 days for Janssen, 35 days for Novavax, and 43 days for Sanofi. The per-protocol cohort included participants who received all planned vaccinations without protocol deviations and, in the first four trials, who were SARS-CoV-2 negative at the last vaccination visit. The per-protocol cohort in the Sanofi trial includes subjects who have been previously infected. Eligibility for correlates analyses in the first four trials required participants to remain SARS-CoV-2 negative up to 6 days post marker-measurement visit.

All trials stratified randomization by age and prospective risk category (based on CDC guidelines for severe COVID-19 risk factors at the time of enrollment). Additionally, a harmonized case-cohort design with two-phase sampling was implemented across trials to measure IgG Spike and nAb ID50. The clinical endpoint was virologically confirmed symptomatic SARS-CoV-2 infection occurring between 7 and 80 days post marker-measurement visit. Table 1 summarizes (i) the study cohort sizes and clinical endpoint counts by randomization arm and (ii) the number of subjects with antibody data by case and vaccine status.

The nAb ID50 in these trials quantifies neutralization against the reference strain; however, this was not the only circulating strain in the trials. Moreover, the trials were conducted in different regions and in different periods, leading to

<sup>12</sup>We interchangeably use surrogate endpoint and correlate of protection in this section.

Table 1: Phase 3 COVID-19 vaccine efficacy trial data included in the surrogate endpoint analysis. The numbers between brackets indicate the number of subjects from the corresponding group with antibody marker measurements. For the Sanofi trials, the first number inside the brackets indicates the number of IgG Spike measurements and the second one indicates the number of nAb ID50 measurements. Naive subjects in the placebo groups should not have an antibody response to SARS-CoV-2; therefore, the corresponding number of antibody marker measurements are indicated by a dash. Note that the counts for the cases include all subjects with an event during the entire trial period (which includes follow-up beyond 80 days post marker-measurement visit). The counts for the non-cases include subjects who were censored.

Phase 3 Trial	n	Placebo		n	Vaccine	
		Cases	Non-Cases		Cases	Non-Cases
Moderna	13,682	656 (-)	13,026 (-)	13,979	47 (36)	13,932 (1,000)
AstraZeneca	6,212	55 (-)	6,157 (-)	13,492	45 (25)	13,447 (438)
Janssen	17,821	818 (-)	17,003 (-)	18,155	420 (373)	17,735 (816)
Novavax	7,250	44 (-)	7,206 (-)	16,143	12 (12)	16,131 (714)
Sanofi (stage 1, naive)	820	84 (-, -)	736 (-, -)	772	77 (69, 72)	695 (178, 268)
Sanofi (stage 1, non-naive)	3,297	114 (102, 109)	3,183 (198, 238)	3,274	72 (62, 67)	3,202 (165, 203)
Sanofi (stage 2, naive)	292	26 (-, -)	266 (-, -)	275	19 (17, 17)	256 (134, 179)
Sanofi (stage 2, non-naive)	4,660	72 (56, 56)	4,588 (236, 413)	4,798	70 (60, 61)	4,728 (245, 456)

between-trial variability in circulating strains. Ideally, the neutralization titer should be measured against the circulating strains to ensure that the surrogate endpoint matches the clinical endpoint (i.e., infection with the circulating strains). This “ideal” surrogate endpoint is not available, however. Instead, we approximated this ideal surrogate endpoint using two information sources: (i) the strains circulating in the subject’s region in the period that the subject was in the trial as obtained from GISAID (GISAID Initiative, 2025) and (ii) the estimated geometric mean titer (GMT) ratios (reference strain to circulating strain) from the literature. The so obtained variable is termed the *adjusted nAb ID50*. Details on this adjustment are provided in Appendix H.2.

## 7.2 Estimating the surrogate index $g_N$

For each potential CoP (IgG Spike, nAb ID50, and adjusted nAb ID50), we consider two estimators for the surrogate index: a Cox proportional hazards (Cox PH) model and a SuperLearner. We briefly discuss these estimators next and provide further details in Appendix H.3.

The Cox PH model includes, in addition to the potential surrogate, the following baseline covariates: age at randomization, sex, BMI category ( $BMI < 18.5$ ,  $18.5 \leq BMI < 25$ ,  $25 \leq BMI < 30$ ,  $BMI \geq 30$ ), and an indicator of whether the subject was at high risk of severe COVID-19 (Polack et al., 2020). We stratified the Cox PH model by trial to account for different forces of infection across the trials. Predictions of the clinical endpoint (i.e., probability of infection by 80 days post marker-measurement visit) are obtained by using the estimated regression coefficients and the estimated baseline hazard function from the Janssen trial.

SuperLearner is an ensemble method that combines multiple candidate prediction algorithms into a single predictive model. It uses cross-validation to evaluate each candidate’s performance and aggregates their predictions via a meta-learner that estimates optimal weights for combining predictions from the different candidates (van der Laan et al., 2007). To estimate the surrogate index, we use a SuperLearner with a set of logistic regression models (varying the included predictors and interaction terms) and a generalized additive logistic regression model as candidate prediction algorithms. The same covariates as in the Cox PH model are included in the candidate algorithms, but we additionally included the logit of the estimated COVID-19 probability (80 days post marker-measurement visit) in the control group by trial as a trial-level covariate to account for different forces of infection across trials. The surrogate is included in each candidate algorithm. We further used a modified cross-validation scheme to avoid trial-level overfitting. Specifically, we use leave-one-trial-out cross-validation: each candidate prediction algorithm is fitted on data from all but one trial and then used to predict on the omitted trial. Repeating this process yields cross-validated predictions for all trials, which serve as inputs to the meta-learner. Finally, all candidate methods are refitted on the full data set, and their predictions are combined using the weights estimated by the meta-learner to produce final predictions.

We have to address missingness in predictors (i.e., in the antibody marker) and in the outcome (i.e., censoring before 80 days) when estimating the surrogate index. For the Cox PH model, we weight observations by the inverse probability of being sampled in the case-cohort design; censoring is automatically handled in the Cox PH model. For the SuperLearner, we weight observations by the product of the inverse probability of being sampled in the case-cohort design and the

inverse probability of censoring weights (IPCWs). The IPCWs are estimated by the Kaplan–Meier estimator for the censoring time stratified by trial and treatment group.

### 7.3 Trial-Level Treatment Effects

The trial-level treatment effects on the clinical endpoint and the estimated surrogate index are estimated using standard methods. The cumulative incidence rates for infection by 80 days post marker-measurement visit are estimated with the Kaplan–Meier estimator. The estimated surrogate index means are estimated by first fitting a linear regression model with the estimated surrogate index as outcome and the treatment indicator, age, sex, BMI category, and the high-risk indicator as covariates. Note that the estimated surrogate index is missing whenever the antibody marker is missing. We, therefore, use the inverse probability of being sampled in the case-cohort design as weights in these linear regression models. The estimated means are obtained as the mean of the predicted values for all subjects in a given trial with the treatment indicator set to 1 (vaccine) and 0 (placebo), respectively. This approach is more efficient than simple sample means and is valid even if the linear model is misspecified (Van Lancker et al., 2024).

We further consider the treatment effects on a transformed scale to ensure that they can take values on the entire real line. For the clinical endpoint, we consider the following transformation of vaccine efficacy (VE):  $\log(1 - VE)$ . Similarly, for the estimated surrogate index, we consider the treatment effect on the following scale:

$$\log\left(1 - \widehat{VE}\right) \quad \text{for} \quad \widehat{VE} = 1 - \frac{E_{PT}(g_N(X, S) \mid Z = 1)}{E_{PT}(g_N(X, S) \mid Z = 0)}.$$

The within-trial covariance matrices of the estimated treatment effects are estimated using the non-parametric bootstrap (with 5,000 replications) in each trial. We keep the case-cohort weights fixed in the bootstrap samples; this is expected to lead to conservative standard errors<sup>13</sup>.

## 7.4 Results

We present the meta-analyses using all trials except the ones with non-naive subjects. We exclude the non-naive trials because the immune response differs substantially between naive and non-naive subjects and, consequently, trial-level surrogacy in a population of trials that mixes naive and non-naive subjects is not meaningful from an immunological perspective. Because the data are limited, it is difficult to reach conclusive results about trial-level surrogacy. We, therefore, also repeat the analyses on a pseudo-real data set with (i) the same six trials, but with a larger within-trial sample size, and (ii) 24 trials obtained by cloning the original six trials.

### 7.4.1 Original Data

**Trial-Level Surrogacy** The trial-level treatment effects on the three antibody markers (as differences in mean base-10 log antibody marker) and the estimated VEs are shown in Figure 3. If we were to exclude the Sanofi trials, this plot would suggest a strong association between both types of treatment effects. However, the Sanofi trials are clear outliers, which seems to suggest that IgG Spike and nAb ID50 are poor trial-level surrogates. The trial-level surrogacy for the adjusted nAb ID50 is less clear from Figure 3, however. The corresponding plot using the estimated surrogate indices is shown in Figure 4. This plot leads to similar conclusions.

Table 2 presents the estimated trial-level correlation coefficients for both the untransformed antibody markers (corresponding to Figure 3) and the estimated surrogate indices (corresponding to Figure 4), along with 95% confidence intervals. Notably, the estimated trial-level correlations are higher for the estimated surrogate indices than the untransformed antibody markers. Furthermore, the estimated trial-level correlations for the adjusted nAb ID50 are higher than those for the unadjusted nAb ID50, indicating that the adjustment for the circulating strains improves the trial-level surrogacy. Nonetheless, the confidence intervals are wide, and the inferences should be interpreted with caution, as they are based on only six independent trials.

In Appendix H.4.2, we also present the results of a Bayesian analysis using weakly informative priors; this is the same Bayesian model as studied in the simulations. This alternative analysis leads to similar conclusions as the frequentist non-parametric analysis. We also repeated the Bayesian analysis assuming a proportional regression of  $\beta$  on  $\alpha^g$ ; this leads to considerably more precise results, but this gain in precision is of course merely due to making additional parametric assumptions.

<sup>13</sup>The estimated standard errors for the treatment effect on the estimated surrogate index are expected to be conservative. The estimator for the treatment effect on the clinical endpoint does not depend on these weights.

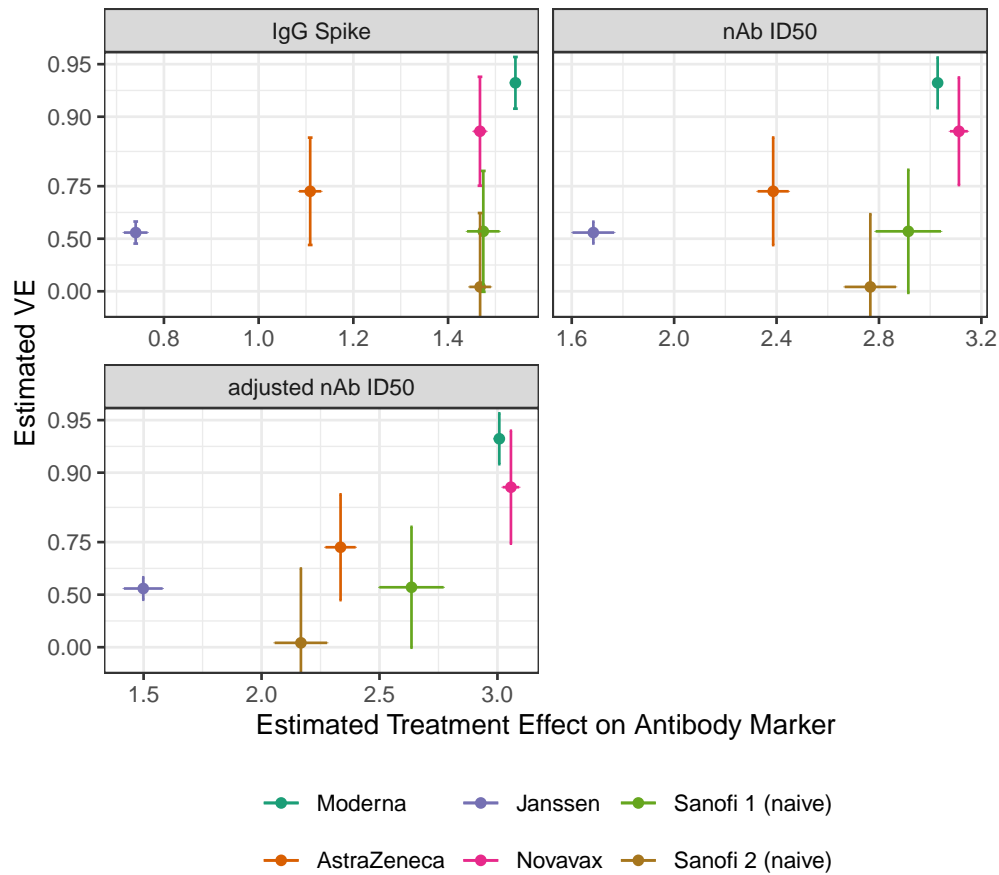


Figure 3: Estimated trial-level treatment effects on the antibody markers (difference in mean base-10 log units) and vaccine efficacies (VEs) with 95% confidence intervals based on the bootstrap standard errors.

Table 2: Estimated trial-level correlations with 95% BCa bootstrap confidence intervals for the meta-analysis that includes all naive trials. The Antibody Marker column indicates the meta-analyses where the antibody marker (without any transformation) is evaluated as a trial-level surrogate endpoint.

Surrogate	Antibody Marker	Est. Surrogate Index	
		Cox Model	SuperLearner
IgG Spike	0.33 (-0.37, 0.83)	0.34 (-0.46, 0.85)	0.33 (-0.45, 0.83)
nAb ID50	0.47 (-0.28, 0.79)	0.56 (-0.34, 0.83)	0.57 (-0.32, 0.82)
Adj. nAb ID50	0.77 (0.12, 0.91)	0.88 (0.34, 0.95)	0.87 (0.25, 0.95)

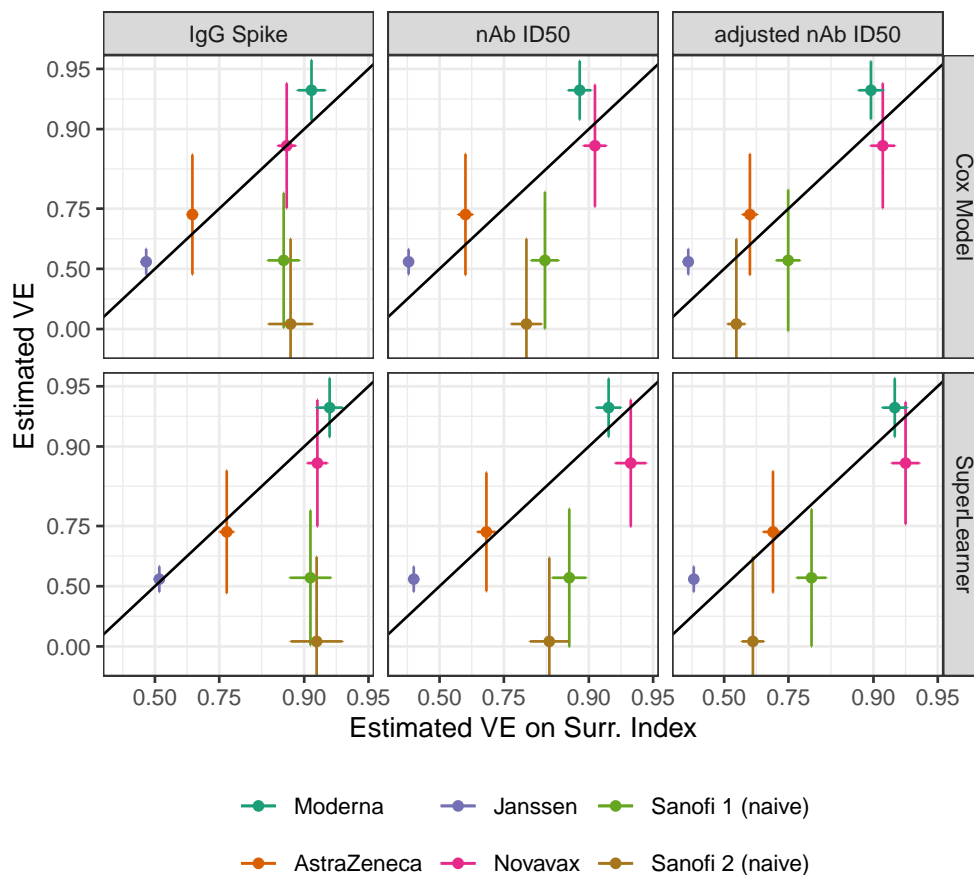


Figure 4: Estimated trial-level treatment effects on the estimated surrogate indices and vaccine efficacies (VEs) with 95% confidence intervals based on the bootstrap standard errors. The black line is the identity line.

**Prediction of Vaccine Efficacy in the non-naive Sanofi Trials** The estimated treatment effects on the estimated surrogate index may serve as predictions for the treatment effects on the clinical endpoint (i.e., for the VE). We further refer to these estimated treatment effects as the predicted VEs. The point estimates for the trial-level correlation suggest that these predictions should be accurate for the estimated surrogate indices based on adjusted nAb ID50 for trials sampled from the same population as the Moderna, AstraZeneca, Janssen, Novavax, and naive Sanofi trials (i.e., for trials sufficiently “similar” to these six). To illustrate this, we show the corresponding predicted VEs for the non-naive Sanofi trials in Figure 5. These predictions are mainly for illustrative purposes, as the non-naive Sanofi trials are not sufficiently similar to the first six trials because, as mentioned before, the immune response in non-naive subjects differs substantially from that in naive subjects. Somewhat surprisingly, the predicted VEs are accurate for the estimated surrogate indices based on the adjusted nAb ID50. However, the confidence intervals for the estimated VEs are wide; hence, it is possible that the predicted VEs do not accurately predict the true VEs.

#### 7.4.2 Pseudo-Real Data

The results of the meta-analysis with the six naive trials are mostly inconclusive because the confidence intervals are wide. To further illustrate the potential of the proposed method, we repeated the analyses on a pseudo-real data set (i) with the same six naive trials as before, but dividing all within-trial variance matrix entries by four, and (ii) with 24 trials obtained by cloning each trial four times. The corresponding estimates and confidence intervals for the trial-level correlation coefficients are shown in Table 3. These results indicate that increasing the precision in each trial increases the precision of the trial-level correlation estimate only slightly; however, increasing the number of trials leads to a substantial increase in precision.

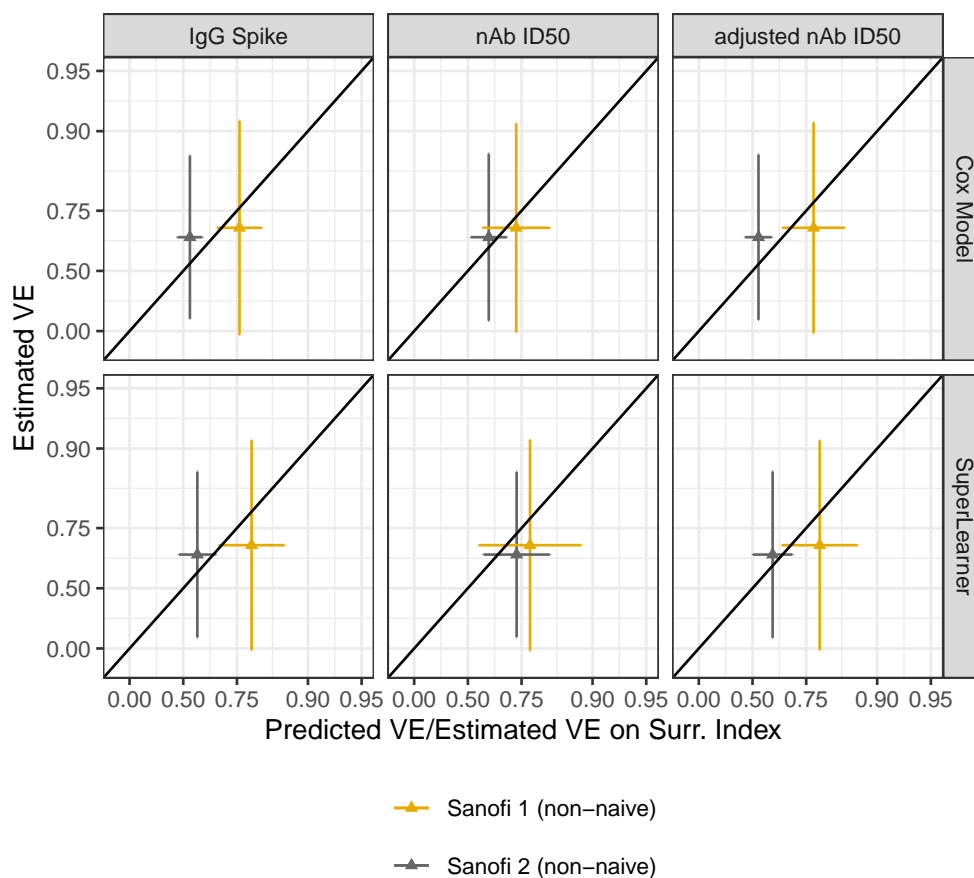


Figure 5: Predicted and estimated vaccine efficacies (VEs) for the non-naive Sanofi trials. The predicted vaccine efficacies are based on the estimated surrogate indices, estimated using the data from the six naive trials. The whiskers are the 95% confidence intervals based on the bootstrap standard errors. The black line is the identity line.

Table 3: Estimated trial-level correlations with 95% BCa bootstrap confidence intervals for the meta-analysis on the pseudo-real data. The Antibody Marker column indicates the meta-analyses where the antibody marker (without any transformation) is evaluated as a trial-level surrogate endpoint.

Pseudo-Real Data	Surrogate	Antibody Marker	Est. Surrogate Index	
			Cox Model	SuperLearner
Increased Precision	IgG Spike	0.32 (-0.29, 0.80)	0.33 (-0.36, 0.81)	0.31 (-0.36, 0.79)
	nAb ID50	0.44 (-0.18, 0.76)	0.54 (-0.21, 0.79)	0.54 (-0.20, 0.79)
	Adjusted nAb ID50	0.73 (0.18, 0.87)	0.84 (0.43, 0.93)	0.83 (0.38, 0.92)
Increased Number of Trials	IgG Spike	0.34 (0.04, 0.60)	0.35 (0.01, 0.63)	0.33 (0.02, 0.61)
	nAb ID50	0.47 (0.23, 0.65)	0.57 (0.31, 0.71)	0.58 (0.32, 0.72)
	Adjusted nAb ID50	0.77 (0.62, 0.85)	0.89 (0.78, 0.93)	0.88 (0.76, 0.92)

## 8 Conclusions

This paper extends the canonical MA framework in a manner that allows for complex surrogate endpoints while also dealing with potential differences in the patient populations across trials. While this approach may be useful in settings where the canonical MA framework can also be used—as, e.g., in the application in Section 7—it may be especially useful in settings where the canonical MA framework cannot be used, such as in settings with complex surrogate endpoints. For instance, the approach as presented in this paper can be used to evaluate the trial-level surrogacy of the information available 3 years after randomization (including, e.g., fasting plasma glucose measurements, but also the presence of diabetes) as a trial-level surrogate for diabetes 4 years after randomization (Agniel & Parast, 2024). A similar analysis is not possible in the canonical MA framework.

The proposed approach runs into the same limitations as the canonical MA framework. Furthermore, whereas the canonical MA framework can be used when appropriate summary-level statistics are available, the proposed approach always requires individual-level data for all trials, where additionally, the same covariates should be measured in all trials. In the data application, such data were available because the trials were designed in a harmonized manner. In practice, however, this is rare and, therefore, an important limitation of the proposed approach. Still, this approach may already be meaningfully applied if  $X$  is a baseline risk score, which is likely to be available in most trials. If the trial populations are similar, one could even apply this approach without any covariates; this may still lead to higher trial-level correlations than the canonical MA framework because treatment effects on  $g_N(S)$  may be better correlated with treatment effects on the clinical endpoint than treatment effects on  $S$ .

We have focused on a particular full-data parameter that reduces to the target parameter of the canonical MA framework when the parametric model is correctly specified. However, one may define different full-data parameters that are identical to the target parameter of the canonical MA framework when the parametric model is correctly specified, but that behave differently when the parametric model is misspecified. The full-data parameter we have considered is appealing because it is easy to interpret even when the parametric model is misspecified; however, it may be more difficult to estimate than alternative full-data parameters. For instance, one could define an alternative full-data parameter in terms of a projection onto the parametric model (used in the canonical MA framework) based on the Kullback-Leibler divergence. Such a projection parameter would be easier to estimate (van der Laan et al., 2023), but it may be more difficult to interpret when the parametric model is misspecified.

## Acknowledgements

The authors thank Craig Magaret from the Fred Hutchinson Cancer Center for preparing the GISAID data for adjusting the neutralization titers.

The authors also thank the participants and study teams that conducted the COVID-19 vaccine efficacy trials of the Moderna, Astra-Zeneca, Janssen, Novavax, and Sanofi SARS-CoV-2 vaccines that are analyzed in this article. The authors thank the US Government Vaccine COVID-19 Vaccine Correlates of Protection Program from the Department of Health and Human Services [including the Administration for Strategic Preparedness and Response; Biomedical Advanced Research and Development Authority; and the National Institute of Allergy and Infectious Diseases of the National Institutes of Health], which co-conducted these clinical trials in public–private partnerships with the vaccine developers. The authors also thank the vaccine developers for these partnerships.

## Supplementary Material

The code to reproduce the results in this paper is available at <https://github.com/florianstijven/ma-surrogate-index>. The individual-level data from the COVID-19 vaccine trials cannot be made available, but the GitHub repo includes a simulated data set that resembles the original data.

## References

- Agniel, D., & Parast, L. (2024). Robust evaluation of longitudinal surrogate markers with censored data. *Journal of the Royal Statistical Society Series B: Statistical Methodology*, qkae119.
- Alonso, A., Bigirimurame, T., Burzykowski, T., Buyse, M., Molenberghs, G., Muchene, L., Perualila, N. J., Shkedy, Z., Van der Elst, W., et al. (2016). *Applied surrogate endpoint evaluation methods with SAS and R*. CRC Press New York.

- Alonso, A., Geys, H., Molenberghs, G., Kenward, M. G., & Vangeneugden, T. (2004). Validation of surrogate markers in multiple randomized clinical trials with repeated measurements: Canonical correlation approach. *Biometrics*, 60(4), 845–853.
- Alonso, A., Van der Elst, W., Molenberghs, G., Buyse, M., & Burzykowski, T. (2015). On the relationship between the causal-inference and meta-analytic paradigms for the validation of surrogate endpoints. *Biometrics*, 71(1), 15–24.
- Athey, S., Chetty, R., Imbens, G. W., & Kang, H. (2019). *The surrogate index: Combining short-term proxies to estimate long-term treatment effects more rapidly and precisely* (tech. rep.). National Bureau of Economic Research.
- Athey, S., Chetty, R., Imbens, G. W., & Kang, H. (2024). *The surrogate index: Combining short-term proxies to estimate long-term treatment effects more rapidly and precisely* (tech. rep.). National Bureau of Economic Research.
- Burzykowski, T., Molenberghs, G., Buyse, M., Geys, H., & Renard, D. (2001). Validation of surrogate end points in multiple randomized clinical trials with failure time end points. *Journal of the Royal Statistical Society Series C: Applied Statistics*, 50(4), 405–422.
- Buyse, M., Burzykowski, T., Michiels, S., & Carroll, K. (2008). Individual-and trial-level surrogacy in colorectal cancer. *Statistical methods in medical research*, 17(5), 467–475.
- Buyse, M., Molenberghs, G., Burzykowski, T., Renard, D., & Geys, H. (2000). The validation of surrogate endpoints in meta-analyses of randomized experiments. *Biostatistics*, 1(1), 49–67.
- Chen, J., Gu, J., & Kwon, S. (2025). Empirical bayes shrinkage (mostly) does not correct the measurement error in regression. *arXiv preprint arXiv:2503.19095*.
- Chen, J., & Ritzwoller, D. M. (2023). Semiparametric estimation of long-term treatment effects. *Journal of Econometrics*, 237(2), 105545.
- Chernozhukov, V., Chetverikov, D., Demirer, M., Duflo, E., Hansen, C., Newey, W., & Robins, J. (2018). Double/debiased machine learning for treatment and structural parameters. *The Econometrics Journal*, 21(1), C1–C68.
- Coyle, J. R., Hejazi, N. S., Malenica, I., Phillips, R. V., & Sofrygin, O. (2021). *sl3: Modern pipelines for machine learning and Super Learning* [R package version 1.4.2]. <https://doi.org/10.5281/zenodo.1342293>
- Daniels, M. J., & Hughes, M. D. (1997). Meta-analysis for the evaluation of potential surrogate markers. *Statistics in medicine*, 16(17), 1965–1982.
- Degtiar, I., & Rose, S. (2023). A review of generalizability and transportability. *Annual Review of Statistics and Its Application*, 10(1), 501–524.
- FDA-NIH Biomarker Working Group. (2016). *BEST (Biomarkers, EndpointS, and other Tools)*. Food; Drug Administration (US). <https://www.ncbi.nlm.nih.gov/books/NBK326791/>
- Fleming, T. R., & Powers, J. H. (2012). Biomarkers and surrogate endpoints in clinical trials. *Statistics in medicine*, 31(25), 2973–2984.
- Frangakis, C. E., & Rubin, D. B. (2002). Principal stratification in causal inference. *Biometrics*, 58(1), 21–29.
- Freedman, L. S., Graubard, B. I., & Schatzkin, A. (1992). Statistical validation of intermediate endpoints for chronic diseases. *Statistics in medicine*, 11(2), 167–178.
- Gabriel, E. E., Daniels, M. J., & Halloran, M. E. (2016). Comparing biomarkers as trial level general surrogates. *Biometrics*, 72(4), 1046–1054.
- Gabriel, E. E., Sachs, M. C., Daniels, M. J., & Halloran, M. E. (2019). Optimizing and evaluating biomarker combinations as trial-level general surrogates. *Statistics in medicine*, 38(7), 1135–1146.
- Gail, M. H., Pfeiffer, R., Van Houwelingen, H. C., & Carroll, R. J. (2000). On meta-analytic assessment of surrogate outcomes. *Biostatistics*, 1(3), 231–246.
- Gilbert, P. B., Peng, J., Han, L., Lange, T., Lu, Y., Nie, L., Shih, M.-C., Waddy, S. P., Wiley, K., Yann, M., et al. (2024). A surrogate endpoint based provisional approval causal roadmap. *arXiv preprint arXiv:2407.06350*.
- GISAID Initiative. (2025). Tracking of hCoV-19 Variants [Accessed: 2025-03-09].
- Hernán, M., & Robins, J. (2023). *Causal Inference*. CRC Press.
- Hubbard, A. E., Kherad-Pajouh, S., & van der Laan, M. J. (2016). Statistical inference for data adaptive target parameters. *The international journal of biostatistics*, 12(1), 3–19.
- Institute of Medicine (US) Committee on Qualification of Biomarkers and Surrogate Endpoints in Chronic Disease. (2011). *Perspectives on biomarker and surrogate endpoint evaluation: Discussion forum summary* [Presentation by Thomas Fleming: Biomarkers and Surrogate Endpoints in Chronic Disease]. National Academies Press (US). <https://www.ncbi.nlm.nih.gov/books/NBK209571/>
- Joffe, M. M., & Greene, T. (2009). Related causal frameworks for surrogate outcomes. *Biometrics*, 65(2), 530–538.
- Kennedy, E. H. (2017). Semiparametric theory. *arXiv preprint arXiv:1709.06418*.
- Korn, E. L., Albert, P. S., & McShane, L. M. (2005). Assessing surrogates as trial endpoints using mixed models. *Statistics in medicine*, 24(2), 163–182.
- Kosorok, M. R. (2008). *Introduction to empirical processes and semiparametric inference* (Vol. 61). Springer.
- Li, S., & Luedtke, A. (2023). Efficient estimation under data fusion. *Biometrika*, 110(4), 1041–1054.

- Lin, Z., Kong, D., & Wang, L. (2023). Causal inference on distribution functions. *Journal of the Royal Statistical Society Series B: Statistical Methodology*, 85(2), 378–398.
- Polack, F. P., Thomas, S. J., Kitchin, N., Absalon, J., Gurtman, A., Lockhart, S., Perez, J. L., Pérez Marc, G., Moreira, E. D., Zerbini, C., et al. (2020). Safety and efficacy of the bnt162b2 mRNA covid-19 vaccine. *New England journal of medicine*, 383(27), 2603–2615.
- Prentice, R. L. (1989). Surrogate endpoints in clinical trials: Definition and operational criteria. *Statistics in medicine*, 8(4), 431–440.
- Rosin, S. P., Stijnen, F., Cross, K. A., Shook-Sa, B. E., Hudgens, M. G., & Gilbert, P. B. (2025). *Doubly standardized trial-level surrogate endpoint evaluation, with application to vaccine trials* [Unpublished manuscript].
- Rubin, D. B. (1981). The bayesian bootstrap. *The annals of statistics*, 130–134.
- Sargent, D. J., Wieand, H. S., Haller, D. G., Gray, R., Benedetti, J. K., Buyse, M., Labianca, R., Seitz, J. F., O’Callaghan, C. J., Francini, G., et al. (2005). Disease-free survival versus overall survival as a primary end point for adjuvant colon cancer studies: Individual patient data from 20,898 patients on 18 randomized trials. *Journal of Clinical Oncology*, 23(34), 8664–8670.
- Sera, F., Armstrong, B., Blangiardo, M., & Gasparrini, A. (2019). An extended mixed-effects framework for meta-analysis. *Statistics in Medicine*, 38(29), 5429–5444.
- Shu, Y., & McCauley, J. (2017). GISAID: Global initiative on sharing all influenza data – from vision to reality. *Eurosurveillance*, 22(13), 30494.
- Stan Development Team. (2025). RStan: The R interface to Stan [R package version 2.32.7]. <https://mc-stan.org/>
- USG COVID-19 Response Team / Coronavirus Prevention Network (CoVPN) Biostatistics Team, Gilbert, P. B., Fong, Y., Benkeser, D., Andriesen, J., Borate, B., Carone, M., Carpp, L. N., Diaz, I., Fay, M. P., Fiore-Gartland, A., Hejazi, N. S., Huang, Y., Huang, Y., Hyrien, O., Janes, H. E., Juraska, M., Li, K., Luedtke, A., . . . Follmann, D. (2022). USG COVID-19 Response Team / CoVPN vaccine efficacy trial immune correlates Statistical Analysis Plan [Version 0.4].
- van der Laan, L., Carone, M., Luedtke, A., & van der Laan, M. (2023). Adaptive debiased machine learning using data-driven model selection techniques. *arXiv preprint arXiv:2307.12544*.
- van der Laan, M. J., & Luedtke, A. R. (2015). Targeted learning of the mean outcome under an optimal dynamic treatment rule. *Journal of causal inference*, 3(1), 61–95.
- van der Laan, M. J., Polley, E. C., & Hubbard, A. E. (2007). Super learner. *Statistical applications in genetics and molecular biology*, 6(1).
- van der Laan, M. J., & Rose, S. (2018). *Targeted learning in data science*. Springer.
- van der Vaart, A. W. (1998). *Asymptotic statistics*. Cambridge University Press.
- Van Houwelingen, H. C., Arends, L. R., & Stijnen, T. (2002). Advanced methods in meta-analysis: Multivariate approach and meta-regression. *Statistics in medicine*, 21(4), 589–624.
- Van Lancker, K., Bretz, F., & Dukes, O. (2024). Covariate adjustment in randomized controlled trials: General concepts and practical considerations. *Clinical Trials*, 21(4), 399–411.
- VanderWeele, T. J. (2013). Surrogate measures and consistent surrogates. *Biometrics*, 69(3), 561–565.
- Vansteelandt, S., & Dukes, O. (2022). Assumption-lean inference for generalised linear model parameters. *Journal of the Royal Statistical Society Series B: Statistical Methodology*, 84(3), 657–685.
- Weir, C. J., & Taylor, R. S. (2022). Informed decision-making: Statistical methodology for surrogacy evaluation and its role in licensing and reimbursement assessments. *Pharmaceutical Statistics*, 21(4), 740–756.
- Zeileis, A. (2004). Econometric computing with HC and HAC covariance matrix estimators. *Journal of Statistical Software*, 11(10), 1–17.
- Zeileis, A., Köll, S., & Graham, N. (2020). Various versatile variances: An object-oriented implementation of clustered covariances in R. *Journal of Statistical Software*, 95(1), 1–36.

## A Surrogate Index

This section summarizes the surrogate-index framework, which approaches the identification of the treatment effect on the clinical endpoint from a missing data perspective (Athey et al., 2019), or equivalently from a data fusion perspective (Li & Luedtke, 2023). Note that the surrogate-index framework is not a surrogacy-evaluation approach; perfect surrogacy is part of the identifying assumptions in this framework.

### A.1 Setting and Notation

In the surrogate-index framework, the full data for subject  $i$  consist of the following variables, a subset of which is assumed to be observed:

- $A \in \{0, 1\}$ : The data source indicator;  $A = 0$  indicates that the data are from the experimental study, and  $A = 1$  indicates that the data are from the observational study. The exact meaning of these two studies is discussed below.
- $Z \in \{0, 1\}$ : Assigned binary treatment. This treatment does not have to be randomized as long as conditional exchangeability holds. However, we will assume simple randomization throughout.
- $X \in \mathcal{X}$ : Baseline covariates.
- $S \in \mathcal{S}$ : Surrogate endpoint.
- $Y \in \mathcal{Y}$  and  $(Y(0), Y(1))' \in \mathcal{Y} \times \mathcal{Y}$ : The observed clinical endpoint is denoted by  $Y$ , and the corresponding potential outcome under treatment  $z$  by  $Y(z)$ . We assume consistency such that  $Y = Z \cdot Y(1) + (1 - Z) \cdot Y(0)$ .

These data are assumed to be i.i.d. sampled from some distribution  $P_0^F$ .

The observed data come from two sources, each with its own missing data pattern:

- In the *experimental study* ( $A = 0$ ), a binary treatment  $Z$  is assigned to all subjects after measuring the baseline covariates  $X$ . The surrogate endpoint  $S$  is measured for all subjects, but the clinical endpoint  $Y$  is missing for all subjects.
- In the *observational study* ( $A = 1$ ), treatment information may or may not be available. We set  $Z = 0$  for all subjects with  $A = 1$ . The same baseline covariates  $X$  and surrogate endpoint  $S$  are measured as in the experimental data, but additionally, the clinical endpoint  $Y$  is measured.

The observed data are thus:

$$(A, X, (1 - A)Z, S, AY)',$$

which are assumed to be i.i.d. sampled from some distribution  $P_0$ , which is implied by the full-data distribution  $P_0^F$ .

The full-data parameter in the surrogate-index framework is the average treatment effect (ATE) in the experimental study:

$$\beta_0 := f \left\{ E_{P_0^F} (Y(1) | A = 0), E_{P_0^F} (Y(0) | A = 0) \right\},$$

where  $f : \mathbb{R}^2 \rightarrow \mathbb{R}$  is a contrast function such that  $f(x, y) = 0$  if  $x = y$  and  $f(x, y) \neq 0$  otherwise.

## A.2 Identification

We present the identification of  $E_{P_0^F}(Y(z) | A = 0)$  from a mean-imputation perspective because this perspective provides intuition into the surrogate-index method and its relation to missing data methods. A first attempt at mean imputation for the missing  $Y$  in the experimental study could be based on  $E_{P_0}(Y | A = 0, X, Z, S)$ . This regression function is not identified because  $Y$  is missing in the experimental study. The first step in the identification is to assume that  $S$  captures the entire treatment effect, formalized in the surrogacy assumption.

**Assumption A.1** (surrogacy). In each study, assigned treatment is independent of the clinical endpoint conditionally on the baseline covariates and the surrogate:

$$Y \perp Z | A, X, S.$$

By the surrogacy assumption,  $E_{P_0}(Y | A = a, X = x, Z, S = s) = E_{P_0}(Y | A = a, X = x, S = s)$ . The latter function is termed the surrogate index by Athey et al. (2019).

**Definition A.1** (surrogate index). The surrogate index is the conditional expectation of the clinical endpoint given the surrogate outcome and the baseline covariates, conditional on the data source:

$$g_0(a, x, s) := E_{P_0}(Y | A = a, X = x, S = s).$$

This definition of the surrogate index differs from the one given in the main text. The surrogate index as defined above is only identified in the observational study (i.e., for  $a = 1$ ) because  $Y$  is missing in the experimental study. We, therefore, also need to make the comparability assumption.

**Assumption A.2** (comparability of samples). Let  $\phi(x, s) = P(A = 0 | X = x, S = s)$  be the sampling score. The comparability assumption requires that:

1.  $A \perp Y | X, S$
2.  $\phi(x, s) < 1 \forall x \in \mathcal{X}, s \in \mathcal{S}$ .

The comparability assumption allows us to identify the surrogate index in the experimental data with the surrogate index in the observational data. The potential outcome means in the application trial are identified with the observed data by replacing the unobserved  $Y$  with the surrogate index:

$$\begin{aligned} E_{P_0^F}(Y(z) \mid A = 0) &= E_{P_0}(Y \mid A = 0, Z = z) && \text{(simple randomization + consistency)} \\ &= E_{P_0}\{g_0(1, X, S) \mid A = 0, Z = z\} && \text{(surrogacy + comparability)} \end{aligned}$$

### A.3 Estimation

Athey et al. (2019) identify multiple representations of  $E_{P_0^F}(Y(z) \mid A = 0)$  as functionals of the observed-data distribution and derive corresponding estimators. Chen and Ritzwoller (2023) derive double machine learning estimators that are semiparametrically efficient under modest assumptions on the rates of convergence of nuisance parameter estimators. In a more applied context, Gilbert et al. (2024) extend the surrogate-index approach to settings with two-phase sampling of  $S$ , which is common in vaccine trials.

### A.4 Limitations

Athey et al. (2019) and Gilbert et al. (2024) note that the surrogacy and comparability assumptions are very strong. These authors suggest sensitivity analyses to assess the impact of violations of surrogacy and comparability on the inferences. However, without additional assumptions, the bias from violations of comparability and surrogacy is unbounded for continuous  $Y$  (Athey et al., 2019). An informative sensitivity analysis requires one to limit the departures from comparability and surrogacy.

Moving away from sensitivity analyses, one could quantify departures from the identifying assumptions in the following “overall” error:

$$e_0 = \beta_0 - f[E_{P_0}\{g_0(X, S) \mid A = 0, Z = 1\}, E_{P_0}\{g_0(X, S) \mid A = 0, Z = 0\}]. \quad (10)$$

Surrogacy and comparability together imply that  $e_0 = 0$ , and  $e_0 \neq 0$  implies that at least one of these assumptions is violated. This error could be estimated if  $Y$  were to become available in the experimental study, allowing one to assess the accuracy of the surrogate-index based prediction. However,  $e_0 = 0$  does not imply that similar surrogate-index based predictions are possible in other experimental studies.

In the context of multiple clinical trials from the same population of trials, one could estimate the “overall” error for each trial and estimate the distribution of these errors. This distribution would reflect violations from surrogacy and comparability in this population of trials. Something similar has been suggested by Athey et al. (2024, p. 40):

“Building on this application, it would be useful to systematically establish surrogate indices that match the long-term treatment effects estimated in other experiments and quasiexperiments. Over time, this would allow researchers to collectively build a public library of surrogate indices for long-term outcomes that could be used to expedite the analysis of future interventions.”

In the above quote, Athey et al. (2024) essentially propose to evaluate the trial-level surrogacy of surrogate indices, which is the focus of our paper.

## B Canonical Parametric Meta-Analysis

In this appendix, we provide an overview of the canonical parametric MA framework. We describe the standard assumptions for estimating the joint distribution of the trial-level treatment effects on the surrogate and clinical endpoints. Next, we explain how the canonical parametric MA framework can be used to construct prediction intervals for the treatment effects on the clinical endpoint in new trials. Finally, we describe a Bayesian implementation of the canonical parametric MA framework.

### B.1 (Approximate) Observed-Data Likelihood

Since the number of trials in a meta-analysis tends to be small, non-parametric methods may be unstable. In most applications, the distribution of  $(\hat{\alpha}^g, \hat{\beta})'$  is, therefore, modelled parametrically in the frequentist or Bayesian paradigm. While parametric approaches are expected to be more stable, they may be sensitive to model misspecification, and as argued in Section 3.1.1, model misspecification is unavoidable when  $g$  is not fixed a priori. If the parametric model holds approximately, however, the parametric approach may be preferred over the non-parametric approach as the

former may be more stable and efficient, even though it will lead to inconsistent estimators. In what follows, we describe the canonical parametric MA framework. Throughout, we make explicit the assumptions that are made in the derivation of the observed-data likelihood. To avoid obfuscating these assumptions with mathematical details, the following arguments ignore some technical details and focus on the main ideas. We further drop the dependency on  $g$  in the notation for the treatment effects.

Let  $f(\cdot; \boldsymbol{\theta})$  be the density of  $(\alpha, \beta)'$  indexed by the finite-dimensional parameter  $\boldsymbol{\theta} \in \Theta \subset \mathbb{R}^p$  where  $\boldsymbol{\theta}_0$  is the true parameter. In most meta-analyses, a bivariate normal model is assumed for  $(\alpha, \beta)'$ . Hence,  $\boldsymbol{\theta} = (\boldsymbol{\mu}, D)'$  and  $f(\cdot; \boldsymbol{\mu}, D)$  is a bivariate normal density with mean  $\boldsymbol{\mu}$  and covariance  $D$  where  $\boldsymbol{\mu} = (\mu_\alpha, \mu_\beta)$  and

$$D = \begin{pmatrix} d_\alpha^2 & \rho_{\text{trial}} d_\alpha d_\beta \\ \rho_{\text{trial}} d_\alpha d_\beta & d_\beta^2 \end{pmatrix}.$$

If  $(\alpha, \beta)'$  were observed directly, estimation of  $\boldsymbol{\theta}_0$  using (restricted) maximum likelihood would be trivial. However, we only observe corresponding estimates  $(\hat{\alpha}, \hat{\beta})'$ . Hence, we have to derive the observed-data likelihood, which is the likelihood for  $O = (\mathbf{y}, n, \Sigma)$  where  $\mathbf{y} = (\hat{\alpha}, \hat{\beta})'$  and  $\Sigma$  is the true within-trial variance matrix. Indeed, in full generality,  $n$  and  $\Sigma$  are part of the observed data. Note that, for the arguments to work below, we need to assume that the within-trial variance matrix  $\Sigma$  is known; we discuss later how this is dealt with in practice. The observed-data likelihood is given by:

$$\begin{aligned} L(O; \boldsymbol{\theta}) &= f(\mathbf{y} | n, \Sigma) \cdot f(n, \Sigma) \\ &= f(n, \Sigma) \cdot \int f(\mathbf{y} | T, \alpha, \beta, n, \Sigma) \cdot f(T | \alpha, \beta, n, \Sigma) \cdot f(\alpha, \beta | n, \Sigma) d\nu(T, \alpha, \beta) \\ &= f(n, \Sigma) \cdot \int f(\mathbf{y} | T) \cdot f(T | \alpha, \beta, n, \Sigma) \cdot f(\alpha, \beta | n, \Sigma) d\nu(T, \alpha, \beta) \quad (\alpha, \beta, n, \text{ and } \Sigma \text{ are known given } T) \end{aligned}$$

where  $f(\mathbf{y} | T)$  is the density of the sampling distribution of the treatment effect estimators given trial  $T$ , and  $\nu$  is an appropriate dominating measure which we leave unspecified. This observed-data likelihood is too complex to use in practice due to the presence of  $T$ . This is ‘‘solved’’ in almost all meta-analytic methods by assuming that this distribution is also bivariate normal.

**Assumption B.1** (normal sampling distributions). For any given trial  $T \in \mathbb{T}$ , the sampling distribution of the treatment effect estimator is bivariate normal with mean  $(\alpha, \beta)' = (\alpha(P^T), \beta(P^T))'$  and known covariance  $\Sigma/n = \Sigma(T)/n(T)$ :

$$\mathbf{y} | T \sim \mathcal{N}((\alpha, \beta)', n^{-1}\Sigma). \quad (11)$$

Under this assumption, the observed-data likelihood simplifies to:

$$\begin{aligned} L(O; \boldsymbol{\theta}) &= f(n, \Sigma) \cdot \int f(\mathbf{y} | \alpha, \beta, n^{-1}\Sigma) \cdot f(T | \alpha, \beta, n, \Sigma) \cdot f(\alpha, \beta | n, \Sigma) d\nu(T, \alpha, \beta) \\ &= f(n, \Sigma) \cdot \int f(\mathbf{y} | \alpha, \beta, n^{-1}\Sigma) \cdot f(\alpha, \beta | n, \Sigma) d\nu(\alpha, \beta) \quad (\text{integrate out } T). \end{aligned}$$

The above expression is still unwieldy because of the presence of  $f(\alpha, \beta | n, \Sigma)$  in the integral. This is solved by making the additional assumption that the within-trial covariance and sample size are unrelated to the true treatment effects.

**Assumption B.2** (independence of treatment effects and covariance and sample size). The within-trial covariance and sample size are independent of the true treatment effects:

$$(\alpha, \beta)' \perp (n, \Sigma).$$

The observed-data likelihood now simplifies to:

$$L(O; \boldsymbol{\theta}) = f(n, \Sigma) \cdot \int f(\mathbf{y} | \alpha, \beta, n^{-1}\Sigma) \cdot f(\alpha, \beta; \boldsymbol{\theta}) d\nu(\alpha, \beta).$$

The presence of  $f(n, \Sigma)$  in the above expression is a nuisance because we are not interested in the distribution of the within-trial sample size and covariance. This is solved by conditioning inference on the observed  $n$  and  $\Sigma$ ; which leads to the following conditional observed-data likelihood:

$$L(\mathbf{y}; \boldsymbol{\theta}, n^{-1}\Sigma) = \int f(\mathbf{y} | \alpha, \beta, n^{-1}\Sigma) \cdot f(\alpha, \beta; \boldsymbol{\theta}) d\nu(\alpha, \beta). \quad (12)$$

In principle, we could now estimate  $\boldsymbol{\theta}$  by maximizing the above likelihood, whatever the model  $\{f(\cdot; \boldsymbol{\theta}) : \boldsymbol{\theta} \in \Theta\}$  for the distribution of the true treatment effects. As mentioned before, a bivariate normal model is often used here.

**Assumption B.3** (bivariate normality of treatment effects). The true treatment effects  $(\alpha, \beta)'$  are bivariate normal with mean  $\boldsymbol{\mu}$  and covariance  $D$ :

$$(\alpha, \beta)' \sim N(\boldsymbol{\mu}, D).$$

Finally, under this additional normality assumption, the conditional observed-data likelihood simplifies to:

$$L(\mathbf{y}; \boldsymbol{\theta}, n^{-1}\Sigma) = f(\mathbf{y}; \boldsymbol{\mu}, D + n^{-1}\Sigma), \quad (13)$$

where  $f(\cdot; \boldsymbol{\mu}, D + n^{-1}\Sigma)$  is a bivariate normal density with mean  $\boldsymbol{\mu}$  and covariance  $D + n^{-1}\Sigma$ . Estimation of  $\boldsymbol{\theta}$  is now straightforward.

**Remark 6.** In reality,  $\Sigma$  is not observed, but it can be consistently estimated as  $\hat{\Sigma} = \hat{\Sigma}(P_n^T)$ . Therefore, the observed-data likelihood used in practice is the following (Daniels & Hughes, 1997; Gail et al., 2000; Korn et al., 2005; Van Houwelingen et al., 2002):

$$L(\mathbf{y}; \boldsymbol{\theta}, n^{-1}\hat{\Sigma}) = f(\mathbf{y}; \boldsymbol{\mu}, D + n^{-1}\hat{\Sigma}), \quad (14)$$

where  $\Sigma$  is replaced with  $\hat{\Sigma}$ . This has also been termed the approximate likelihood by some authors (Gabriel et al., 2016). This strategy has been implemented in R packages for multivariate meta-analysis such as *mixmeta* (Sera et al., 2019). However, ignoring the estimation error in  $\hat{\Sigma}$  generally leads to inconsistent estimators under the asymptotic regime of Section 2 (where within-trial sample sizes do not increase with the number of independent trials). Furthermore, the sampling distribution of estimators is generally not normal for a fixed sample size, but this is required by assumption B.1.

## B.2 Prediction of $\beta_0$

The two bivariate normality assumptions (on the level of the estimated and true treatment effects) simplify prediction of treatment effects in new trials. For instance, suppose we have conducted a new trial, indicated by  $j = 0$ , where  $S$  was measured but  $Y$  was not. In this trial, we are interested in the treatment effect on  $Y$ , which clearly cannot be estimated directly. Still, we can estimate the treatment effect on  $S$  as  $\hat{\alpha}_0$  where  $\hat{\alpha}_0 \sim N(\alpha_0, \sigma^2)$ , or equivalently,  $\hat{\alpha}_0 - \alpha_0 \sim N(0, \sigma^2)$ . Because the sampling error is independent from  $\alpha_0$  (viewed as random treatment effect), it can be shown that

$$(\hat{\alpha}_0, \beta_0)' \sim N \left\{ \boldsymbol{\mu}, \begin{pmatrix} d_\alpha^2 + \sigma^2 & \rho_{\text{trial}} d_\alpha d_\beta \\ \rho_{\text{trial}} d_\alpha d_\beta & d_\beta^2 \end{pmatrix} \right\}.$$

The conditional distribution  $\beta \mid \hat{\alpha} = \hat{\alpha}_0$ , which can be used for empirical Bayes prediction and inference, follows directly as

$$\beta \mid \hat{\alpha} = \hat{\alpha}_0 \sim N \left( \mu_\beta + \rho_{\text{trial}} \cdot \frac{d_\beta}{\sqrt{d_\alpha^2 + \sigma^2}} \cdot (\hat{\alpha}_0 - \mu_\alpha), d_\beta^2 - \frac{(\rho_{\text{trial}} d_\alpha d_\beta)^2}{d_\alpha^2 + \sigma^2} \right). \quad (15)$$

Above, the prediction for  $\beta_0$  is shrunk towards  $\mu_\beta$ ; the amount of shrinkage depends on  $\sigma^2$  (i.e., the sampling variability of  $\hat{\alpha}$ ). This shrinkage approach to prediction is applied, among others, in Gail et al. (2000) and Korn et al. (2005) and is appropriate if the new trial and the trials in the meta-analysis are sampled independently from the same population of trials (i.e., from  $P_0^F$ ) and the parametric assumptions hold.

**Remark 7.** For a new trial  $j = 0$ , we could consider  $\alpha_0$  as fixed and assume that the conditional distribution of  $\beta_0 \mid \alpha_0$  is the same for the new trial and the trials in the meta-analysis. The shrinkage present in (15) is then not appropriate anymore because  $(\alpha_0, \beta_0)'$  is not sampled from the distribution of  $(\alpha, \beta)$  implied by  $P_0^F$ . Instead, we start from the following conditional distribution with  $\alpha$  known:

$$\beta \mid \alpha = \alpha_0 \sim N \left( \mu_\beta + \rho_{\text{trial}} \cdot \frac{d_\beta}{d_\alpha} \cdot (\alpha_0 - \mu_\alpha), d_\beta^2 (1 - \rho_{\text{trial}}^2) \right). \quad (16)$$

In the above prediction, we can simply replace  $\alpha_0$  with  $\hat{\alpha}_0$ . This prediction is unbiased for a fixed  $\alpha_0$ :

$$\begin{aligned} E(\mu_\beta + \rho_{\text{trial}} \cdot \frac{d_\beta}{d_\alpha} \cdot (\hat{\alpha}_0 - \mu_\alpha) \mid \alpha_0) &= E(\mu_\beta + \rho_{\text{trial}} \cdot \frac{d_\beta}{d_\alpha} \cdot (\hat{\alpha}_0 - \alpha_0 + \alpha_0 - \mu_\alpha) \mid \alpha_0) \\ &= \mu_\beta + \rho_{\text{trial}} \cdot \frac{d_\beta}{d_\alpha} \cdot (\alpha_0 - \mu_\alpha) + \rho_{\text{trial}} \cdot \frac{d_\beta}{d_\alpha} \cdot E(\hat{\alpha}_0 - \alpha_0 \mid \alpha_0) \\ &= E(\beta_0 \mid \alpha_0). \end{aligned}$$

This approach is used throughout Alonso et al. (2016).

**Remark 8.** Ideally, after having evaluated  $S$  as a good surrogate and having estimated  $\alpha_0$  with  $\hat{\alpha}_0$ , one would like to do inference about  $\beta_0$  even if  $Y$  was not observed in this trial. Such inference is possible using a prediction interval for  $\beta_0$ , based on (i) the meta-analysis and (ii)  $\hat{\alpha}_0$ , which covers  $\beta_0$  with  $1 - \alpha$  probability. Such inferences resemble classic frequentist inferences except that the above coverage probability is with respect to repeatedly sampling (i) the new study (where  $\beta_0$  is a random variable) and (ii) the data used for estimating the meta-analytic model parameters. This deviates from classic frequentist inferences which are with respect to repeatedly sampling observations from the same study where  $\beta_0$  is, consequently, fixed.

### B.3 Bayesian Implementation

In the data application and the simulation study, we also considered a Bayesian implementation of the canonical parametric meta-analysis. This approach is in general asymptotically invalid because the parametric assumptions are unlikely to hold for a fixed  $g$ . Moreover, for a data-adaptive  $g$ , these parametric assumptions cannot hold in principle, as explained in Section 3.1.1. Still,  $N$  is very small in most meta-analyses, so non-parametric methods that are asymptotically valid may be unstable and perform poorly, whence asymptotically invalid parametric methods may be preferred in practice. In this section, we describe the Bayesian implementation of the canonical parametric meta-analysis that was used in the data application and the simulation study.

We implemented the Bayesian hierarchical model for bivariate trial-level treatment effects as follows. For  $i = 1, \dots, N$  trials, let  $\mathbf{y}_i = (\hat{\alpha}_i, \hat{\beta}_i)'$  denote the observed estimated treatment effects on the surrogate and clinical endpoints, with known within-trial covariance matrix  $\Sigma_i := \hat{\Sigma}_i$  and sample size  $n_i$ .

$$\begin{aligned} \text{Data model:} & \quad \mathbf{y}_i \mid \boldsymbol{\theta}_i, \Sigma_i, n_i \sim \mathcal{N}(\boldsymbol{\theta}_i, \Sigma_i/n_i) \\ \text{Latent effects:} & \quad \boldsymbol{\theta}_i \mid \boldsymbol{\mu}, D \sim \mathcal{N}(\boldsymbol{\mu}, D) \\ \text{where} & \quad \boldsymbol{\mu} = \begin{pmatrix} \mu_\alpha \\ \mu_\beta \end{pmatrix}, \quad D = \begin{pmatrix} d_\alpha^2 & \rho_{\text{trial}} d_\alpha d_\beta \\ \rho_{\text{trial}} d_\alpha d_\beta & d_\beta^2 \end{pmatrix} \end{aligned}$$

The hyperparameters have the following priors:

$$\begin{aligned} \mu_\alpha, \mu_\beta & \sim \mathcal{N}(0, 2^2) \\ d_\alpha, d_\beta & \sim \mathcal{N}^+(0, 2^2) \quad (\text{truncated to } [0, \infty)) \\ \rho & \sim \text{Uniform}(-1, 1) \end{aligned}$$

In the data application, we also consider the analysis where the regression of  $\beta$  on  $\alpha$  is assumed to go through the origin. This is implemented by setting  $\mu_\beta = \rho_{\text{trial}} \cdot d_\beta / d_\alpha \cdot \mu_\alpha$ .

## C Plug-In Estimator and Efficiency

### C.1 Plug-In Estimator

In the following, we describe the estimating equations for the plug-in estimator as given in (7) of the main text and corresponding finite-sample corrections. We also explain how approximate prediction intervals can be constructed in this setting.

#### C.1.1 Estimating Function

The plug-in estimator for  $\Psi^g(P_0)$ , as given in (7) of the main text, is defined through the estimating function  $\phi_{\boldsymbol{\theta}}^g : \mathbb{N} \times \mathcal{M}_{NP}^* \rightarrow \mathbb{R}^5$ , which is indexed by the parameter vector  $\boldsymbol{\theta} := (\mu_\alpha^g, \mu_\beta^g, d_\alpha^g, d_\beta^g, d_{\alpha,\beta}^g)'$ .

$$\phi_{\boldsymbol{\theta}}^g := \begin{pmatrix} \phi_{\boldsymbol{\theta},1}^g \\ \phi_{\boldsymbol{\theta},2}^g \\ \phi_{\boldsymbol{\theta},3}^g \\ \phi_{\boldsymbol{\theta},4}^g \\ \phi_{\boldsymbol{\theta},5}^g \end{pmatrix} = \begin{pmatrix} \hat{\alpha}^g - \mu_\alpha^g \\ \hat{\beta} - \mu_\beta^g \\ (\hat{\alpha}^g - \mu_\alpha^g)^2 - n^{-1} \hat{\sigma}_{\hat{\alpha}^g} - d_\alpha^g \\ (\hat{\beta} - \mu_\beta^g)^2 - n^{-1} \hat{\sigma}_{\hat{\beta}} - d_\beta^g \\ (\hat{\alpha}^g - \mu_\alpha^g) \cdot (\hat{\beta} - \mu_\beta^g) - n^{-1} \hat{\sigma}_{\hat{\alpha}^g, \hat{\beta}} - d_{\alpha,\beta}^g \end{pmatrix} \quad (17)$$

where

$$\hat{\Sigma}^g =: \begin{pmatrix} \hat{\sigma}_{\hat{\alpha}^g} & \hat{\sigma}_{\hat{\alpha}^g, \hat{\beta}} \\ \hat{\sigma}_{\hat{\alpha}^g, \hat{\beta}} & \hat{\sigma}_{\hat{\beta}} \end{pmatrix}$$

is the estimated within-trial covariance matrix. The expectation of the estimating function  $\Phi^g(\boldsymbol{\theta}) := P_0 \phi_{\boldsymbol{\theta}}^g$  is as follows:

$$\Phi^g(\boldsymbol{\theta}) = \begin{pmatrix} P_0 \hat{\alpha}^g - \mu_{\alpha}^g \\ P_0 \hat{\beta} - \mu_{\beta}^g \\ P_0 (\hat{\alpha}^g - \mu_{\alpha}^g)^2 - P_0 (n^{-1} \hat{\sigma}_{\hat{\alpha}^g}) - d_{\alpha}^g \\ P_0 (\hat{\beta} - \mu_{\beta}^g)^2 - P_0 (n^{-1} \hat{\sigma}_{\hat{\beta}}) - d_{\beta}^g \\ P_0 \{(\hat{\alpha}^g - \mu_{\alpha}^g) \cdot (\hat{\beta} - \mu_{\beta}^g)\} - P_0 (n^{-1} \hat{\sigma}_{\hat{\alpha}^g, \hat{\beta}}) - d_{\alpha, \beta}^g \end{pmatrix}. \quad (18)$$

The partial derivative matrix of  $\Phi^g(\boldsymbol{\theta})$  with respect to  $\boldsymbol{\theta}$  is as follows:

$$\dot{\Phi}^g(\boldsymbol{\theta}) = \begin{pmatrix} -1 & 0 & 0 & 0 & 0 \\ 0 & -1 & 0 & 0 & 0 \\ -2 \cdot (P_0 \hat{\alpha}^g - \mu_{\alpha}^g) & 0 & -1 & 0 & 0 \\ 0 & -2 \cdot (P_0 \hat{\beta} - \mu_{\beta}^g) & 0 & -1 & 0 \\ -1 \cdot (P_0 \hat{\beta} - \mu_{\beta}^g) & -1 \cdot (P_0 \hat{\alpha}^g - \mu_{\alpha}^g) & 0 & 0 & -1 \end{pmatrix}$$

From the above expressions, we can see that  $\dot{\Phi}^g(\boldsymbol{\theta}_0^g)$  for  $\boldsymbol{\theta}_0^g$  such that  $\Phi^g(\boldsymbol{\theta}_0^g) = 0$  is a diagonal matrix with  $-1$  on the diagonal.

### C.1.2 Finite-Sample Corrections

The estimator that solves the estimation equation in (17) uses the biased variance estimator for the variance of  $(\hat{\alpha}^g, \hat{\beta})'$  that divides by  $N$  instead of  $N - 1$ . We can resolve this, and expect better finite-sample performance, by changing the estimating functions for the covariance parameters as follows:

$$\begin{pmatrix} \phi_{\boldsymbol{\theta},3}^g \\ \phi_{\boldsymbol{\theta},4}^g \\ \phi_{\boldsymbol{\theta},5}^g \end{pmatrix} = \begin{pmatrix} \frac{N}{N-1} (\hat{\alpha}^g - \mu_{\alpha}^g)^2 - \hat{\sigma}_{\hat{\alpha}^g} - d_{\alpha} \\ \frac{N}{N-1} (\hat{\beta} - \mu_{\beta}^g)^2 - \hat{\sigma}_{\hat{\beta}} - d_{\beta} \\ \frac{N}{N-1} (\hat{\alpha}^g - \mu_{\alpha}^g) \cdot (\hat{\beta} - \mu_{\beta}^g) - \hat{\sigma}_{\hat{\alpha}^g, \hat{\beta}} - d_{\alpha, \beta} \end{pmatrix} \quad (19)$$

A finite-sample adjusted sandwich estimator is as follows:

$$\left( P_N \dot{\phi}_{\boldsymbol{\theta}_0^{gN}}^{gN} \right)^{-1} \cdot \frac{N}{N-1} P_N \left( \phi_{\boldsymbol{\theta}_0^{gN}}^{gN} \right)^{\otimes 2} \cdot \left( P_N \dot{\phi}_{\boldsymbol{\theta}_0^{gN}}^{gN} \right)^{-1}. \quad (20)$$

Both corrections described above are used in the data application and the simulation study.

### C.1.3 Approximate Prediction Intervals

The parameters described before are appealing because they are well defined in a non-parametric model; however, they are not immediately useful for prediction in new trials where the clinical endpoint is not observed. Given the low number of independent trials in practice, strong parametric assumptions are needed for predictions with corresponding prediction intervals. Although such parametric assumptions are in principle testable, such tests have very low power because  $N$  is small. At the same time, some parametric assumptions could be argued, from a substantive perspective, to hold approximately (although never exactly). We take this idea further next, realizing that ensuing prediction intervals are really only approximations of the uncertainty as the parametric assumptions on which they rely only hold approximately at best. Hence, they are not guaranteed to have nominal coverage, even as  $N \rightarrow \infty$ .

Under the surrogacy and comparability assumptions, treatment effects on the surrogate index  $g_0$  equal treatment effects on the clinical endpoint:  $\beta(T) = \alpha^{g_0}(T)$  for all  $T \in \mathbb{T}$ . In practice, surrogacy and comparability only hold approximately at best and the surrogate index is only estimated. We, therefore, introduce an error term  $\epsilon$  so that, given the estimated surrogate index  $g_N$ ,  $\beta = \alpha^{g_N} + \epsilon$  where  $E(\epsilon \mid \alpha^{g_N}) \approx 0$ . To compute prediction intervals, we need to make parametric assumptions about this error term. We further assume that  $\epsilon \sim N(0, \sigma_{g_N}^2)$ , which can only hold approximately in reality. Let  $\hat{\alpha}_0^g$  be the estimated treatment effect in a new trial—where subscript 0 indicates the new trial—with estimated standard error  $\hat{\sigma}_{\hat{\alpha}^{gN}, 0}$ . If we additionally assume that  $\hat{\alpha}_0^{gN} - \alpha_0^{gN} \sim N(0, \sigma_{\hat{\alpha}^{gN}, 0}^2/n_0)$ , we have the following:

$$\begin{aligned} \beta_0 - \hat{\alpha}_0^{gN} &= (\beta_0 - \alpha_0^{gN}) + (\alpha_0^{gN} - \hat{\alpha}_0^{gN}) \\ &= \epsilon_0 - (\alpha_0^{gN} - \hat{\alpha}_0^{gN}) \sim N(0, \sigma_{g_N}^2 + \sigma_{\hat{\alpha}^{gN}, 0}^2/n_0) \end{aligned}$$

because  $\epsilon_0$  and  $\alpha_0^{gN} - \hat{\alpha}_0^{gN}$  are independent by design. An approximate  $1 - \alpha$  prediction interval for the corresponding  $\beta_0$  is then as follows:

$$\hat{\alpha}_0^{gN} \pm z_{1-\alpha/2} \cdot \sqrt{\hat{\sigma}_{\hat{\alpha}^{gN}, 0}^2/n_0 + \hat{\sigma}_{gN}^2},$$

where  $z_{1-\alpha/2}$  is the  $1 - \alpha/2$  percentile of the standard normal distribution and  $\hat{\sigma}_{gN}^2$  is an estimate of  $\sigma_{gN}^2$ .

**Remark 9** (estimation of  $\sigma_{gN}^2$ ). In the above setup, the full-data parameter  $\sigma_{gN}^2$  is defined as  $\sigma_{gN}^2 := E_{P^F} \{(\beta - \alpha^{gN})^2\}$ . Under assumptions 3.3 and 3.4,  $\sigma_{gN}^2$  is identified with the observed-data distribution as follows:

$$\sigma_{gN}^2 = E_P \left\{ (\hat{\beta} - \hat{\alpha}^{gN})^2 \right\} - E_P \left\{ \hat{\sigma}_{\hat{\beta}}^2/n + \hat{\sigma}_{\hat{\alpha}^{gN}}^2/n - 2\hat{\sigma}_{\hat{\alpha}^{gN}, \hat{\beta}}/n \right\},$$

where  $\hat{\sigma}_{\hat{\beta}}^2$ ,  $\hat{\sigma}_{\hat{\alpha}^{gN}}^2$  and  $\hat{\sigma}_{\hat{\alpha}^{gN}, \hat{\beta}}$  are the corresponding entries of  $\hat{\Sigma}^{gN}$ . We can estimate  $\sigma_{gN}^2$  by replacing  $P$  with  $P_N$  in the above expression.

## C.2 Semi-Parametric Efficiency Analysis

### C.2.1 Results for General Multivariate Meta-Analysis

The following analysis is more general than the bivariate meta-analysis setting considered in the main text. It applies to any multivariate meta-analysis where the estimated treatment effects are denoted by  $\hat{X} \in \mathbb{R}^k$  and the estimated variance matrices are denoted by  $\hat{\Sigma} \in \mathbb{R}^{k \times k}$ , where  $k$  is the number of treatment effects. Note that this variance matrix is an estimate of the variance of the treatment effect estimator in a given trial, without root- $n$  standardization (in contrast to the presentation in the main text). We further ignore within-trial sample sizes because treating them as part of the observed data does not change the following results.

We first present a more specific lemma that is relevant for the canonical meta-analysis approach where it is assumed that  $\hat{\Sigma} = \Sigma$  and that  $\hat{X} | X, \Sigma \sim \mathcal{N}(X, \Sigma)$  where  $X$  is the vector of true treatment effects. Even though these are strong (identifying) assumptions, the implied observed-data model is already locally non-parametric if we don't make assumptions about the distribution of  $(X, \Sigma)$ . Note that these results, and the corresponding proofs, closely follow the arguments in van der Vaart (1998, Example 25.35) and Chen et al. (2025, Appendix B).

**Lemma C.1.** Let  $Y = (\hat{X}, \hat{\Sigma}, X, \Sigma)$  be a full-data vector distributed according to  $P^F \in \mathcal{M}^F$  where  $\mathcal{M}^F$  satisfies the following assumptions:

$$\hat{X} | X, \Sigma \sim \mathcal{N}(X, \Sigma) \quad \text{and} \quad \hat{\Sigma} = \Sigma \quad P^F\text{-a.s.}$$

and  $(\hat{X}, \hat{\Sigma})$  are observed. No further assumptions are made on  $\mathcal{M}^F$ . If the true full-data distribution  $P_0^F \in \mathcal{M}^F$  is such that the distribution of  $X | \Sigma$  contains an interval  $P_0^F$ -a.s. and  $\Sigma$  is positive definite  $P_0^F$ -a.s., then the observed-data model  $\mathcal{M} := \{P : P = h(P^F) \text{ for some } P^F \in \mathcal{M}^F\}$ , where  $h(P^F)$  is the observed-data distribution implied by  $P^F$ , is locally non-parametric at  $P_0 = h(P_0^F)$ .

The conditions in Lemma C.1 are not satisfied in practice and, moreover, we do not assume these conditions in the main text. The following corollary corresponds to the conditions that we do assume in the main text (i.e., Assumptions 3.3 and 3.4).

**Corollary 1.** Under the same conditions as in Lemma C.1, but now only requiring that

$$E(\hat{X} | X, \Sigma) = X \quad \text{and} \quad \text{Var}(\hat{X} | X, \Sigma) = \Sigma \quad P_0^F\text{-a.s.},$$

and

$$E(\hat{\Sigma} | X, \Sigma) = \Sigma \quad P_0^F\text{-a.s.}$$

the observed-data model  $\mathcal{M} := \{P : P = h(P^F) \text{ for some } P^F \in \mathcal{M}^F\}$  is locally non-parametric at  $P_0$ .

### C.2.2 Implications

We stated in Remark 2 that, because the observed-data model  $\mathcal{M}$  is locally non-parametric at  $P_0$ , there is only one regular asymptotically linear estimator. Hence, the plug-in estimator is efficient. This is counterintuitive for two reasons:

1. In finite samples, the plug-in estimator may return estimated variance matrices that are not positive semi-definite. Hence, in finite samples, the plug-in estimator may be improved by truncating estimated variance matrices to be positive semi-definite by finding the closest positive semi-definite matrix to the estimated matrix. This is a well-known problem in the literature and can be solved using the `nearPD` function in R. However, the plug-in estimator will return positive semi-definite estimates with probability tending to one as  $N \rightarrow \infty$ .

2. It seems that the plug-in estimator could be improved by weighting trials by, for example, the within-trial sample size or the inverse of  $\hat{\Sigma}^g/n$ . This is not the case, however, because this would only be valid under the additional assumption that within-trial samples sizes and  $\hat{\Sigma}^g/n$  are unrelated to the treatment effects. If we would assume this, the observed-data model  $\mathcal{M}$  would no longer be locally non-parametric and, indeed, there would generally exist multiple regular asymptotically linear estimators. The plug-in estimator would be one of them, but not necessarily the most efficient one.

## D Conditions of Theorem 2

In the first part of this appendix, we discuss the conditions of Theorem 2 in more detail without reference to the MA framework. In the second part, we discuss a set of conditions, specific to the MA framework, that is sufficient for the conditions of Theorem 2. In the third part, we discuss how some of these conditions are related to overfitting of the surrogate index estimator and how this can be mitigated in practice.

### D.1 General Discussion

We discuss the conditions of Theorem 2 in more detail next.

Condition (i) is a standard identifiability condition for Z-estimators.

Condition (ii) requires that the class of estimating functions  $\{\phi_{\theta}^g : g \in \mathcal{G}, \theta \in \Theta\}$  is not too complex, which is satisfied if the class  $\mathcal{G}$  is not too large. For example, if  $\mathcal{G}$  is a class of real-valued functions, this condition may be satisfied if  $\mathcal{G}$  itself is Glivenko–Cantelli and  $\phi_{\theta}^g$  is smooth in  $g$  and  $\theta$ . Condition (iii) requires that the class of estimating functions  $\{\phi_{\theta}^g : g \in \mathcal{G}, \|\theta - \theta_0^g\|_2 < \delta\}$  is not too complex—as for condition (ii), this is satisfied if the class  $\mathcal{G}$  is not too large. The second part of Condition (iii) requires that  $(\theta, g) \mapsto \phi_{\theta}^g$  is sufficiently smooth.

The first part of Condition (iv) is a standard regularity condition for Z-estimators. The second part again imposes a smoothness condition on the estimating function. Condition (v) asks that both the empirical and bootstrap estimators solve their respective estimating equations up to  $o_P(N^{-1/2})$ . This allows for some numerical error in solving the estimating equations and is a standard condition for Z-estimators.

Condition (vi) is a new condition that is specific to the data-adaptive setting. It requires that the expectation of the estimating function,  $\Phi^g(\theta)$ , is sufficiently smooth in  $g$ . Essentially, small changes in  $g$  should not cause large changes in  $\Phi^g(\theta)$ , regardless of the value of  $\theta$ . This condition is required for showing that (i)  $\theta_0^g$  is a continuous function of  $g$  and that (ii)  $\hat{\theta}_N^{g_N}$  is consistent for  $\theta_0^{g^*}$ . These two intermediate results are used in the proof of Theorem 2. Intuitively, if condition (vi) is not satisfied, a small change in  $g$  could lead to a large change in the estimating function, which would make it difficult to establish the continuity of  $g \mapsto \theta_0^g$  and the consistency of  $\hat{\theta}_N^{g_N}$ .

### D.2 Plug-in Estimator for Data-Adaptive Target Parameter in MA Framework

We next propose a set of conditions specialized to the MA setting which are sufficient for the conditions in Theorem 2. The relation between the notation in Theorem 2 and the notation in Section 3 was discussed in Remark 5 of the main text.

The first condition requires that the estimated surrogate index  $g_N$  converges to a fixed function in the supremum norm.

- (a) There exists a  $g^* \in \mathcal{G}$  such that  $\|g_N - g^*\|_{\infty} \xrightarrow{P} 0$  and  $g_N \in \mathcal{G}$  with probability tending to one.

This is a very weak condition that should be satisfied for practically any algorithm that returns  $g_N$  based on the observed data. However, it has important implications (related to overfitting and positivity violations) for finite samples as discussed in Appendix D.3. This condition does not require that  $g_N$  converges at a certain rate, which would be a strong condition for the supremum norm. Also note that the supremum norm cannot easily be replaced by other norms because some of the next conditions are not plausible for other norms like the  $L_2(P)$  norm.

The second condition is a regularity condition on the set of parameters:

- (b)  $\theta$  can be restricted to a bounded open set  $\Theta$ .

The third and fourth conditions restrict the complexity of the trial-specific treatment effect estimators and the estimator for  $g_N$ :  $\hat{\alpha}^g$  should be smooth in  $g$  and  $\mathcal{G}$  should not be too complex.

- (c) The following classes of real- or matrix-valued functions on  $\mathbb{N} \times \mathcal{M}_{NP}^*$  are bounded  $P_0$ -Donsker classes:  $\{\hat{\alpha}^g : g \in \mathcal{G}\}$ ,  $\{\hat{\beta} : g \in \mathcal{G}\}$ , and  $\{\hat{\Sigma}^g : g \in \mathcal{G}\}$ . This is understood to hold element wise for the latter class.
- (d) Consider  $g \mapsto \hat{\alpha}^g(n, P_n^T)$  and  $g \mapsto \hat{\Sigma}^g(n, P_n^T)$  as random real- and matrix-valued functions on  $\mathcal{G}$  indexed by  $(n, P_n^T)$ . These functions are  $P_0$ -a.e. continuous at  $g^*$  with respect to the metric induced by the supremum norm.

Conditions (c–d) can be shown using many strategies. In the following remark, we outline one such strategy that (practically) does not restrict the class of estimators for the trial-specific treatment effects.

**Remark 10.** By van der Vaart (1998, Theorem 19.5),  $\hat{\alpha}^{\mathcal{G}} := \{\hat{\alpha}^g : g \in \mathcal{G}\}$  is a  $P_0$ -Donsker class if

$$\int_0^1 \sqrt{\log N_{[]}(\epsilon, \hat{\alpha}^{\mathcal{G}}, L_2(P_0))} d\epsilon < \infty.$$

where  $N_{[]}$  is the bracketing number. If we additionally assume that<sup>14</sup> for all  $g_1, g_2 \in \mathcal{G}$ ,

$$|\hat{\alpha}^{g_1}(n, P_n^T) - \hat{\alpha}^{g_2}(n, P_n^T)| \leq F(n, P_n^T) \cdot \|g_1 - g_2\|_{\infty} \quad (21)$$

where  $P_0 F^2 < \infty$ , then Kosorok (2008, Theorem 9.23) shows that

$$N_{[]} (2\epsilon \|F\|_{2, P_0}, \hat{\alpha}^{\mathcal{G}}, L_2(P_0)) \leq N(\epsilon, \mathcal{G}, \|\cdot\|_{\infty})$$

where  $N$  is the covering number and  $\|F\|_{2, P_0} = (P_0 F^2)^{1/2}$ . This implies that  $\hat{\alpha}^{\mathcal{G}}$  is a  $P_0$ -Donsker class if

$$\int_0^1 \sqrt{\log N(\epsilon, \mathcal{G}, \|\cdot\|_{\infty})} d\epsilon < \infty,$$

which holds, for instance, for a parametric class of functions indexed by a bounded subset of  $\mathbb{R}^d$  (by van der Vaart (1998, Example 19.7) combined with Kosorok (2008, Lemma 9.18)). Note that (21) also implies condition (d).

Remark 10 shows that parametric estimators for  $g_N$  may be used in combination with practically any within-trial estimator  $\hat{\alpha}^g$ . However, if we impose mild smoothness conditions on the estimator  $(n, P_n^T) \mapsto \hat{\alpha}^g(n, P_n^T)$ , we have that  $\{\hat{\alpha}^g : g \in \mathcal{G}\}$  is a  $P_0$ -Donsker class whenever  $\mathcal{G}$  is a Donsker class for a certain set of measures, which allows one to use many machine learning methods to estimate  $g_N$ . This is made precise in the following lemma.

**Lemma D.1.** Let  $(n, P_n^T) \mapsto a_i(n, P_n^T) \in \mathcal{X} \times \mathcal{Z} \times \mathcal{S} \times \mathcal{Y}$  be a mapping that extracts the  $i$ 'th observation from the observed data for a given trial, where  $a_i(n, P_n^T) = 0$  for  $i > n$ . Define  $z_i(n, P_n^T)$  and  $x_i(n, P_n^T)$  similarly as  $a_i(n, P_n^T)$  as mappings that extract the assigned treatment and the observed covariate, respectively, from the  $i$ 'th observation, also setting them to 0 for  $i > n$ . Assume the following conditions hold:

1. The within-trial sample sizes are bounded above by  $n^* < \infty$ .
2.  $\mathcal{X}$  is a bounded subset of  $\mathbb{R}^d$  for some  $d < \infty$ .
3.  $P_0 |\hat{\alpha}^g|^2 < \infty$  for some  $g \in \mathcal{G}$ .
4.  $\hat{\alpha}^g$  depends on  $(n, P_n^T)$  only through  $\{(x_1, z_1, g \circ a_1)(n, P_n^T), \dots, (x_n, z_n, g \circ a_n)(n, P_n^T)\}$ . Moreover, if we shift  $g \circ a_i(n, P_n^T)$  by  $\Delta$  for some  $i \in \{1, \dots, n^*\}$ , then the estimate changes by less than  $c|\Delta|$  for some constant  $c < \infty$ .
5.  $\mathcal{G}$ , as a uniformly bounded set of real-valued functions on  $\mathcal{X} \times \mathcal{Z} \times \mathcal{S} \times \mathcal{Y}$  is  $P_{a_i, 0}$ -Donsker for all  $i = 1, \dots, n^*$  for the pushforward measure  $P_{a_i, 0} := P_0 \circ a_i^{-1}$ .

We then have that  $\{\hat{\alpha}^g : g \in \mathcal{G}\}$  is a  $P_0$ -Donsker class.

Conditions (e) and (f) are again smoothness conditions on  $g \mapsto \hat{\alpha}^g(n, P_n^T)$  and  $g \mapsto \hat{\Sigma}^g(n, P_n^T)$  as functions of  $g$  indexed by  $(n, P_n^T)$ .

<sup>14</sup>This holds for any reasonable estimator. Let  $d := \|g_1 - g_2\|_{\infty}$ . Then the maximum difference between the transformed surrogate, using  $g_1$  or  $g_2$ , for data points with non-zero probability under  $P_n^T$  is  $d$ . Most reasonable estimators will satisfy the following: shifting the observed outcomes with at most  $d$  will not change the estimated treatment effect by more than  $d$ . These estimators satisfy the stated condition. Note, however, that this may fail for estimators of ratios (e.g., estimator for the relative risk) if the denominator is close to zero.

- (e) Consider  $\hat{\alpha}^g$  as a random variable indexed by  $g$ , we require that the functions  $P_0\hat{\alpha}^g, P_0(\hat{\alpha}^g)^2, P_0\hat{\alpha}^g\hat{\beta} : \mathcal{G} \rightarrow \mathbb{R}$  are Lipschitz continuous:  $|P_0\hat{\alpha}^g - P_0\hat{\alpha}^{g'}| \leq M \cdot \|g - g'\|_\infty$  for some  $M < \infty$  and for all  $g, g' \in \mathcal{G}$  (and similarly for  $P_0(\hat{\alpha}^g)^2$  and  $P_0\hat{\alpha}^g\hat{\beta}$ ).
- (f) Consider  $\hat{\Sigma}^g$  as a random matrix indexed by  $g$ , we require that the function  $P_0\hat{\Sigma}^g : \mathcal{G} \rightarrow \mathbb{R}^{2 \times 2}$  is element-wise Lipschitz continuous in the same sense as in condition (e).

These are minor regularity conditions that follow from the same reasoning as in the footnote of Remark 10.

The following lemma summarizes the above discussion. As for all other lemmas and theorems, this is proved in Appendix F.

**Lemma D.2.** For the setup described in Sections 2 and 3, Conditions (a–f) listed in Appendix D.2 are sufficient for the conditions of Theorem 2.

### D.3 Overfitting of the Surrogate Index Estimator

Condition (a) requires that  $\|g_N - g^*\|_\infty \xrightarrow{P} 0$  as  $N \rightarrow \infty$ . Although this is a weak requirement asymptotically, it has important finite-sample implications. The next paragraphs illustrate how this condition can fail, how this is relevant in finite samples, and how this can be resolved by using SuperLearner with a modified cross-validation procedure (van der Laan et al., 2007).

If a surrogate index estimator includes a trial indicator in  $X$ , the estimated surrogate index, evaluated in  $(x, s)$ -values occurring in any observed trial  $t$ , will be close to  $E[Y | X = x, S = s, T = t]$  if the estimator is sufficiently flexible and the within-trial sample sizes are sufficiently large. In this case,  $g_N$  will not converge to some fixed  $g^*$  if the comparability assumption is violated. If we now assume surrogacy without comparability, the mean of  $g_N(X, S)$  in trial  $t$  under treatment  $z$  is approximately equal to the mean of  $Y$  in trial  $t$  under treatment  $z$ :

$$\begin{aligned} E(g_N(X, S) | Z = z, T = t) &\approx E\{E(Y | X, S, T = t) | Z = z, T = t\} \\ &= E\{E(Y | X, Z = z, S, T = t) | Z = z, T = t\} \quad (\text{surrogacy}) \\ &= E(Y | Z = z, T = t) \quad (\text{iterated expectations}) \end{aligned}$$

Hence, the treatment effects on  $g_N(X, S)$  and  $Y$  will be close in all observed trials, even if the comparability assumption is severely violated. The surrogate index will then appear to be a perfect trial-level surrogate, yet it will fail for unobserved trials. This shows that adjusting for trial indicators is problematic. This seems like a trivial point; however, the same type of overfitting can occur when there is limited overlap of  $(X, S)$  across trials. (This corresponds to a violation of the so-called positivity or overlap assumption in the transportability and data-fusion literature (Degtiar & Rose, 2023; Li & Luedtke, 2023).) Especially worrisome is the fact that, in such cases, even parametric models can overfit, especially if the number of trials is small. For instance, if  $S$  is a categorical variable where one category is almost exclusively observed in one trial, a parametric model may be overfitting to that trial.

The trial-level type of overfitting can be avoided by using SuperLearner in combination with a modified cross-validation scheme (van der Laan et al., 2007). Specifically, the SuperLearner should use a leave-one-trial-out cross-validation scheme and should include at least one very simple learner that cannot overfit at a trial level. If certain  $(X, S)$  regions occur only in one trial, flexible learners may extrapolate poorly, while simpler learners typically extrapolate more robustly. Thus, the trained SuperLearner will place more weight on simple learners if there is little overlap in  $(X, S)$  across trials. If there is sufficient overlap, the SuperLearner will place more weight on flexible learners if the underlying regression function is more complex.

## E Alternative Asymptotic Regime

### E.1 Setting and Notation

In the data-generating mechanism introduced in Section 2, we assumed that the within-trial sample size  $n$  was a random variable whose distribution does not depend on the number of independent trials  $N$ . Consequently, the full- and observed-data distributions,  $P_0^F$  and  $P_0$ , were unknown but fixed distributions—fixed in the sense that they do not change with  $N$ . We now deviate from this setting and let  $P_{0,n} \in \mathcal{M}$  be the observed-data distribution where all within-trial sample sizes are set to  $n$  and  $\mathcal{M}$  is a model for the distribution of the trial-level observations:  $P_n^T \in \mathcal{M}_{NP}^*$ . As in Section 2, the observed-data distribution is determined by the full-data distribution as represented by the mapping

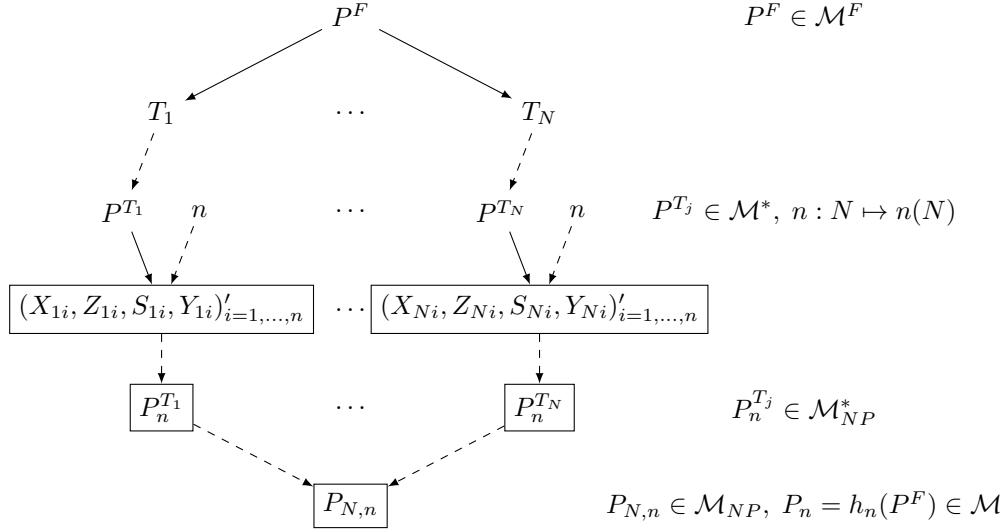


Figure 6: Data-generating mechanism underlying the meta-analytic framework where the within-trial samples size,  $n$ , increases with the total number of independent trials,  $N$ . Dashed arrows represent mappings. Full arrows represent sampling. Objects surrounded by a rectangle represent the observed data.  $\mathcal{M}^F$ : full-data model;  $\mathcal{M}^*$ : within-trial model;  $\mathcal{M}_{NP}^*$ : non-parametric within-trial model;  $\mathcal{M}_{NP}$ : non-parametric observed-data model;  $\mathcal{M}$ : observed-data model.

$h_n : \mathcal{M}^F \rightarrow \mathcal{M}$ . In contrast to the setting in Section 2, this mapping is now indexed by  $n$ . Note that  $P_0^F$  and  $\mathcal{M}^F$  remain unchanged as the distribution of trials does not depend on  $n$ , but the way the observed data for a given trial are generated does. This is visualized in Figure 6, which replaces Figure 1 from the main text.

For a fixed  $n$ , the new data-generating mechanism is a special case of the previous setting where the distribution of  $n$  is degenerate. Hence, under identifying assumptions 3.3 and 3.4, all methods presented in the main text are valid for this new setting (i.e., with  $P_0$  replaced with  $P_{0,n}$  and  $n$  fixed). However, in reality, the identifying assumptions 3.3 and 3.4 will not be satisfied exactly for a fixed  $n$ . Nonetheless, we expect these assumptions to be satisfied approximately, and more specifically, we expect this “approximation error” to decrease with increasing  $n$ . We, therefore, now consider the setting where the within-trial sample size  $n$  is a function of the number of independent trials  $N$  (i.e.,  $n = n(N)$ ) such that  $n(N) \rightarrow \infty$  as  $N \rightarrow \infty$ , as also visualized in Figure 6. In most of the notations, we leave the dependence of the within-trial sample size  $n$  on the number of independent trials  $N$  implicit. So, when we’re using  $n$ , we mean  $n(N)$ .

In the following arguments, we first consider a fixed  $g$  and denote the trial-level treatment-effect estimates by a tilde to emphasize that they do not satisfy the identifying assumptions:  $(\tilde{\alpha}^g, \tilde{\beta})'$  and  $\tilde{\Sigma}^g$ . We then consider finite-sample unbiased counterparts, denoted by  $(\hat{\alpha}^g, \hat{\beta})'$  and  $\hat{\Sigma}^g$ , which satisfy the identifying assumptions; the latter will be obtained by debiasing the former. We will consider the “augmented” data as  $(\tilde{\alpha}^g, \tilde{\beta}, \tilde{\Sigma}^g, \hat{\alpha}^g, \hat{\beta}, \hat{\Sigma}^g)$  whose distribution is implied by  $P_0^F$  and  $n$  (but only the first part is observable). We further let the empirical distribution of  $(\tilde{\alpha}^g, \tilde{\beta}, \tilde{\Sigma}^g)$  be denoted by  $\tilde{P}_{N,n}$  and the empirical distribution of  $(\hat{\alpha}^g, \hat{\beta}, \hat{\Sigma}^g)$  be denoted by  $\hat{P}_{N,n}$ . Note that the latter distribution is actually not observed. Our goal in this section is to study when  $\hat{\Psi}^g(\tilde{P}_{N,n})$  is asymptotically equivalent to  $\hat{\Psi}^g(\hat{P}_{N,n})$ . If these two estimators are asymptotically equivalent, then we can ignore the fact that the trial-specific estimates only satisfy the identifying assumptions approximately. In the remainder of this section, we formalize this goal further and derive sufficient conditions for this asymptotic equivalence to hold. We also discuss when these conditions are theoretically non-trivial and how they may be practically relevant.

## E.2 Alternative Assumptions

We relax Assumptions 3.3 and 3.4 in Assumptions E.1 and E.2, respectively. The latter assumptions allow for a finite-sample bias that converges to zero as  $n \rightarrow \infty$ .

**Assumption E.1** (vanishing bias for trial-level treatment effect estimators). Let  $\mathcal{G}$  be a set of real-valued functions on  $\mathcal{S} \times \mathcal{X}$  and define the trial-level bias  $b_n^g$  as follows for  $P^T \in \mathcal{M}^*$ :

$$b_n^g := n^{1/2} E_{P^T, n} \left\{ (\tilde{\alpha}^g, \tilde{\beta})' \right\} - \left\{ \alpha^g(P^T), \beta(P^T) \right\}'$$

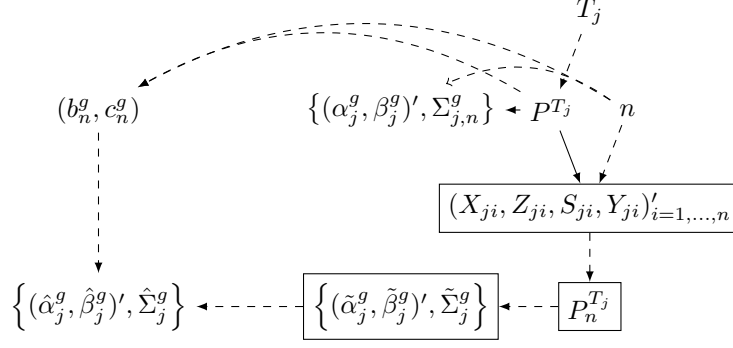


Figure 7: True, estimated and debiased treatment effects as functionals of the true and empirical within-trial distributions, respectively. Some objects are indexed by  $n$  while others are not, this is on purpose as further explained in Section E.2: The true treatment effects are not indexed by  $n$  because they are fixed functionals of the true within-trial distribution, the true within-trial covariance matrix  $\Sigma_{j,n}^g$  is indexed by  $n$  because the root- $n$  standardized variance of the estimators may change with  $n$ . The estimated treatment effects and within-trial covariance matrix are not indexed by  $n$  because they are fixed functionals of the empirical within-trial distribution. The debiased estimators,  $(\hat{\alpha}_{j,n}^g, \hat{\beta}_{j,n}^g)'$  and  $\hat{\Sigma}_{j,n}^g$  are indexed by  $n$  because the bias terms  $b_n^g$  and  $c_n^g$  depend on  $n$ . Dashed arrows represent deterministic mappings. Full arrows represent sampling. Objects surrounded by a rectangle represent the observed data.

where  $E_{P^{T,n}}$  is the expectation over the empirical distributions  $P_n^T$  generated by sampling  $n$  i.i.d. observations from  $P^T$ . We then require that  $P_0^F \|b_n^g\|_2^2 = O(n^{-\delta_1})$  and  $P_0^F \|b_n^g\|_2^4 < K < \infty$  for  $n \geq n_0 \in \mathbb{N}$  for all  $g \in \mathcal{G}$ , where  $\delta_1 > 0$ ,  $n_0$ , and  $K$  are constants.

The trial-level bias  $b_n^g$  defined above is a random variable (indexed by  $g$  and  $n$ ) whose distribution is implied by  $P_0^F$  since it is a real-valued function (i) of the random element  $P^T$  (whose distribution also depends on  $P_0^F$ ) and (ii) of  $n$ . If we could observe  $b_n^g$ , we could simply subtract it from the finite-sample biased estimators  $(\tilde{\alpha}^g, \tilde{\beta})'$  to obtain finite-sample unbiased estimators  $(\hat{\alpha}_n^g, \hat{\beta}_n)'$ :

$$(\hat{\alpha}_n^g, \hat{\beta}_n)' := (\tilde{\alpha}^g, \tilde{\beta})' - n^{-1/2} b_n^g. \quad (22)$$

These debiased estimators are asymptotically equivalent to the original estimators because

$$n^{1/2} \left\{ (\tilde{\alpha}^g, \tilde{\beta})' - (\hat{\alpha}_n^g, \hat{\beta}_n)' \right\} = b_n^g = o_{P_0^F}(1)$$

where the second equality follows from  $P_0^F \|b_n^g\|_2^2 = O(n^{-\delta_1})$ . Note that the debiased estimators are indexed by  $n$  to emphasize that the root- $n$  standardized bias of estimators may change with  $n$ <sup>15</sup>.

The debiased estimators are needed in the following assumption.

**Assumption E.2** (vanishing bias for within-trial variance estimators). Let  $\mathcal{G}$  be a set of real-valued functions on  $\mathcal{S} \times \mathcal{X}$ . For  $g \in \mathcal{G}$ , let  $\Sigma_n^g : P^T \mapsto n \cdot \text{Var}_{P^{T,n}} \left\{ (\hat{\alpha}_n^g, \hat{\beta}_n)' \right\}$  be the within-trial variance<sup>16</sup> for within-trial distribution  $P^T$  and sample size  $n$ . Further let  $\tilde{\Sigma}^g : P_n^T \mapsto \tilde{\Sigma}(P_n^T)$  be the within-trial variance estimator. Define the trial-level bias matrix  $c_n^g$  as follows for  $P^T \in \mathcal{M}^*$ :

$$c_n^g := E_{P^{T,n}} \left( \tilde{\Sigma}^g \right) - \Sigma_n^g(P^T)$$

where  $E_{P^{T,n}}$  is the expectation over the empirical distributions  $P_n^T$  generated by sampling  $n$  i.i.d. observations from  $P^T$ . Let  $\|\cdot\|_F$  be the Frobenius norm. We then require that  $P_0^F \|c_n^g\|_F = O(n^{-\delta_2})$  and  $P_0^F \|c_n^g\|_F^2 < K < \infty$  for  $n \geq n_0 \in \mathbb{N}$  for all  $g \in \mathcal{G}$ , where  $\delta_2 > 0$ ,  $n_0$ , and  $K$  are constants.

<sup>15</sup>In principle, we could also explicitly index  $(\tilde{\alpha}, \tilde{\beta})'$  by  $n$  because, viewing these as functionals of the trial-level observations, we defined these in Section 2.2.2 to depend on both the within-trial empirical distribution and the within-trial sample size. To be consistent with notation in the main text, we leave this indexing implicit.

<sup>16</sup>This is the sampling variance of the root- $n$  standardized **debiased** estimators. Note also that this variance matrix is indexed by  $n$ , allowing for the fact that the root- $n$  standardized variance of estimators may change with  $n$ .

Like we debiased the treatment effect estimators in (22), we can also debias the within-trial variance estimators by subtracting the bias  $c_n^g$  from the finite-sample biased  $\tilde{\Sigma}^g$ :

$$\hat{\Sigma}_n^g := \tilde{\Sigma}^g - c_n^g. \quad (23)$$

By construction,  $\hat{\Sigma}_n^g$  is an unbiased estimator for the root- $n$  standardized variance of  $(\hat{\alpha}_n^g, \hat{\beta}_n^g)'$  in a given trial. Hence, Assumptions 3.3 and 3.4 are satisfied for the debiased estimators. Consequently, for a fixed  $n$ , everything from the Sections 3 and 4 applies to the estimator  $\hat{\Psi}^g(\hat{P}_{N,n})$ , defined in (7), that uses the debiased estimates. In these sections, we had derived the asymptotic distribution of

$$N^{1/2} \left( \hat{\Psi}^g(\hat{P}_{N,n}) - \Psi^{F,g}(P_0^F) \right) \text{ and } N^{1/2} \left( \hat{\Psi}^{gN}(\hat{P}_{N,n}) - \Psi^{F,gN}(P_0^F) \right)$$

for a fixed and a data-adaptive parameter, respectively, where  $n$  is fixed and  $N \rightarrow \infty$ .

**Remark 11** (Within-Trial Covariance). Note that  $c_n^g$  concerns a non-standardized bias, whereas  $b_n^g$  concerns a root- $n$  standardized bias. This difference in notation reflects the fact that, given any trial  $T$ , treatment effect estimators typically converge at the root- $n$  rate—which is assumed throughout this paper—whereas estimators of the variance of  $n^{1/2} \left( (\hat{\alpha}_n, \hat{\beta}_n)' - (\alpha, \beta)' \right)$  are typically only required to be consistent.

### E.3 Rate Conditions

In this subsection, we derive conditions under which the following holds for  $N \rightarrow \infty$  and  $n = n(N)$ :

$$\|\hat{\Psi}^g(\tilde{P}_{N,n}) - \hat{\Psi}^g(\hat{P}_{N,n})\|_2 = o_{P_0^F}(N^{-1/2}) \text{ and } \|\hat{\Psi}^{gN}(\tilde{P}_{N,n}) - \hat{\Psi}^{gN}(\hat{P}_{N,n})\|_2 = o_{P_0^F}(N^{-1/2}). \quad (24)$$

Under these conditions, the limiting distributions of  $\hat{\Psi}^g(\tilde{P}_{N,n})$  and  $\hat{\Psi}^g(\hat{P}_{N,n})$  are the same because (24) implies that

$$N^{1/2} \left( \hat{\Psi}^g(\tilde{P}_{N,n}) - \Psi^{F,g}(P_0^F) \right) = N^{1/2} \left( \hat{\Psi}^g(\hat{P}_{N,n}) - \Psi^{F,g}(P_0^F) \right) + o_{P_0^F}(1)$$

and similarly for  $\hat{\Psi}^{gN}$ . Hence, if  $N^{1/2} \left( \hat{\Psi}^g(\hat{P}_{N,n}) - \Psi^{F,g}(P_0^F) \right)$  converges in distribution to  $Z$ , then  $N^{1/2} \left( \hat{\Psi}^g(\tilde{P}_{N,n}) - \Psi^{F,g}(P_0^F) \right)$  converges in distribution to  $Z$  as well, by Slutsky's theorem.

**Remark 12.** Sections 3 and 4 of the main text only apply to the asymptotic regime where  $n$  is fixed and  $N \rightarrow \infty$ . In the current setting,  $n$  increases with  $N$ ; consequently, the limiting distribution of  $\hat{\Psi}(\hat{P}_{N,n})$  (i.e., the distribution of  $Z$  above) may differ from the one derived in these sections (even though Assumptions 3.3 and 3.4 hold). This is further discussed in Appendix E.4.

In the following lemma, we present restrictions on  $\delta_1$  and  $\delta_2$  (appearing in Assumptions E.1 and E.2) such that (24) holds.

**Lemma E.1.** Let  $n(N) = N^\gamma$  with  $\gamma > 0$  and assume that Assumptions E.1 and E.2 hold. If  $\gamma > \max \left\{ \frac{1}{1+2\delta_1}, \frac{1}{2} \frac{1}{1+\delta_2} \right\}$ , then

$$\|\hat{\Psi}^g(\tilde{P}_{N,n}) - \hat{\Psi}^g(\hat{P}_{N,n})\|_2 = o_{P_0^F}(N^{-1/2}), \quad (25)$$

for  $\hat{\Psi}^g$  as defined in (7).

Furthermore, if  $P_0^F \|b_n^{gN} - b_n^{g*}\|_2^2 = O(N^{-\gamma\delta_1})$  and  $P_0^F \|c_n^{gN} - c_n^{g*}\|_2 = O(N^{-\gamma\delta_2})$  where  $g_N \xrightarrow{P} g^*$ , and  $P_0^F \|b_n^{gN} - b_n^{g*}\|_2^4$  and  $P_0^F \|c_n^{gN} - c_n^{g*}\|_2^2$  are bounded, then we also have that

$$\|\hat{\Psi}^{gN}(\tilde{P}_{N,n}) - \hat{\Psi}^{gN}(\hat{P}_{N,n})\|_2 = o_{P_0^F}(N^{-1/2}). \quad (26)$$

**Remark 13** (Rates of convergence). We discuss the consequences of Lemma E.1 for special values of  $\delta_1$  and  $\delta_2$ :

- $\delta_1 = 1$  and  $\delta_2 = 0$ . The within-trial estimator's root- $n$  standardized bias converges<sup>17</sup> with rate  $n^{-\frac{1}{2}}$  and the estimator for the within-trial covariance matrix remains biased as  $n \rightarrow \infty$ . The conditions in Lemma E.1 are satisfied, however, if  $\gamma > \frac{1}{2}$ . This is not an appropriate asymptotic regime because it would allow one to ignore the within-trial estimation error completely, see remark 14.

<sup>17</sup>  $P_0^F \|b_n^{g*}\|_2 \leq (P_0^F \|b_n^{g*}\|_2^2)^{1/2} = O(n^{-\delta_1/2})$

- $\delta_1 > \frac{1}{2}$  and  $\delta_2 > 0$ . In this scenario, the within-trial sample size is allowed to grow slower than  $N^{1/2}$ . In this setting, completely ignoring estimation error is not valid, see remark 14.

**Remark 14** (Non-trivial rates of convergence). To determine which values for  $\gamma$  are reasonable, we can impose the condition on  $\gamma$  that the corresponding asymptotic regime does not lead to valid “unadjusted” estimators that ignore sampling variability in the trial-level treatment effect estimators. Specifically, the estimators of the covariance between  $\alpha^g$  and  $\beta$ , based on (i) the unobservable  $(\alpha^g, \beta)'$  and (ii) the unbiased within-trial estimators  $(\hat{\alpha}_n^g, \hat{\beta}_n)'$  should not be asymptotically equivalent in the sense that

$$N^{1/2} \left\{ \widehat{\text{Cov}}(\hat{\alpha}_n^g, \hat{\beta}_n)_N - \widehat{\text{Cov}}(\alpha^g, \beta)_N \right\}$$

may not be  $o_{P_0^F}(1)$ .

We now show that  $\widehat{\text{Cov}}(\hat{\alpha}_n^g, \hat{\beta}_n)_N$  and  $\widehat{\text{Cov}}(\alpha^g, \beta)_N$  are asymptotically equivalent in the above sense if  $\gamma > \frac{1}{2}$ . Consider the setting where  $\mu_{\alpha,0}^g := E_{P_0^F}(\alpha^g)$  and  $\mu_{\beta,0} := E_{P_0^F}(\beta)$  are known and  $(\hat{\alpha}_n^g, \hat{\beta}_n)'$  are finite-sample unbiased. For simplicity, we use the known  $\mu_{\alpha,0}^g$  and  $\mu_{\beta,0}$  instead of the corresponding sample means in  $\widehat{\text{Cov}}(\hat{\alpha}_n^g, \hat{\beta}_n)_N$  and  $\widehat{\text{Cov}}(\alpha^g, \beta)_N$ . The root- $N$  standardized difference is then as follows<sup>18</sup>:

$$\begin{aligned} & N^{1/2} \left\{ \widehat{\text{Cov}}(\hat{\alpha}_n^g, \hat{\beta}_n)_N - \widehat{\text{Cov}}(\alpha^g, \beta)_N \right\} \\ &= N^{1/2} P_N \left\{ (\hat{\alpha}_n^g - \mu_{\alpha,0}^g)(\hat{\beta}_n - \mu_{\beta,0}) - (\alpha^g - \mu_{\alpha,0}^g)(\beta - \mu_{\beta,0}) \right\} \\ &= N^{1/2} \left\{ P_N(\hat{\alpha}_n^g - \alpha^g)(\hat{\beta}_n - \beta) + P_N(\hat{\alpha}_n^g - \alpha^g)(\beta - \mu_{\beta,0}) + P_N(\alpha^g - \mu_{\alpha,0}^g)(\hat{\beta}_n - \beta) \right\} \end{aligned}$$

The second and third terms above are sample means of mean-zero variables, the variance of which decreases to zero as  $n \rightarrow \infty$ ; hence, these terms are asymptotically negligible for any  $\gamma > 0$ . The first term above, however, is only asymptotically negligible under further conditions on  $\gamma$ . Let  $n^{-1}\sigma_{\hat{\alpha},\hat{\beta}}^g$  be the within-trial covariance between  $(\hat{\alpha}_n^g, \hat{\beta}_n)$ ; we then have that

$$\begin{aligned} N^{1/2} P_N(\hat{\alpha}_n^g - \alpha^g)(\hat{\beta}_n - \beta) &= N^{1/2}(P_N - P_0^F)(\hat{\alpha}_n^g - \alpha^g)(\hat{\beta}_n - \beta) + N^{1/2}n^{-1}P_0^F\sigma_{\hat{\alpha},\hat{\beta}}^g \\ &= N^{1/2}V_{N,n} + N^{1/2-\gamma}P_0^F\sigma_{\hat{\alpha},\hat{\beta}}^g. \end{aligned}$$

The term  $V_{N,n}$  is  $o_{P_0^F}(N^{-1/2})$  as long as  $n \rightarrow \infty$  because it is the sample mean of a mean-zero random variable with a variance that decreases to zero as  $n \rightarrow \infty$ . The second term is  $o_{P_0^F}(1)$  if  $\gamma > \frac{1}{2}$ ; hence, the naive estimator of the covariance is asymptotically equivalent to the estimator based on the true treatment effects if  $\gamma > \frac{1}{2}$ .

#### E.4 Practical Relevance

By allowing the within-trial sample sizes to increase with the number of independent trials, our approach becomes more practically useful because we are allowed to use more within-trial estimators (e.g., asymptotically efficient but finite-sample biased estimators). However, this comes at the cost of requiring within-trial sample sizes to increase sufficiently fast as a function of  $N$ . In realistic meta-analyses,  $n$  tends to be very large relative to  $N$ ; hence, this section’s asymptotic regime seems reasonable. Two caveats should be raised here, however. First, one should generally be mindful that our results are asymptotic (in the sense that  $N \rightarrow \infty$ ) regardless of the asymptotic regime. When  $N$  is small—as is almost always the case in a meta-analysis—one should interpret the results carefully. Second, when  $n \not\gg N$ , one should interpret the results with even more suspicion as the current asymptotic regime may not hold up very well.

To some degree, the arguments and results in this section are not satisfactory. In Sections 3 and 4, we derived the asymptotic distribution of the plug-in estimator  $\hat{\Psi}^g(\hat{P}_{N,n})$  and  $\hat{\Psi}^{gN}(\hat{P}_{N,n})$  when  $n$  is fixed and  $N \rightarrow \infty$ . As already mentioned in Remark 12, when  $n$  increases with  $N$ , the limiting distributions may differ from the ones derived in Sections 3 and 4. This is indeed the case as the limiting distribution of

$$N^{1/2} \left( \hat{\Psi}^g(\hat{P}_{N,n}) - \Psi^F(P_0^F) \right),$$

for  $n$  increasing with  $N$  and any  $\gamma > 0$ , is the same as the limiting distribution of

$$N^{1/2} \left( \widehat{\text{Cov}}(\alpha^g, \beta) - \Psi^F(P_0^F) \right).$$

<sup>18</sup>We abuse notation here and let  $P_N$  be the empirical distribution of the (unobserved) data  $(\hat{\alpha}_n^g, \hat{\beta}_n, \hat{\Sigma}_n^g, \alpha^g, \beta)$ .

for  $n$  increasing with  $N$ . Indeed, following similar derivations as in Remark 14, we can show that

$$N^{1/2} \left( \hat{\Psi}^g(\hat{P}_{N,n}) - \widehat{\text{Cov}}(\alpha^g, \beta) \right) = N^{1/2} n^{-1} (P_N - P_0^F) \hat{\sigma}_{\hat{\alpha}, \hat{\beta}, n}^g + o_{P_0^F}(1)$$

whenever  $\gamma > 0$ . Clearly, the remaining term on the right-hand side is also  $o_{P_0^F}(1)$  if  $\hat{\sigma}_{\hat{\alpha}, \hat{\beta}, n}^g$  has a finite variance because that term then is the root- $N$  standardized mean of a mean-zero random variable with a variance that converges to zero. Hence, in the current asymptotic regime, the measurement error in the trial-level treatment effects has no effect on the asymptotic distribution if we adjust for the measurement error<sup>19</sup>. While this result is not fully satisfactory, it is not surprising that the measurement error becomes negligible if  $n, N \rightarrow \infty$  because the variance of the measurement error is  $O(n^{-1})$ . At the same time, if one does not want to work under the regime where  $n, N \rightarrow \infty$ , there seems no way forward without making Assumptions 3.3 and 3.4 (or other similar assumptions).

## F Proofs

### F.1 Proof of Lemma 3.1

**Lemma 3.1.** Define the statistical parameter  $\Psi^g := (\Psi_1^g, \dots, \Psi_5^g)'$  as follows:

$$\begin{pmatrix} \Psi_1^g(P) \\ \Psi_2^g(P) \end{pmatrix} = \begin{pmatrix} E_P \hat{\alpha}^g \\ E_P \hat{\beta} \end{pmatrix} \quad \text{and} \quad \begin{pmatrix} \Psi_3^g(P) & \Psi_5^g(P) \\ \Psi_4^g(P) & \Psi_2^g(P) \end{pmatrix} = \text{Var}_P \left\{ \begin{pmatrix} \hat{\alpha}^g \\ \hat{\beta} \end{pmatrix} \right\} - E_P \left( n^{-1} \hat{\Sigma}^g \right), \quad (6)$$

where  $P \in \mathcal{M}$  is an observed-data distribution. Under Assumptions 3.3 and 3.4, the full-data parameter (5) is identified in the sense that  $\Psi^{F,g}(P^F) = \Psi^g(h(P^F))$  for all  $P^F \in \mathcal{M}^F$  and  $g \in \mathcal{G}$  where  $h$  is the mapping from the full-data distribution to the implied observed-data distribution, as defined in Section 2.2.1.

*Proof.* Let  $P^F \in \mathcal{M}^F$  be an arbitrary full-data distribution where all elements of  $\mathcal{M}^F$  satisfy Assumptions 3.3 and 3.4, and let  $P := h(P^F)$  be the corresponding observed-data distribution.

We first show that  $\Psi_1^{F,g}(P^F) = \Psi_1^g(P)$ . The derivations for  $\Psi_2^{F,g}(P^F)$  and  $\Psi_2^g(P)$  follow the same steps.

$$\begin{aligned} \Psi_1^{F,g}(P^F) &= E_{P^F}(\alpha^g) \\ &= E_{P^F} \{ E_{P^F}(\hat{\alpha}^g \mid \alpha^g) \} && \text{(assumption 3.3)} \\ &= E_{P^F}(\hat{\alpha}^g) && \text{(iterated expectation)} \\ &= E_P(\hat{\alpha}^g) && (P = h(P^F)) \\ &= \Psi_1^g(P) \end{aligned}$$

We now show that  $\Psi_3^{F,g}(P^F) = \Psi_3^g(P)$ . The derivations for  $\Psi_4^{F,g}(P^F) = \Psi_4^g(P)$  and  $\Psi_5^{F,g}(P^F) = \Psi_5^g(P)$  follow the same steps.

$$\begin{aligned} \Psi_3^{F,g}(P^F) &= \text{Var}_{P^F}(\alpha^g) \\ &= \text{Var}_{P^F}(E_{P^F}(\hat{\alpha}^g \mid \alpha^g)) && \text{(assumption 3.3)} \\ &= \text{Var}_{P^F}(\hat{\alpha}^g) - E_{P^F}(\text{Var}_{P^F}(\hat{\alpha}^g \mid \alpha^g)) && \text{(law of total variation)} \\ &= \text{Var}_{P^F}(\hat{\alpha}^g) - E_{P^F} [ E_{P^F}(\text{Var}_{P^F}(\hat{\alpha}^g \mid \alpha^g, T, n) \mid \alpha^g) + \text{Var}_{P^F}(E_{P^F}(\hat{\alpha}^g \mid \alpha^g, T, n) \mid \alpha^g) ] && \text{(law of total variation)} \\ &= \text{Var}_{P^F}(\hat{\alpha}^g) - E_{P^F} [ E_{P^F}(\text{Var}_{P^F}(\hat{\alpha}^g \mid \alpha^g, T, n) \mid \alpha^g) + \text{Var}_{P^F}(\alpha^g \mid \alpha^g) ] && \text{(assumption 3.3)} \\ &= \text{Var}_{P^F}(\hat{\alpha}^g) - E_{P^F} [ E_{P^F}(\text{Var}_{P^F}(\hat{\alpha}^g \mid \alpha^g, T, n) \mid \alpha^g) ] \\ &= \text{Var}_{P^F}(\hat{\alpha}^g) - E_{P^F} [ E_{P^F}(n^{-1} \cdot \Sigma_{11}^g \mid \alpha^g) ] \\ &= \text{Var}_{P^F}(\hat{\alpha}^g) - E_{P^F} [ E_{P^F}(E_{P^F}(n^{-1} \cdot \Sigma_{11}^g \mid \alpha^g, T, n) \mid \alpha^g) ] && \text{(iterated expectation)} \\ &= \text{Var}_{P^F}(\hat{\alpha}^g) - E_{P^F} [ E_{P^F}(E_{P^F}(n^{-1} \cdot \hat{\Sigma}_{11}^g \mid \alpha^g, T, n) \mid \alpha^g) ] && \text{(assumption 3.4)} \\ &= \text{Var}_{P^F}(\hat{\alpha}^g) - E_{P^F} (n^{-1} \cdot \hat{\Sigma}_{11}^g) && \text{(iterated expectation)} \\ &= \text{Var}_P(\hat{\alpha}^g) - E_P (n^{-1} \cdot \hat{\Sigma}_{11}^g) && (P = h(P^F)) \\ &= \Psi_3^g(P) \end{aligned}$$

□

<sup>19</sup>This only holds when we effectively adjust for measurement error because, as shown in Remark 14, not adjusting for the measurement error when  $\gamma \leq \frac{1}{2}$  can lead to incorrect inferences.

## E.2 Proof of Lemma E.1

**Lemma E.1.** Let  $n(N) = N^\gamma$  with  $\gamma > 0$  and assume that Assumptions E.1 and E.2 hold. If  $\gamma > \max\left\{\frac{1}{1+2\delta_1}, \frac{1}{2} \frac{1}{1+\delta_2}\right\}$ , then

$$\|\hat{\Psi}^g(\tilde{P}_{N,n}) - \hat{\Psi}^g(\hat{P}_{N,n})\|_2 = o_{P_0^F}(N^{-1/2}), \quad (25)$$

for  $\hat{\Psi}^g$  as defined in (7).

Furthermore, if  $P_0^F \|b_n^{gN} - b_n^{g*}\|_2^2 = O(N^{-\gamma\delta_1})$  and  $P_0^F \|c_n^{gN} - c_n^{g*}\|_2 = O(N^{-\gamma\delta_2})$  where  $g_N \xrightarrow{P} g^*$ , and  $P_0^F \|b_n^{gN} - b_n^{g*}\|_2^4$  and  $P_0^F \|c_n^{gN} - c_n^{g*}\|_2^2$  are bounded, then we also have that

$$\|\hat{\Psi}^{gN}(\tilde{P}_{N,n}) - \hat{\Psi}^{gN}(\hat{P}_{N,n})\|_2 = o_{P_0^F}(N^{-1/2}). \quad (26)$$

*Proof.* We prove the lemma first for the mean parameters and then for the covariance parameters. For simplicity of notation, we let  $P_N$  be the empirical distribution of the data, including the unobserved bias terms  $b_n^g$  and  $c_n^g$  where  $n = N^\gamma$ . Hence,  $P_N$  contains the information necessary to compute the observed trial-level estimators  $(\tilde{\alpha}^g, \tilde{\beta})'$  and  $\tilde{\Sigma}^g$ , and the (unobserved) debiased trial-level estimators  $(\hat{\alpha}_n^g, \hat{\beta}_n^g)'$  and  $\hat{\Sigma}_n^g$ .

**Mean Parameters** The estimators for  $E_{P_0^F}(\alpha^g)$  are given by

$$\hat{\Psi}^g(\tilde{P}_{N,n}) = P_N \tilde{\alpha}^g \quad \text{and} \quad \hat{\Psi}^g(\hat{P}_{N,n}) = P_N \hat{\alpha}_n^g$$

for the observed trial-level estimators and the debiased estimators, respectively. We now show that they are asymptotically equivalent under conditions.

$$\begin{aligned} N^{1/2} \left( \hat{\Psi}^g(\tilde{P}_{N,n}) - \hat{\Psi}^g(\hat{P}_{N,n}) \right) &= N^{1/2} P_N (\tilde{\alpha}^g - \hat{\alpha}_n^g) \\ &\leq N^{1/2} P_N n^{-1/2} \|b_n^g\|_2 && \text{(Assumption E.1)} \\ &= N^{1/2} n^{-1/2} \cdot (P_N - P_0^F) \|b_n^g\|_2 + N^{1/2} n^{-1/2} P_0^F \|b_n^g\|_2 && \text{(add and subtract } N^{1/2} n^{-1/2} P_0^F \|b_n^g\|_2) \end{aligned}$$

By Assumption E.1,  $\|b_n^g\|_2$  has finite variance for  $n \geq n_0 \in \mathbb{R}$ ; hence, the first term above is the root- $N$  standardized empirical mean of mean-zero i.i.d. random variables with variance going to zero as  $n \rightarrow \infty$ . The first term is thus  $o_{P_0^F}(1)$  whenever  $\gamma > 0$ . The second term is  $o_{P_0^F}(1)$  if

$$N^{1/2} n^{-1/2} P_0^F \|b_n^g\|_2 \leq N^{1/2} n^{-1/2} (P_0^F \|b_n^g\|_2^2)^{1/2} = N^{\frac{1}{2} - \frac{1}{2}\gamma} \cdot O(N^{-\frac{1}{2}\gamma\delta_1}) = N^{\frac{1}{2} - \frac{1}{2}\gamma - \frac{1}{2}\gamma\delta_1} \cdot O(1) = o(1).$$

This holds for  $\gamma > \frac{1}{1+\delta_1}$ .

The same derivation holds for the estimator of  $E_{P_0^F}(\beta)$ .

**Covariance Parameters** The estimators for  $E_{P_0^F}(\alpha^g - E_{P_0^F}(\alpha^g))^2$  are given by

$$\hat{\Psi}^g(\tilde{P}_{N,n}) = P_N (\tilde{\alpha}^g - P_N \tilde{\alpha}^g)^2 - P_N (n^{-1} \tilde{\sigma}_\alpha^g) \quad \text{and} \quad \hat{\Psi}^g(\hat{P}_{N,n}) = P_N (\hat{\alpha}_n^g - P_N \hat{\alpha}_n^g)^2 - P_N (n^{-1} \hat{\sigma}_{\alpha,n}^g),$$

for the observed trial-level estimators and the debiased estimators, respectively. We now show that they are asymptotically equivalent under conditions.

$$\begin{aligned}
N^{1/2} \left( \hat{\Psi}^g(\tilde{P}_{N,n}) - \hat{\Psi}^g(\hat{P}_{N,n}) \right) &= N^{1/2} n^{-1} P_N (\tilde{\sigma}_\alpha^g - \hat{\sigma}_{\alpha,n}^g) + N^{1/2} P_N \left\{ (\tilde{\alpha}^g - P_N \tilde{\alpha}^g)^2 - (\hat{\alpha}_n^g - P_N \hat{\alpha}_n^g)^2 \right\} \\
&= N^{1/2} n^{-1} P_N (\tilde{\sigma}_\alpha^g - \hat{\sigma}_{\alpha,n}^g) \\
&\quad + N^{1/2} P_N \left\{ (\tilde{\alpha}^g - P_N \tilde{\alpha}^g)^2 - \left( \tilde{\alpha}_n^g - n^{-1/2} b_n^g - P_N (\tilde{\alpha}_n^g - n^{-1/2} b_n^g) \right)^2 \right\} \\
&= N^{1/2} n^{-1} P_N (\tilde{\sigma}_\alpha^g - \hat{\sigma}_{\alpha,n}^g) \\
&\quad + N^{1/2} P_N \left\{ (\tilde{\alpha}^g - P_N \tilde{\alpha}^g)^2 - \left( (\tilde{\alpha}_n^g - P_N \tilde{\alpha}_n^g) - n^{-1/2} (b_n^g - P_N b_n^g) \right)^2 \right\} \\
&= N^{1/2} n^{-1} P_N (\tilde{\sigma}_\alpha^g - \hat{\sigma}_{\alpha,n}^g) \\
&\quad + N^{1/2} P_N \left\{ 2n^{-1/2} (b_n^g - P_N b_n^g) (\tilde{\alpha}_n^g - P_N \tilde{\alpha}_n^g) - n^{-1} (b_n^g - P_N b_n^g)^2 \right\} \\
&\leq N^{1/2} n^{-1} P_N \|c_n^g\|_2 \\
&\quad + 2N^{1/2} n^{-1/2} P_N (b_n^g - P_N b_n^g) (\tilde{\alpha}_n^g - P_N \tilde{\alpha}_n^g) \\
&\quad + N^{1/2} n^{-1} P_N (b_n^g - P_N b_n^g)^2
\end{aligned}$$

We now bound each of the three terms above. The first term,  $N^{1/2} n^{-1} P_N \|c_n^g\|_2$ , can be written as  $N^{1/2} n^{-1} \cdot (P_N - P_0^F) \|c_n^g\|_2 + N^{1/2} n^{-1} P_0^F \|c_n^g\|_2$  where  $N^{1/2} n^{-1} \cdot (P_N - P_0^F) \|c_n^g\|_2$  is the root- $N$  standardized empirical mean of mean-zero i.i.d. random variables with variance going to zero as  $n \rightarrow \infty$  because  $\|c_n^g\|_2$  has finite variance by assumption E.2; hence,  $N^{1/2} n^{-1} \cdot (P_N - P_0^F) \|c_n^g\|_2 = o_{P_0^F}(1)$  whenever  $\gamma > 0$ . Further,  $N^{1/2} n^{-1} \cdot P_0^F \|c_n^g\|_2$  is  $o_{P_0^F}(1)$  if

$$N^{1/2} n^{-1} P_0^F \|c_n^g\|_2 = N^{1/2} N^{-\gamma} \cdot O(n^{-\delta_2}) = N^{1/2-\gamma-\delta_2} \cdot O(1) = o_P(1).$$

This holds for  $\gamma > \frac{1}{2} \cdot \frac{1}{1+\delta_2}$ .

For the second term, we have that by the Cauchy-Schwarz inequality:

$$N^{1/2} n^{-1/2} P_N (b_n^g - P_N b_n^g) (\tilde{\alpha}^g - P_N \tilde{\alpha}^g) \leq N^{1/2} n^{-1/2} \left\{ P_N (b_n^g - P_N b_n^g)^2 \right\}^{1/2} \cdot \left\{ P_N (\tilde{\alpha}^g - P_N \tilde{\alpha}^g)^2 \right\}^{1/2}.$$

The elements on the right-hand side correspond to sample variances. The sample variance corresponding to  $\tilde{\alpha}^g$  is  $O_{P_0^F}(1)$  and the sample variance corresponding to  $b_n^g$  is bounded by above by

$$\begin{aligned}
P_N (b_n^g - P_N b_n^g)^2 &= P_N (b_n^g - P_0^F b_n^g + P_0^F b_n^g - P_N b_n^g)^2 \\
&= P_N (b_n^g - P_0^F b_n^g)^2 + (P_0^F b_n^g - P_N b_n^g)^2 + 2P_N (b_n^g - P_0^F b_n^g) (P_0^F b_n^g - P_N b_n^g) \\
&= (P_N - P_0^F) (b_n^g - P_0^F b_n^g)^2 + P_0^F (b_n^g - P_0^F b_n^g)^2 \\
&\quad + ((P_N - P_0^F) b_n^g)^2 - 2((P_N - P_0^F) b_n^g)^2 \\
&\leq (P_N - P_0^F) (b_n^g - P_0^F b_n^g)^2 + P_0^F \|b_n^g\|_2^2 - ((P_N - P_0^F) b_n^g)^2 \\
&= O_{P_0^F}(N^{-1/2}) + O(n^{-\delta_1})
\end{aligned}$$

In the last equality, we used the fact that  $P_0^F \|b_n^g\|_2^4 < K < \infty$  for the mean-zero sample averages and  $P_0^F \|b_n^g\|_2^2 = O(n^{-\delta_1})$ . Hence, the second term is  $o_{P_0^F}(1)$  if  $N^{1/2} n^{-1/2} \cdot O(n^{-\delta_1}) = o_{P_0^F}(1)$ , which holds for  $\gamma > \frac{1}{2} \cdot \frac{1}{\frac{1}{2} + \delta_1}$ .

The third term is automatically  $o_{P_0^F}(1)$  by the above derivations. The same derivations hold for the other covariance parameters.

**Estimated  $g_N$**  The above derivations can be repeated for an estimated  $g_N$  because

$$\|b_n^{g_N}\|_2^2 \leq \|b_n^{g_N} - b_n^{g^*}\|_2^2 + \|b_n^{g^*}\|_2^2 \quad \text{and} \quad \|c_n^{g_N}\|_2 \leq \|c_n^{g_N} - c_n^{g^*}\|_2 + \|c_n^{g^*}\|_2.$$

By assumption,  $P_0^F \|b_n^{g_N} - b_n^{g^*}\|_2^2$  and  $P_0^F \|c_n^{g_N} - c_n^{g^*}\|_2$  are of the same order as  $P_0^F \|b_n^{g^*}\|_2^2 = O(n^{-\delta_1}) = O(N^{-\gamma\delta_1})$  and  $P_0^F \|c_n^{g^*}\|_2 = O(n^{-\delta_2}) = O(N^{-\gamma\delta_2})$ , respectively. The same argument can be repeated for  $\|b_n^{g_N}\|_2^4$  and  $\|c_n^{g_N}\|_2^2$ .  $\square$

### E.3 Proof of Theorem 2

**Theorem 2.** Let  $\Theta \subset \mathbb{R}^p$  be open and define  $g \mapsto \theta_0^g$  such that  $\Phi^g(\theta_0^g) = 0$  for all  $g \in \mathcal{G} \subset \mathbb{D}$ . Further assume that  $g_N \in \mathcal{G}$  with probability tending to one as  $N \rightarrow \infty$ , where  $g_N$  depends on the observed data and  $(\mathbb{D}, d)$  is a metric space with metric  $d$ . Further assume there exists  $g^* \in \mathcal{G}$  such that  $d(g_N, g^*) = o_P(1)$  and define  $\rho\{(\theta_1, g_1), (\theta_2, g_2)\} := \|\theta_1 - \theta_2\|_2 + d(g_1, g_2)$  as a metric on  $\Theta \times \mathbb{D}$ .

Additionally assume the following conditions:

- (i)  $\Phi^g(\theta_N) \rightarrow 0$  implies that  $\theta_N \rightarrow \theta_0^g$  for all  $g \in \mathcal{G}$ .
- (ii)  $\{\phi_\theta^g : g \in \mathcal{G}, \theta \in \Theta\}$  is strong  $P_0$ -Glivenko–Cantelli.
- (iii)  $\exists \delta_1 > 0$  such that  $\{\phi_\theta^g : g \in \mathcal{G}, \|\theta - \theta_0^{g^*}\|_2 < \delta_1\}$  is  $P_0$ -Donsker and  $P_0\|\phi_\theta^g - \phi_{\theta_0^{g^*}}^{g^*}\|_2^2 \rightarrow 0$  if  $\rho\{(\theta, g), (\theta_0^{g^*}, g^*)\} \rightarrow 0$ .
- (iv)  $P_0\|\phi_{\theta_0^{g^*}}^{g^*}\|_2^2 < \infty$  and  $\theta \mapsto \Phi^g(\theta)$  is differentiable in  $\|\theta - \theta_0^{g^*}\|_2 < \delta_2$  for some  $\delta_2 > 0$  for all  $g \in \mathcal{G}$  with the matrix of partial derivatives, denoted by  $\dot{\Phi}^g(\theta)$ , being invertible at  $\theta_0^{g^*}$  for  $g = g^*$ . Further assume that  $(\theta, g) \mapsto \dot{\Phi}^g(\theta)$  is continuous at  $(\theta_0^{g^*}, g^*)$  with respect to the metric  $\rho$ .
- (v)  $\hat{\theta}_N^{g_N}$  and  $\tilde{\theta}_N^{g_N}$  solve the empirical and bootstrapped estimating equations approximately:  $P_N\phi_{\hat{\theta}_N^{g_N}}^{g_N} = o_P(N^{-1/2})$  and  $\tilde{P}_N\phi_{\tilde{\theta}_N^{g_N}}^{g_N} = o_P(N^{-1/2})$ .
- (vi)  $g \mapsto \Phi^g(\theta)$  is Lipschitz continuous uniformly over  $\theta \in \Theta$ :  $\|\Phi^{g_1}(\theta) - \Phi^{g_2}(\theta)\|_2 \leq L \cdot d(g_1, g_2)$  for all  $g_1, g_2 \in \mathcal{G}$  and  $\theta \in \Theta$  for some  $L > 0$ .

Under conditions (i) to (vi), we have that

$$N^{1/2} \left( \hat{\theta}_N^{g_N} - \theta_0^{g_N} \right) \xrightarrow{d} Z \sim N(0, \Sigma_0^{g^*}) \text{ as } N \rightarrow \infty,$$

and

$$N^{1/2} \left( \tilde{\theta}_N^{g_N} - \hat{\theta}_N^{g_N} \right) \xrightarrow{P_W} Z \sim N(0, \Sigma_0^{g^*}) \text{ as } N \rightarrow \infty,$$

where  $\Sigma_0^{g^*} = \left( \dot{\Phi}^{g^*}(\theta_0^{g^*}) \right)^{-1} P_0 \left( \phi_{\theta_0^{g^*}}^{g^*} \right)^{\otimes 2} \left( \dot{\Phi}^{g^*}(\theta_0^{g^*}) \right)^{-1}$ .

*Proof.* We split the proof into three parts. First, we show that  $\hat{\theta}_N^{g_N}$  and  $\tilde{\theta}_N^{g_N}$  are consistent estimators of  $\theta_0^{g^*}$  and  $\theta_0^{g_N}$ . Second, we prove the convergence in distribution of  $N^{1/2}(\hat{\theta}_N^{g_N} - \theta_0^{g_N})$ . Third, we prove the bootstrap result.

**Part 1: Consistency** We first show consistency of  $\hat{\theta}_N^{g_N}$  for the non-data-adaptive estimand  $\theta_0^{g^*}$ ; afterwards, we show that this also implies that  $\|\hat{\theta}_N^{g_N} - \theta_0^{g_N}\|_2 = o_P(1)$ . We then repeat similar steps for the bootstrapped estimator  $\tilde{\theta}_N^{g_N}$ .

$$\begin{aligned} \|\Phi^{g_N}(\hat{\theta}_N^{g_N})\|_2 &= \|\Phi^{g_N}(\hat{\theta}_N^{g_N}) - P_N\phi_{\hat{\theta}_N^{g_N}}^{g_N} + P_N\phi_{\hat{\theta}_N^{g_N}}^{g_N}\|_2 \\ &= \|P_0\phi_{\hat{\theta}_N^{g_N}}^{g_N} - P_N\phi_{\hat{\theta}_N^{g_N}}^{g_N} + P_N\phi_{\hat{\theta}_N^{g_N}}^{g_N}\|_2 \\ &\leq \sup_{\theta \in \Theta, g \in \mathcal{G}} \|P_0\phi_\theta^g - P_N\phi_\theta^g\|_2 + \|P_N\phi_{\hat{\theta}_N^{g_N}}^{g_N}\|_2 \\ &\leq \sup_{\theta \in \Theta, g \in \mathcal{G}} \|P_0\phi_\theta^g - P_N\phi_\theta^g\|_2 + o_P(N^{-1/2}) && \text{(condition (v))} \\ &\leq o_P(1) + o_P(N^{-1/2}) = o_P(1) && \text{(condition (ii))} \end{aligned}$$

We use the above result in the following derivations, note that we used  $g_N$  above and are using  $g^*$  below.

$$\begin{aligned} \|\Phi^{g^*}(\hat{\theta}_N^{g_N})\|_2 &= \|P_0\phi_{\hat{\theta}_N^{g_N}}^{g^*} - P_0\phi_{\hat{\theta}_N^{g_N}}^{g_N} + P_0\phi_{\hat{\theta}_N^{g_N}}^{g_N}\|_2 \\ &\leq \|P_0\phi_{\hat{\theta}_N^{g_N}}^{g^*} - P_0\phi_{\hat{\theta}_N^{g_N}}^{g_N}\|_2 + o_P(1) && \text{(previous equation)} \\ &\leq L \cdot d(g^*, g_N) + o_P(1) && \text{(condition (vi))} \\ &= o_P(1) \end{aligned}$$

By condition (i),  $\|\Phi^{g^*}(\hat{\theta}_N^{g_N})\|_2 = o_P(1)$  implies that  $\|\hat{\theta}_N^{g_N} - \theta_0^{g^*}\|_2 = o_P(1)$ . Lemma F.1 then implies that  $\|\hat{\theta}_N^{g_N} - \theta_0^{g_N}\|_2 = o_P(1)$ .

We now repeat the same steps for the bootstrapped estimator  $\tilde{\theta}_N^{g_N}$ .

$$\begin{aligned} \|\Phi^{g_N}(\tilde{\theta}_N^{g_N})\|_2 &= \|P_0\phi_{\tilde{\theta}_N^{g_N}}^{g_N} - \tilde{P}_N\phi_{\tilde{\theta}_N^{g_N}}^{g_N} + \tilde{P}_N\phi_{\tilde{\theta}_N^{g_N}}^{g_N}\|_2 \\ &\leq \sup_{\theta \in \Theta, g \in \mathcal{G}} \|P_0\phi_{\theta}^g - \tilde{P}_N\phi_{\theta}^g\|_2 + \|\tilde{P}_N\phi_{\tilde{\theta}_N^{g_N}}^{g_N}\|_2 \\ &= \sup_{\theta \in \Theta, g \in \mathcal{G}} \|P_0\phi_{\theta}^g - \tilde{P}_N\phi_{\theta}^g\|_2 + o_P(N^{-1/2}) && \text{(condition (v))} \\ &\leq \sup_{\theta \in \Theta, g \in \mathcal{G}} \|P_0\phi_{\theta}^g - P_N\phi_{\theta}^g\|_2 + \sup_{\theta \in \Theta, g \in \mathcal{G}} \|P_N\phi_{\theta}^g - \tilde{P}_N\phi_{\theta}^g\|_2 + o_P(N^{-1/2}) \\ &= o_P(1) + o_P(1) + o_P(N^{-1/2}) \end{aligned}$$

The last equality follows from condition (iii) and Kosorok (2008, corollary 10.14). The remaining arguments are the same as for  $\hat{\theta}_N^{g_N}$  and are omitted to avoid repetition. We conclude that  $\|\hat{\theta}_N^{g_N} - \theta_0^{g^*}\|_2 = o_P(1)$  and  $\|\tilde{\theta}_N^{g_N} - \theta_0^{g_N}\|_2 = o_P(1)$ .

**Part 2: Convergence in Distribution of  $N^{1/2}(\hat{\theta}_N^{g_N} - \theta_0^{g_N})$ .** From condition (ii) and Kosorok (2008, lemma 13.3) follows that  $N^{1/2}(P_N - P_0)\phi_{\hat{\theta}_N^{g_N}}^{g_N} - N^{1/2}(P_N - P_0)\phi_{\theta_0^{g^*}}^{g^*} = o_P(1)$ . We start from this result in the following derivations:

$$\begin{aligned} N^{1/2}(P_N - P_0)\phi_{\theta_0^{g^*}}^{g^*} &= N^{1/2}P_N\phi_{\hat{\theta}_N^{g_N}}^{g_N} - N^{1/2}P_0\phi_{\hat{\theta}_N^{g_N}}^{g_N} + o_P(1) \\ &= -N^{1/2}P_0\phi_{\hat{\theta}_N^{g_N}}^{g_N} + o_P(1) && \text{(condition (v))} \\ &= -N^{1/2}P_0\phi_{\theta_0^{g^*}}^{g^*} - N^{1/2}\dot{\Phi}^{g_N}(\bar{\theta}) \cdot (\hat{\theta}_N^{g_N} - \theta_0^{g_N}) + o_P(1) && \text{(mean value theorem + condition (iv))} \\ &= -N^{1/2}\dot{\Phi}^{g_N}(\bar{\theta}) \cdot (\hat{\theta}_N^{g_N} - \theta_0^{g_N}) + o_P(1) \end{aligned}$$

where  $\bar{\theta}$  is a point between  $\hat{\theta}_N^{g_N}$  and  $\theta_0^{g_N}$ . Note that we're abusing notation here if  $p > 1$  because the mean-value theorem only exists for real-valued functions. In that case, the mean-value theorem is applied to each element of the vector-valued function  $\Phi^{g_N}(\theta)$  where  $\bar{\theta}$  may differ from element to element. Anyhow, any such  $\bar{\theta}$  converges in probability to  $\theta_0^{g^*}$  by virtue of it being between  $\hat{\theta}_N^{g_N}$  and  $\theta_0^{g^*}$ . By condition (iv) and the fact that  $\|\bar{\theta} - \theta_0^{g^*}\|_2 + d(g^*, g_N) = o_P(1)$ , we have that  $\dot{\Phi}^{g_N}(\bar{\theta}) = \dot{\Phi}^{g^*}(\theta_0^{g^*}) + o_P(1)$  by the continuous mapping theorem. It now follows immediately that the rate of convergence is root- $N$  by using the fact that  $N^{1/2}(P_N - P_0)\phi_{\theta_0^{g^*}}^{g^*} = O_P(1)$  by the central limit theorem.

$$\begin{aligned} N^{1/2}(P_N - P_0)\phi_{\theta_0^{g^*}}^{g^*} &= -N^{1/2}\dot{\Phi}^{g^*}(\theta_0^{g^*}) \cdot (\hat{\theta}_N^{g_N} - \theta_0^{g_N}) + o_P(1) \\ &\implies O_P(1) = N^{1/2}\|\hat{\theta}_N^{g_N} - \theta_0^{g_N}\|_2 \end{aligned}$$

Note that this does not imply that  $N^{1/2}\|\hat{\theta}_N^{g_N} - \theta_0^{g^*}\|_2 = O_P(1)$ . It further follows by condition (iv) that

$$N^{1/2}(\hat{\theta}_N^{g_N} - \theta_0^{g_N}) = -\left(\dot{\Phi}^{g^*}(\theta_0^{g^*})\right)^{-1} \cdot N^{1/2}(P_N - P_0)\phi_{\theta_0^{g^*}}^{g^*} + o_P(1).$$

By the central limit theorem and Slutsky's theorem, we thus have that  $N^{1/2}(\hat{\theta}_N^{g_N} - \theta_0^{g_N}) \sim Z$  for  $Z \sim \mathcal{N}(0, \Sigma_0^{g^*})$  where

$$\Sigma_0^{g^*} = \left(\dot{\Phi}^{g^*}(\theta_0^{g^*})\right)^{-1} \cdot P_0 \left(\phi_{\theta_0^{g^*}}^{g^*}\right)^{\otimes 2} \cdot \left(\dot{\Phi}^{g^*}(\theta_0^{g^*})\right)^{-1}.$$

**Part 3: Bootstrap Result** We first state some general results about the bootstrap that will be used later on. First, by Kosorok (2008, p. 198) and condition (iii), we have that

$$N^{1/2}(\tilde{P}_N - P_N) \rightsquigarrow \mathbb{G} \quad \text{in } l^\infty(\mathcal{F})$$

where  $\mathcal{F} = \left\{ \phi_{\theta}^g : g \in \mathcal{G}, \|\theta - \theta_0^{g*}\|_2 \leq \delta \right\}$  and  $\rightsquigarrow$  denotes weak convergence and  $\mathbb{G}$  is a tight Gaussian process. Applying the same asymptotic equicontinuity argument as in Kosorok (2008, Lemma 13.3) to the above bootstrapped process, we have that

$$N^{1/2} \left( \tilde{P}_N - P_N \right) \phi_{\theta_N^{g_N}}^{g_N} = N^{1/2} \left( \tilde{P}_N - P_N \right) \phi_{\theta_0^{g*}}^{g*} + o_P(1).$$

By the previous results, we have that

$$N^{1/2} (P_N - P_0) \left( \phi_{\theta_N^{g_N}}^{g_N} - \phi_{\theta_0^{g*}}^{g*} \right) + N^{1/2} \left( \tilde{P}_N - P_N \right) \left( \phi_{\theta_N^{g_N}}^{g_N} - \phi_{\theta_0^{g*}}^{g*} \right) = o_P(1).$$

In the above equation, several terms cancel out. We can rewrite the above equation as follows:

$$-N^{1/2} P_0 \phi_{\theta_N^{g_N}}^{g_N} + N^{1/2} P_0 \phi_{\theta_0^{g*}}^{g*} + N^{1/2} \tilde{P}_N \phi_{\theta_N^{g_N}}^{g_N} - N^{1/2} \tilde{P}_N \phi_{\theta_0^{g*}}^{g*} = o_P(1),$$

where, additionally,  $N^{1/2} P_0 \phi_{\theta_0^{g*}}^{g*} = 0$  by definition and  $N^{1/2} \tilde{P}_N \phi_{\theta_N^{g_N}}^{g_N} = o_P(1)$  by condition (v). Hence, we have that, following similar steps as in part 2,

$$\begin{aligned} N^{1/2} \tilde{P}_N \phi_{\theta_0^{g*}}^{g*} &= -N^{1/2} P_0 \phi_{\theta_N^{g_N}}^{g_N} + o_P(1) \\ &= -N^{1/2} P_0 \phi_{\theta_N^{g_N}}^{g_N} - N^{1/2} \dot{\Phi}^{g_N}(\bar{\theta}) \cdot \left( \tilde{\theta}_N^{g_N} - \theta_0^{g_N} \right) + o_P(1) \quad (\text{mean value theorem} + \text{condition (iv)}) \\ &= -N^{1/2} \dot{\Phi}^{g_N}(\bar{\theta}) \cdot \left( \tilde{\theta}_N^{g_N} - \theta_0^{g_N} \right) + o_P(1). \end{aligned}$$

By the same arguments as in part 2, we have that  $\dot{\Phi}^{g_N}(\bar{\theta}) = \dot{\Phi}^{g*}(\theta_0^{g*}) + o_P(1)$ . We, therefore, have that

$$N^{1/2} \left( \tilde{\theta}_N^{g_N} - \theta_0^{g_N} \right) = - \left( \dot{\Phi}^{g*}(\theta_0^{g*}) \right)^{-1} \cdot N^{1/2} \tilde{P}_N \phi_{\theta_0^{g*}}^{g*} + o_P(1).$$

Finally, we have that

$$\begin{aligned} N^{1/2} \left( \tilde{\theta}_N^{g_N} - \hat{\theta}_N^{g_N} \right) &= N^{1/2} \left( \tilde{\theta}_N^{g_N} - \theta_0^{g_N} \right) - N^{1/2} \left( \hat{\theta}_N^{g_N} - \theta_0^{g_N} \right) \\ &= - \left( \dot{\Phi}^{g*}(\theta_0^{g*}) \right)^{-1} \cdot N^{1/2} \tilde{P}_N \phi_{\theta_0^{g*}}^{g*} + o_P(1) + \left( \dot{\Phi}^{g*}(\theta_0^{g*}) \right)^{-1} \cdot N^{1/2} P_N \phi_{\theta_0^{g*}}^{g*} + o_P(1) \\ &= - \left( \dot{\Phi}^{g*}(\theta_0^{g*}) \right)^{-1} \cdot N^{1/2} \left( \tilde{P}_N - P_N \right) \phi_{\theta_0^{g*}}^{g*} + o_P(1) \end{aligned}$$

From Kosorok (2008, Theorem 2.6) now follows that

$$N^{1/2} \left( \tilde{\theta}_N^{g_N} - \hat{\theta}_N^{g_N} \right) \xrightarrow{P} \underset{W}{Z},$$

where  $Z$  is as defined in part 2. □

#### F.4 Proof of Lemma F.1

**Lemma F.1.** Under the conditions (i) and (vi) of Theorem 2, we have that  $g \mapsto \Psi^g(P_0)$  is continuous at  $g^*$ . This in turn implies that  $\hat{\Psi}^{g_N}(P_N) \xrightarrow{P} \Psi^{g_N}(P_0)$  if  $\hat{\Psi}^{g_N}(P_N) \xrightarrow{P} \Psi^{g*}(P_0)$ .

*Proof.* If  $\Psi^g(P_0)$  is continuous in  $g$  at  $g^*$ , then it automatically follows that  $\Psi^{g_N}(P_0) \xrightarrow{P} \Psi^{g*}(P_0)$  whenever  $g_N \xrightarrow{P} g^*$  by the continuous mapping theorem, and hence also  $\hat{\Psi}^{g_N}(P_N) \xrightarrow{P} \Psi^{g_N}(P_0)$  if  $\hat{\Psi}^{g_N}(P_N) \xrightarrow{P} \Psi^{g*}(P_0)$ . We thus only need to show that this continuity holds under the conditions of Theorem 2.

Let  $\theta_0^{g*} := \Psi^{g*}(P_0)$  where, by definition of the estimand and condition (i) of Theorem 2,  $P_0 \phi_{\theta_0^{g*}}^{g*} = 0$  and  $P_0 \phi_{\theta}^{g*} \neq 0$  for  $\theta \neq \theta_0^{g*}$ . Let  $g_N$  be a sequence of functions in  $\mathcal{G}$  such that  $d(g_N, g^*) \rightarrow 0$  and let  $\theta_N := \Psi^{g_N}(P_0)$  such that  $P_0 \phi_{\theta_N}^{g_N} = 0$ . We now have by condition (vi) of Theorem 2 that

$$\left| P_0 \phi_{\theta_N}^{g_N} - P_0 \phi_{\theta_N}^{g*} \right| \leq C \cdot d(g_N, g^*) \rightarrow 0.$$

Because  $P_0 \phi_{\theta_N}^{g_N} = 0$  for all  $N$ , we have that  $P_0 \phi_{\theta_N}^{g*} \rightarrow 0$ . By condition (i) of Theorem 2, this implies that  $\theta_N \rightarrow \theta_0^{g*}$ . This shows that  $\Psi^{g_N}(P_0) \rightarrow \Psi^{g*}(P_0)$  whenever  $d(g_N, g^*) \rightarrow 0$ ; hence,  $g \mapsto \Psi^g(P_0)$  is continuous at  $g^*$ . □

### E.5 Proof of Lemma C.1 and Corollary 1

**Lemma C.1.** Let  $Y = (\hat{X}, \hat{\Sigma}, X, \Sigma)$  be a full-data vector distributed according to  $P^F \in \mathcal{M}^F$  where  $\mathcal{M}^F$  satisfies the following assumptions:

$$\hat{X} \mid X, \Sigma \sim \mathcal{N}(X, \Sigma) \quad \text{and} \quad \hat{\Sigma} = \Sigma \quad P^F\text{-a.s.}$$

and  $(\hat{X}, \hat{\Sigma})$  are observed. No further assumptions are made on  $\mathcal{M}^F$ . If the true full-data distribution  $P_0^F \in \mathcal{M}^F$  is such that the distribution of  $X \mid \Sigma$  contains an interval  $P_0^F$ -a.s. and  $\Sigma$  is positive definite  $P_0^F$ -a.s., then the observed-data model  $\mathcal{M} := \{P : P = h(P^F) \text{ for some } P^F \in \mathcal{M}^F\}$ , where  $h(P^F)$  is the observed-data distribution implied by  $P^F$ , is locally non-parametric at  $P_0 = h(P_0^F)$ .

*Proof.* Let  $\mathbf{X} := (\hat{X}, \hat{\Sigma})$  and  $\mathbf{Z} := (X, \Sigma)$ , and let  $Q_0 := Q_{P_0^F}$  be the distribution of  $\mathbf{Z}$  under  $P_0^F$ . The model for  $Q$  implied by  $\mathcal{M}^F$  is denoted by  $\mathcal{Q} := \{Q_{P^F} : P^F \in \mathcal{M}^F\}$ . The model  $\mathcal{Q}$  is locally non-parametric at  $Q_0$ . Indeed, the only restrictions on  $\mathcal{Q}$  are that the distribution of  $X \mid \Sigma$  contains an interval  $P_0^F$ -a.s. and that  $\Sigma$  is positive definite  $P_0^F$ -a.s., which will remain true for all local perturbations of  $Q_0$  in the direction of  $h \in L_0^2(Q_0)$  where  $L_0^2(Q_0)$  is the space of mean-zero square-integrable functions with respect to  $Q_0$ . Hence,  $\overline{\mathcal{T}}(Q_0)$ , denoting the closure of the tangent set of  $\mathcal{Q}$  at  $Q_0$ , is  $L_0^2(Q_0)$ .

The density of  $\mathbf{X} \mid \mathbf{Z}$  with respect to the dominating measure  $\lambda_{\mathbb{R}^k} \otimes \delta_{\Sigma}$ , where  $\lambda_{\mathbb{R}^k}$  is the Lebesgue measure on  $\mathbb{R}^k$  and  $\delta_{\Sigma}$  is the Dirac measure at  $\Sigma$ , is given by

$$p_{\mathbf{X} \mid \mathbf{Z}}(\hat{x}, \hat{\Sigma} \mid \mathbf{Z} = (x, \Sigma)) = \frac{1}{(2\pi)^{k/2} |\Sigma|^{1/2}} \exp \left\{ -\frac{1}{2} (\hat{x} - x)^\top \Sigma^{-1} (\hat{x} - x) \right\}.$$

Note that the observed-data distribution only depends on  $P^F$  through  $Q_{P^F}$ ; hence, the observed-data distributions can also be indexed by  $Q$ . Let  $b(X, \Sigma)$  be a score for  $Q_0$  in  $\mathcal{Q}$ . The tangent set of  $\mathcal{M}$  at  $P_0$  is given by

$$\mathcal{T}(P_0) = \{A_{Q_0} b : b \in L_0^2(Q_0)\},$$

where  $A_{Q_0}$  is the score operator that maps a score  $b$  for the unobserved-data model  $\mathcal{Q}$  to the corresponding score for the observed-data model  $\mathcal{M}$ . This operator is given by

$$(A_{Q_0} b)(\mathbf{x}) = E_{P_0^F} \{b(\mathbf{Z}) \mid \mathbf{X} = \mathbf{x}\}.$$

The proof is complete if we can show that  $\overline{\mathcal{T}}(P_0) = L_0^2(P_0)$ . This holds if the range of the score operator  $A_{Q_0} : L_0^2(Q_0) \rightarrow L_0^2(P_0)$ , denoted by  $R(A_{Q_0})$ , is dense in  $L_0^2(P_0)$ , or equivalently, its closure  $\overline{R}(A_{Q_0})$  is equal to  $L_0^2(P_0)$ . Because  $A_{Q_0}$  is a bounded linear operator from  $L_0^2(Q_0)$  to  $L_0^2(P_0)$ , we have that  $\overline{R}(A_{Q_0}) = N(A_{Q_0}^*)^\perp$ , where  $N(A_{Q_0}^*)$  is the null space of  $A_{Q_0}^* : L_0^2(P_0) \rightarrow L_0^2(Q_0)$ , which is the adjoint operator, which is defined as follows:

$$(A_{Q_0}^* g)(\mathbf{z}) = E_{P_0^F} \{g(\mathbf{X}) \mid \mathbf{Z} = \mathbf{z}\}.$$

Hence, we only need to show that  $N(A_{Q_0}^*) = \{0\}$ . This follows if the following

$$(A_{Q_0}^* g)(\mathbf{z}) = E_{P_0^F} \{g(\mathbf{X}) \mid \mathbf{Z} = (x, \Sigma)\} = 0 \quad P_0^F\text{-a.s.}$$

implies that  $g(\mathbf{x}) = 0$   $P_0^F$ -a.e. We can rewrite the above equation as follows, also using the assumption that  $\hat{\Sigma} = \Sigma$   $P_0^F$ -a.s.:

$$E_{P_0^F} \left\{ g(\hat{X}, \Sigma) \mid \mathbf{Z} = (x, \Sigma) \right\} = 0 \quad P_0^F\text{-a.s.}$$

The above expectation is with respect to a multivariate normal distribution with mean  $x$  and variance  $\Sigma$ . Given a certain  $\Sigma$ , the above equation should hold for all  $x$  in the support of  $X \mid \Sigma$  under  $P_0^F$ , which contains an interval  $P_0^F$ -a.s. by assumption. This implies that  $g(\hat{X}, \Sigma) = 0$   $P_0^F$ -a.s. because the multivariate normal distribution (with fixed  $\Sigma$ ) is complete.  $\square$

**Corollary 1.** Under the same conditions as in Lemma C.1, but now only requiring that

$$E(\hat{X} \mid X, \Sigma) = X \quad \text{and} \quad \text{Var}(\hat{X} \mid X, \Sigma) = \Sigma \quad P_0^F\text{-a.s.},$$

and

$$E(\hat{\Sigma} \mid X, \Sigma) = \Sigma \quad P_0^F\text{-a.s.}$$

the observed-data model  $\mathcal{M} := \{P : P = h(P^F) \text{ for some } P^F \in \mathcal{M}^F\}$  is locally non-parametric at  $P_0$ .

*Proof.* The observed-data model under the conditions of this corollary is larger than the observed-data model under the conditions of the previous lemma because fewer restrictions are imposed on  $\mathcal{M}^F$ . The latter observed-data model was shown to be locally non-parametric. Hence, the former observed-data model is also non-parametric.  $\square$

## E.6 Proof of Lemma D.1

**Lemma D.1.** Let  $(n, P_n^T) \mapsto a_i(n, P_n^T) \in \mathcal{X} \times \mathcal{Z} \times \mathcal{S} \times \mathcal{Y}$  be a mapping that extracts the  $i$ 'th observation from the observed data for a given trial, where  $a_i(n, P_n^T) = 0$  for  $i > n$ . Define  $z_i(n, P_n^T)$  and  $x_i(n, P_n^T)$  similarly as  $a_i(n, P_n^T)$  as mappings that extract the assigned treatment and the observed covariate, respectively, from the  $i$ 'th observation, also setting them to 0 for  $i > n$ . Assume the following conditions hold:

1. The within-trial sample sizes are bounded above by  $n^* < \infty$ .
2.  $\mathcal{X}$  is a bounded subset of  $\mathbb{R}^d$  for some  $d < \infty$ .
3.  $P_0|\hat{\alpha}^g|^2 < \infty$  for some  $g \in \mathcal{G}$ .
4.  $\hat{\alpha}^g$  depends on  $(n, P_n^T)$  only through  $\{(x_1, z_1, g \circ a_1)(n, P_n^T), \dots, (x_n, z_n, g \circ a_n)(n, P_n^T)\}$ . Moreover, if we shift  $g \circ a_i(n, P_n^T)$  by  $\Delta$  for some  $i \in \{1, \dots, n^*\}$ , then the estimate changes by less than  $c|\Delta|$  for some constant  $c < \infty$ .
5.  $\mathcal{G}$ , as a uniformly bounded set of real-valued functions on  $\mathcal{X} \times \mathcal{Z} \times \mathcal{S} \times \mathcal{Y}$  is  $P_{a_i,0}$ -Donsker for all  $i = 1, \dots, n^*$  for the pushforward measure  $P_{a_i,0} := P_0 \circ a_i^{-1}$ .

We then have that  $\{\hat{\alpha}^g : g \in \mathcal{G}\}$  is a  $P_0$ -Donsker class.

*Proof.* We assume without loss of generality that  $\mathcal{X} \subset \mathbb{R}$ . The same arguments (using  $d$  projection mappings) can be applied whenever  $\mathcal{X} \subset \mathbb{R}^d$  for  $d < \infty$ .

As assumed,  $\hat{\alpha}^g$  only depends on  $(n, P_n^T)$  through  $\{x_i(n, P_n^T), z_i(n, P_n^T), g \circ a_i(n, P_n^T)\}$  for  $i = 1, \dots, n$ . Since  $n$  is random, this function does not have a fixed number of arguments. We, therefore, define a corresponding  $\hat{\alpha}$  as a function of  $3n^* + 1$  arguments such that  $\hat{\alpha}$  evaluated in

$$\{g \circ a_1(n, P_n^T), \dots, g \circ a_{n^*}(n, P_n^T), z_1(n, P_n^T), \dots, z_{n^*}(n, P_n^T), x_1(n, P_n^T), \dots, x_{n^*}(n, P_n^T), n\}$$

equals the former function evaluated in  $\{x_i(n, P_n^T), z_i(n, P_n^T), g \circ a_i(n, P_n^T)\}$  for  $i = 1, \dots, n$ .

We now define  $\mathcal{F}_i$  as follows:

$$\mathcal{F}_i = \begin{cases} \mathcal{G} \circ a_i & \text{for } 1 \leq i \leq n^* \\ \{z_i\} & \text{for } n^* < i \leq 2n^* \\ \{x_i\} & \text{for } 2n^* < i \leq 3n^* \\ \{(n, P_n^T) \mapsto n\} & \text{for } i = 3n^* + 1 \end{cases}$$

The class  $\{\hat{\alpha}^g : g \in \mathcal{G}\}$  is smaller than  $\hat{\alpha} \circ (\mathcal{F}_1 \times \dots \times \mathcal{F}_{3n^*+1}) := \{\hat{\alpha} \circ f : f \in \mathcal{F}_1 \times \dots \times \mathcal{F}_{3n^*+1}\}$  because the former restricts the first  $n^*$  elements of  $f$  to be  $(g \circ a_1, \dots, g \circ a_{n^*})$  for  $g \in \mathcal{G}$ , whereas the latter allows for a different  $g \in \mathcal{G}$  in each of the first  $n^*$  elements. Hence, it is sufficient to show that the latter (larger) class is  $P_0$ -Donsker.

We can apply Kosorok, 2008, Theorem 9.31 to conclude that  $\hat{\alpha} \circ (\mathcal{F}_1 \times \dots \times \mathcal{F}_{3n^*+1})$  is a  $P_0$ -Donsker class if the following conditions hold:

- (i)  $\|P_0\|_{\mathcal{F}_i} < \infty$  for all  $i = 1, \dots, 3n^* + 1$ .
- (ii)  $\hat{\alpha} \circ f$  is square-integrable for at least one  $f \in \mathcal{F}_1 \times \dots \times \mathcal{F}_{3n^*+1}$ .
- (iii)  $|\hat{\alpha} \circ f(n, P_n^T) - \hat{\alpha} \circ h(n, P_n^T)|^2 \leq c^2 \sum_{i=1}^{3n^*+1} (f_i(n, P_n^T) - h_i(n, P_n^T))^2$  for every  $f, h \in \mathcal{F}$  and some constant  $c < \infty$ .
- (iv)  $\mathcal{F}_i$  is a  $P_0$ -Donsker class for all  $i = 1, \dots, 3n^* + 1$ .

Condition (i) holds because  $\mathcal{G}$  is uniformly bounded by condition (5.),  $\mathcal{Z} = \{0, 1\}$  is bounded, and  $\mathcal{X}$  is bounded by condition (2.). Condition (ii) holds by condition (3.). Condition (iii) is implied by condition (4.) Condition (iv) holds for all  $i$  because:

- For  $i \leq n^*$ :  $\mathcal{G}$  is a  $P_{a_i,0} = P_0 \circ a_i^{-1}$ -Donsker class by condition (5.), which implies that  $\mathcal{G} \circ a_i$  is a  $P_0$ -Donsker class.
- For  $n^* < i \leq 2n^*$ :  $\{z_i\}$  contains a single function with bounded image and is thus a  $P_0$ -Donsker class.

- For  $2n^* < i \leq 3n^*$ :  $\{x_i\}$  contains a single function with bounded image and is thus a  $P_0$ -Donsker class.
- For  $i = 3n^* + 1$ :  $\{(n, P_n^T) \mapsto n\}$  contains a single function with bounded image and is thus a  $P_0$ -Donsker class.

□

## F.7 Proof of Lemma D.2

**Lemma D.2.** For the setup described in Sections 2 and 3, Conditions (a–f) listed in Appendix D.2 are sufficient for the conditions of Theorem 2.

*Proof.* We first derive some intermediate results. Next, we verify the conditions of Theorem 2.

**Intermediate Results** From the form of the estimating function, as given in Appendix C, we see that  $\Phi^g(\theta)$  only depends on  $g$  through  $P_0\hat{\alpha}^g$ ,  $P_0(\hat{\alpha}^g)^2$ ,  $P_0\hat{\alpha}^g\hat{\beta}$ , and  $P_0\frac{1}{n}\hat{\Sigma}^g$ . Furthermore, each element of  $\Phi^g(\theta)$  is a linear function of these arguments where the coefficients depend on  $\theta$ :

$$\Phi^g(\theta) = \begin{pmatrix} P_0\hat{\alpha}^g - \mu_\alpha \\ P_0\hat{\beta} - \mu_\beta \\ P_0(\hat{\alpha}^g)^2 - 2\mu_\alpha \cdot P_0\hat{\alpha}^g - P_0\frac{1}{n}\hat{\sigma}_{\hat{\alpha}^g} - d_\alpha + \mu_\alpha^2 \\ P_0\hat{\beta}^2 - 2\mu_\beta \cdot P_0\hat{\beta} - P_0\frac{1}{n}\hat{\sigma}_{\hat{\beta}} - d_\beta + \mu_\beta^2 \\ P_0\hat{\alpha}^g\hat{\beta} - \mu_\beta \cdot P_0\hat{\alpha}^g - \mu_\alpha \cdot P_0\hat{\beta} + P_0\frac{1}{n}\hat{\sigma}_{\hat{\alpha}^g, \hat{\beta}} + \mu_\alpha\mu_\beta - d_{\alpha, \beta} \end{pmatrix}$$

Hence,  $\Phi^g(\theta)$  is a Lipschitz continuous function of  $(P_0\hat{\alpha}^g, P_0(\hat{\alpha}^g)^2, P_0\hat{\alpha}^g\hat{\beta}, P_0\frac{1}{n}\hat{\Sigma}^g)$  indexed by  $\theta$  where the Lipschitz constants are upper bounded by  $C < \infty$  if  $\theta$  is restricted to a bounded set  $\Theta$  (as required in condition (b)). Hence, for any  $\theta \in \Theta$  and any  $g_1, g_2 \in \mathcal{G}$ , we have that (where  $\|\cdot\|_F$  is the Frobenius norm):

$$\begin{aligned} \|\Phi^{g_1}(\theta) - \Phi^{g_2}(\theta)\|_2 &\leq C \cdot \left( |P_0\hat{\alpha}^{g_1} - P_0\hat{\alpha}^{g_2}| + |P_0(\hat{\alpha}^{g_1})^2 - P_0(\hat{\alpha}^{g_2})^2| + |P_0\hat{\alpha}^{g_1}\hat{\beta} - P_0\hat{\alpha}^{g_2}\hat{\beta}| + \left\| P_0\frac{1}{n}\hat{\Sigma}^{g_1} - P_0\frac{1}{n}\hat{\Sigma}^{g_2} \right\|_F \right) \\ &\leq C \cdot (M_1 \cdot \|g_1 - g_2\|_\infty + M_2 \cdot \|g_1 - g_2\|_\infty + M_3 \cdot \|g_1 - g_2\|_\infty + M_4 \cdot \|g_1 - g_2\|_\infty) \\ &\quad \text{(Lipschitz continuity in conditions (e–f))} \\ &\leq C^* \cdot \|g_1 - g_2\|_\infty \\ &\quad (C^* := C \cdot (M_1 + M_2 + M_3 + M_4)) \end{aligned}$$

Similar to above, note that the estimating function  $\phi_\theta^g$  only depends on  $g$  through  $\hat{\alpha}^g$  and  $\frac{1}{n}\hat{\Sigma}^g$ . It additionally depends on the observed data through  $\hat{\beta}$ . We will therefore sometimes write  $\phi_\theta^g(n, P_n^T)$  as  $\phi_\theta(\hat{\alpha}^g, \hat{\beta}, n^{-1}\hat{\Sigma}^g)$  to simplify the notation in some of the arguments. Following the same argument as above,  $\phi_\theta^g$  is a linear function of  $\hat{\alpha}^g$ ,  $(\hat{\alpha}^g)^2$ ,  $\hat{\alpha}^g\hat{\beta}$ , and  $\frac{1}{n}\hat{\Sigma}^g$  with coefficients that depend on  $\theta$ . Together with condition (b) and (c), this implies that  $\phi_\theta^g$  is a Lipschitz continuous function of  $(\hat{\alpha}^g, (\hat{\alpha}^g)^2, \hat{\alpha}^g\hat{\beta}, \frac{1}{n}\hat{\Sigma}^g, \theta)$ . It now follows from Kosorok (2008, Theorem 9.31) that  $\{\phi_\theta^g : g \in \mathcal{G}, \theta \in \Theta\}$  is  $P_0$ -Donsker if

1.  $\mathcal{F}_1 = \{\hat{\alpha}^g : g \in \mathcal{G}\}$ ,  $\mathcal{F}_2 = \{(\hat{\alpha}^g)^2 : g \in \mathcal{G}\}$ ,  $\mathcal{F}_3 = \{\hat{\alpha}^g\hat{\beta} : g \in \mathcal{G}\}$ ,  $\mathcal{F}_4 = \{\frac{1}{n}\hat{\Sigma}^g : g \in \mathcal{G}\}$ , and  $\mathcal{F}_5 = \{\theta : \theta \in \Theta\}$  are  $P_0$ -Donsker classes,
2.  $\|P_0\|_{\mathcal{F}_i} < \infty$  for  $i = 1, \dots, 5$ , and
3.  $\phi_\theta^g$  is square integrable for some  $(\theta, g) \in \Theta \times \mathcal{G}$ .

Condition (1.) follows from condition (c) for  $i = 1, 4$ ; for  $i = 2, 3$ , it follows from the fact that the product of bounded Donsker classes is a bounded Donsker class (Kosorok, 2008, Corollary 9.32); and for  $i = 5$ , it trivially holds because  $\Theta$  is a bounded set. Condition (2.) follows from the involved classes of functions being uniformly bounded by conditions (b) and (c). Condition (3.) follows from  $\phi_\theta^g$  being a finite sum of finite products of elements from these classes of functions and the fact that these functions are uniformly bounded by conditions (b) and (c).

**Verification of the Conditions** Condition (i) of Theorem 2 follows from  $\theta_0^g$  being the unique root of  $\Phi^g(\theta)$  for  $g \in \mathcal{G}$  and  $\theta \mapsto \Phi^g(\theta)$  being a continuous function.

Condition (ii) of Theorem 2 follows from  $\{\phi_\theta^g : g \in \mathcal{G}, \theta \in \Theta\}$  being a  $P_0$ -Donsker class (intermediate result) because a  $P_0$ -Donsker class is a  $P_0$ -Glivenko-Cantelli class.

The first part of Condition (iii) of Theorem 2 follows from the intermediate Donsker result and the fact that  $\Theta$  is open. Indeed, for  $\theta_0^{g^*} \in \Theta$ , there exists a  $\delta > 0$  such that  $\{\theta \in \mathbb{R}^5 : \|\theta - \theta_0^{g^*}\|_2 < \delta\} \subset \Theta$  (and a subset of a Donsker class is a Donsker class). For the second part, we write the estimating function  $\phi_\theta^g : \mathbb{N} \times \mathcal{M}_{NP}^* \times \Theta \rightarrow \mathbb{R}^5$  as the following composite function:

$$\mathbb{N} \times \mathcal{M}_{NP}^* \times \Theta \mapsto \phi_\theta^g = \phi \circ (\hat{\alpha}^g, \hat{\beta}, n^{-1}\hat{\Sigma}^g, \theta)$$

where  $\hat{\alpha}^g, \hat{\beta} : \mathbb{N} \times \mathcal{M}_{NP}^* \rightarrow \mathbb{R}$  and  $n^{-1}\hat{\Sigma}^g : \mathbb{N} \times \mathcal{M}_{NP}^* \rightarrow \mathbb{R}^{2 \times 2}$ . The function  $\phi$  above is a second-degree polynomial function and, hence, continuous in its arguments. Hence, if for every  $(n, P_n^T) \in \mathbb{N} \times \mathcal{M}_{NP}^*$ , the arguments converge to the appropriate limits indexed by  $g^*$  and  $\theta_0^{g^*}$  as  $\|\theta - \theta_0^{g^*}\|_2 + \|g - g^*\|_\infty \rightarrow 0$ , then  $\phi_\theta^g(n, P_n^T) \rightarrow \phi_{\theta_0^{g^*}}^{g^*}(n, P_n^T)$  pointwise. By condition (d),  $\hat{\alpha}^g$  and  $n^{-1}\hat{\Sigma}^g$  converge pointwise to  $\hat{\alpha}^{g^*}$  and  $n^{-1}\hat{\Sigma}^{g^*}$ , respectively, if  $\|g - g^*\|_\infty \rightarrow 0$ . The other arguments,  $\hat{\beta}$  and  $\theta$  trivially converge to  $\hat{\beta}$  and  $\theta_0^{g^*}$  as  $\|\theta - \theta_0^{g^*}\|_2 \rightarrow 0$ . The pointwise convergence implies, by the dominated convergence theorem, that  $P_0\|\phi_{\theta_0^g}^g - \phi_{\theta_0^{g^*}}^{g^*}\|_2^2 \rightarrow 0$  as  $\|\theta - \theta_0^{g^*}\|_2 + \|g - g^*\|_\infty \rightarrow 0$ .

The first part of condition (iv) of Theorem 2 follows from  $\hat{\alpha}^g, \hat{\beta}, \hat{\Sigma}^g$ , and  $\theta$  being bounded (uniformly in  $\mathcal{G}$ ) by conditions (b) and (c). The second part follows from the expression for  $\hat{\Phi}^g(\theta)$  given in (18).

Condition (v) of Theorem 2 follows from the definition of the estimators as the exact solutions of the corresponding estimating equations.

Condition (vi) of Theorem 2 follows from the intermediate results.  $\square$

## G Simulations

### G.1 Data-Generating Mechanism

We consider two data-generating mechanisms: a proof-of-concept scenario and a vaccine scenario. The proof-of-concept scenario is meant to illustrate the potential advantage of using an estimated surrogate index over the surrogate endpoint itself, but is not very realistic. The vaccine scenario is meant to reflect a set of vaccine trials and is more realistic. We will show that our methods work in principle in the proof-of-concept scenario and that they work reasonably well in practice in the realistic scenario.

#### G.1.1 Proof-of-Concept Scenario

The data-generating mechanism described next is meant to (i) illustrate the potential advantage of using an estimated surrogate index over the surrogate endpoint itself and (ii) show that the methods work in principle. We first describe the data-generating mechanism for a fixed trial. Next, we describe how between-trial heterogeneity is simulated and how this relates to the comparability and surrogacy assumptions.

**Within-Trial Data-Generating Mechanism** We observe in each trial one binary baseline covariate  $X_1$ , the treatment indicator  $Z$ , the univariate continuous surrogate  $S$ , and the univariate continuous clinical endpoint  $Y$ . The within-trial observed-data distribution is determined by the following set of equations:

$$\begin{cases} X_1 \sim \text{Bernoulli}(p) \\ S = \beta_{S,Z} \cdot Z + \epsilon_S \text{ where } \epsilon_S \sim \mathcal{N}(0, 1) \\ Y = -0.25 \cdot S \cdot X_1 + S \cdot (1 - X_1) + \beta_{Y,Z} \cdot Z + \beta_{Y,S^2} \cdot S^2 + \epsilon_Y \text{ where } \epsilon_Y \sim \mathcal{N}(0, 1) \end{cases} \quad (27)$$

where the first  $n/2$  subjects are assigned to treatment  $Z = 1$  and the last  $n/2$  subjects to treatment  $Z = 0$ . We let  $n = 2,000$ . Further note that the surrogate is negatively associated with the clinical endpoint if  $X_1 = 1$ , but positively associated if  $X_1 = 0$ . This is unrealistic: we expect the direction of this association to be the same for all patient subgroups for a "good" surrogate. Nonetheless, our methods can be applied in this artificial scenario.

**Trial-Level Random Parameters** In (27), several parameters vary across trials and are treated as random parameters. We consider two scenarios for the distributions of these trial-level parameters: one with moderate violations of the surrogacy and comparability assumptions, and another with only slight violations.

First, the trial-level parameter  $p$ , which determines the distribution of the baseline covariate  $X$ , is sampled from a uniform distribution:  $p \sim \text{Uniform}(0.30, 0.70)$ . This reflects differences in patient populations across trials. Second, the trial-level parameter  $\beta_{S,Z}$ , which determines the treatment effect on the surrogate, is sampled as follows:  $\beta_{S,Z} \sim \mathcal{N}(0.5, 0.3^2)$ . The variance of this distribution captures the between-trial variability in treatment effects on the surrogate. Third, the trial-level parameter  $\beta_{Y,Z}$  determines the treatment effect on the clinical endpoint, adjusted<sup>20</sup> for the surrogate and the baseline covariate. It is sampled as follows:  $\beta_{Y,Z} \sim \mathcal{N}(0, \sigma_{\beta_{Y,Z}}^2)$ . This parameter directly relates to the surrogacy assumption, which holds if  $\beta_{Y,Z} = 0$ . The magnitude of the surrogacy violation depends on the variance  $\sigma_{\beta_{Y,Z}}^2$ . Finally, the trial-level parameter  $\beta_{Y,S^2}$  represents a quadratic effect of the surrogate on the clinical endpoint. It is sampled as follows:  $\beta_{Y,S^2} \sim \mathcal{N}(0, \sigma_{\beta_{Y,S^2}}^2)$ . This parameter directly relates to the comparability assumption, which holds if  $\beta_{Y,S^2}$  (and  $\beta_{Y,Z}$ ) are constant across all trials. The magnitude of the comparability violation depends on the variance  $\sigma_{\beta_{Y,S^2}}^2$ .

In the first scenario, we set  $\sigma_{\beta_{Y,Z}}^2 = \sigma_{\beta_{Y,S^2}}^2 = 0.1^2$ , representing moderate violations of surrogacy and comparability. In the second scenario, we set  $\sigma_{\beta_{Y,Z}}^2 = \sigma_{\beta_{Y,S^2}}^2 = 0.05^2$ , representing slight violations of these assumptions.

We illustrate the data-generating mechanism—and the implied violations of the comparability assumption—for the proof-of-concept scenario in Figure 8. This figure is based on simulated individual-patient data from six trials for (i) slight and (ii) moderate violations of the surrogacy and comparability assumptions. In Figure 8 (a), the surrogate is plotted against the clinical endpoint separately by trial and by the degree of violations of the surrogacy and comparability assumptions. Smooth regression curves, stratified by  $X_1$ , were added to further illustrate that the sign of the association between the surrogate and the clinical endpoint depends on  $X_1$ . We show the smooth regression curves in a single plot in Figure 8 (b) to demonstrate more clearly that the comparability assumption is more severely violated in the first scenario than in the second scenario.

**Implementation** The surrogate index is estimated through a linear regression model with main effects for  $S$  and  $X_1$ , the corresponding interaction, and a quadratic effect for  $S$ . The parameters are estimated by pooling data from the  $N$  simulated trials in each replication of the simulation study. The data-adaptive target parameter  $\rho^{g_N}$  is approximated in each replication by sampling  $2 \cdot 10^4$  trials with sample size 200 and estimating  $\rho_{\text{trial}}^{g_N}$  where  $g_N$  is the previously estimated surrogate index and where the trial-level treatments effects are estimated by corresponding sample mean differences<sup>21</sup>.

The trial-level treatment effects on the surrogate, the estimated surrogate index, and the clinical endpoint are estimated through fitting a linear regression model for  $S$  and  $Y$  with main effects for  $X_1$  and  $Z$ . The estimated coefficients for the treatment indicator is a consistent and asymptotically normal estimator for the treatment effect  $\alpha^g$  and  $\beta$  in terms of mean differences. The covariance matrix of  $(\hat{\alpha}^g, \hat{\beta})'$  is estimated through the sandwich estimator using the `vcovHC()` function from the `sandwich` R package with `type = "HC0"` (Zeileis, 2004; Zeileis et al., 2020). This procedure is generally more efficient than simple mean differences but valid even if the linear model is misspecified (Van Lancker et al., 2024). The sandwich estimator for the covariance matrix is consistent but not finite-sample unbiased; hence, we have to appeal to the alternative asymptotic regime of Section 5 to justify our inferences.

### G.1.2 Vaccine Scenario

The data-generating mechanism described next is meant to reflect a set of vaccine trials and is more complex than the one above. We first describe the data-generating mechanism for a fixed trial. Next, we describe how between-trial heterogeneity is simulated and how this relates to the comparability and surrogacy assumptions.

**Within-Trial Data-Generating Mechanism** We observe in each trial three baseline covariates:  $X_1$  is an “internal” measure of exposure (e.g., the average number of contacts per week),  $X_2$  is an external covariate associated with the amount of exposure (e.g., calendar time), and  $X_3$  indicates whether the subject is naive (i.e., whether they have been previously infected). The treatment indicator  $Z$  is as before. Further,  $S$  is the neutralizing antibody titer measured 20

<sup>20</sup>Because we have adjusted here for post-randomization covariates, this parameter lacks a causal interpretation.

<sup>21</sup>Sample mean differences are unbiased estimators of the population mean differences; the covariance estimator based on the sample covariance is also unbiased. So, there is no need for large within-trial sample sizes when approximating  $\rho_{\text{trial}}^{g_N}$  through Monte Carlo integration.

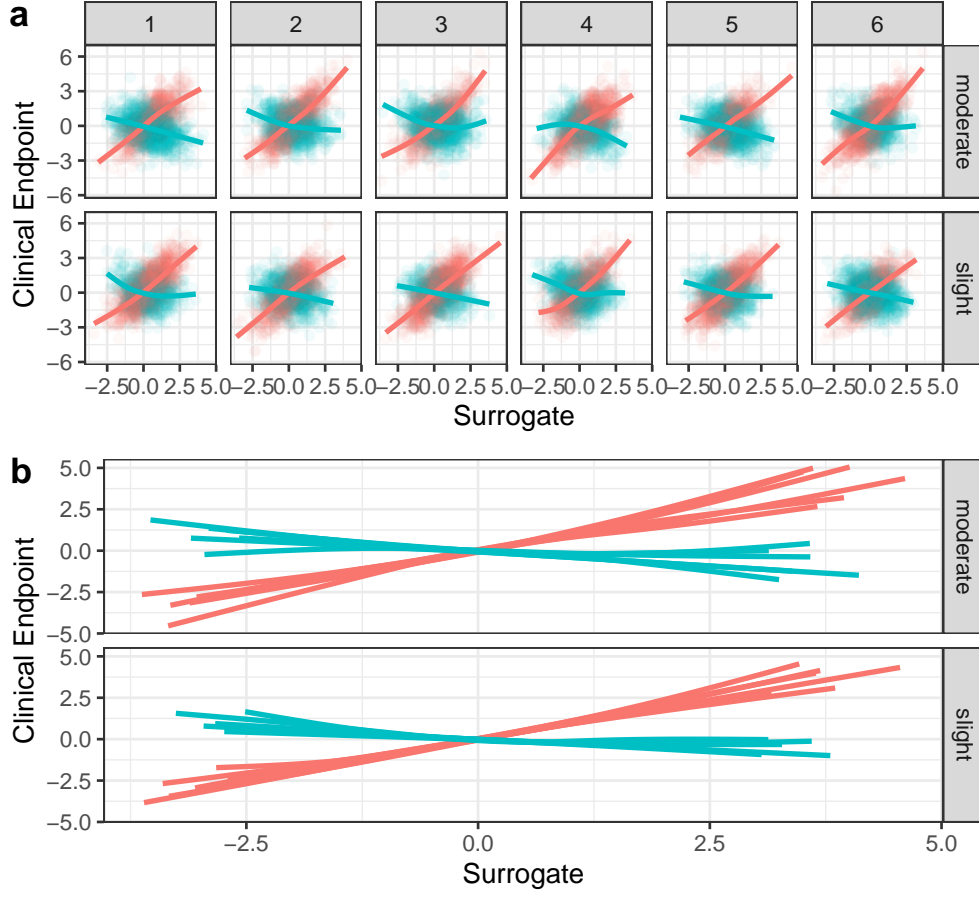


Figure 8: Proof-of-concept scenario: simulated individual-patient data in six simulated trials under slight ( $\sigma_{\beta_{Y,Z}}^2 = \sigma_{\beta_{Y,S^2}}^2 = 0.05^2$ ) and moderate ( $\sigma_{\beta_{Y,Z}}^2 = \sigma_{\beta_{Y,S^2}}^2 = 0.1^2$ ) violations of the surrogacy and comparability assumptions. Dots and smooth regression curves are colored by the value for  $X_1$ . Panel a shows the simulated individual-patient data separately by trial (columns) and degree of violations of surrogacy and comparability (rows). Note that these plots pool observations across treatment groups. Smooth regression curves (full lines) are fitted to these data in each trial, stratified by  $X_1$ . Panel b shows the smooth regression curves from panel a in a single plot for each scenario.

days after vaccination, and  $Y$  is the infectious disease outcome 80 days after measuring  $S$  (e.g., confirmed symptomatic infection). The within-trial observed-data distribution is determined by the following set of equations:

$$\begin{cases} X_1 \sim \mathcal{N}(\mu_1, 1) \\ X_2 \sim \mathcal{N}(\mu_2, 1) \\ X_3 \sim \text{Bernoulli}(p) \\ S \sim \beta_{S,Z} \cdot Z + \epsilon_S \text{ where } \epsilon_S \sim \mathcal{N}(0, 1) \\ P(Y = 1 | \cdot) = \text{expit} \{ \beta_{Y,Z} \cdot Z + (1 + \beta_{Y,S} + X_3) \cdot S + X_1 - 2 \cdot X_3 \} \cdot 0.10 \cdot \exp(\sin(X_2) + 1) \end{cases} \quad (28)$$

where the first  $n/2$  subjects are assigned to treatment  $Z = 1$  and the last  $n/2$  subjects to treatment  $Z = 0$ . We let  $n = 5,000$ .

**Trial-Level Random Parameters** As for the proof-of-concept scenario, we consider two scenarios for the distributions of the trial-level parameters: one with moderate violations of the surrogacy and comparability assumptions and another with only slight violations.

First, the trial-level parameters  $\mu_1$ ,  $\mu_2$ , and  $p$  reflect population differences across trials. These parameters are sampled as follows:

$$\mu_1 \sim \text{Uniform}(-1, 1), \quad \mu_2 \sim \text{Uniform}(-1, 1), \quad p \sim \text{Uniform}(0.25, 0.75).$$

Second, the trial-level parameter  $\beta_{S,Z}$ , which determines the treatment effect on the surrogate, is sampled as follows:  $\beta_{S,Z} \sim \mathcal{N}(1, 0.5^2)$ . Third, the trial-level parameter  $\beta_{Y,Z}$  determines the treatment effect on the clinical endpoint, adjusted for the surrogate and baseline covariates, and is sampled as follows  $\beta_{Y,Z} \sim \mathcal{N}(0, \sigma_{\beta_{Y,Z}}^2)$ . The surrogacy assumption holds if  $\beta_{Y,Z} = 0$ . Fourth, the trial-level parameter  $\beta_{Y,S}$  corresponds to the association between the surrogate on the clinical endpoint and is sampled as  $\beta_{Y,S} \sim \mathcal{N}(0, \sigma_{\beta_{Y,S}}^2)$ . This parameter directly relates to the comparability assumption, which holds if  $\beta_{Y,S}$  (and  $\beta_{Y,Z}$ ) are constant across all trials.

In the first scenario, we set  $\sigma_{\beta_{Y,Z}}^2 = \sigma_{\beta_{Y,S}}^2 = 0.30^2$ , representing moderate violations of surrogacy and comparability. In the second scenario, we set  $\sigma_{\beta_{Y,Z}}^2 = \sigma_{\beta_{Y,S}}^2 = 0.15^2$ , representing slight violations of these assumptions.

**Remark 15.** In these simulations, we assume that  $S$  is measured for all subjects; however, in practice, this may not always be the case. Indeed,  $S$  is often measured some time after randomization, and if a subject is infected beforehand,  $S$  is generally no longer well defined. A similar issue arises in the COVID-19 trials we analyze in Section 7.

We illustrate the data-generating mechanism—and the implied violations of the comparability assumption—for the vaccine scenario in Figure 9. This figure is based on simulated individual-patient data from six trials for (i) slight and (ii) moderate violations of the surrogacy and comparability assumptions. In Figure 9 (a), the estimated surrogate index is plotted against the clinical endpoint separately by trial and by the degree of violations of the surrogacy and comparability assumptions. Smooth regression curves were added: under the surrogacy and comparability assumptions, these curves should be close to the identity line for all trials; deviations from this indicate a violation of comparability. We show the smooth regression curves in a single plot in Figure 9 (b) to demonstrate more clearly that the comparability assumption is more severely violated in the first scenario than in the second scenario. Note that variability in the curves for the  $[0, 0.2]$ -range of the estimated surrogate index is most important because most values of the estimated surrogate index are in this range.

**Implementation** The treatment effect on the clinical endpoint is defined—as in the data application—as the log relative risk and similarly for the treatment effect on the surrogate index. The treatment effect on the untransformed surrogate is the mean difference. These treatment effects are estimated using sample means and the covariance matrix is estimated through the delta method. The surrogate index is estimated (pooling all data from the simulated  $N$  trials in each replication) through the SuperLearner with several logistic regression models and a generalized additive logistic regression models as candidate learners (van der Laan et al., 2007). The meta-learner uses leave-one-trial-out cross-validation with the binomial loglikelihood as the loss function. The SuperLearner is implemented using the *s3* R package (Coyle et al., 2021).

The data-adaptive target parameter  $\rho_{\text{trial}}^{g_N}$  is approximated by sampling  $5 \cdot 10^3$  trials<sup>22</sup> with sample size 3000 and estimating  $\rho_{\text{trial}}^{g_N}$  where  $g_N$  is the previously estimated surrogate index and where the trial-level treatments effects are estimated using sample means and the corresponding covariance matrices through the delta method.

## G.2 Results

In this section, we present the results of the simulations using the earlier described data-generating mechanisms and implementations. In each scenario, we simulated 500 data sets. This number of replications is on the lower end of what is typically used in simulation studies, but it is sufficient to illustrate the main points of this paper. More replications would have been computationally too expensive because each replication requires us to generate individual-level data from multiple trials and, in each replication, we have to numerically approximate the data-adaptive estimand  $\rho_{\text{trial}}^{g_N}$  through Monte Carlo integration.

We focus on estimation of and inference about the  $\rho_{\text{trial}}(\rho_{\text{trial}}^{g_N})$  parameter (the Pearson correlation between  $\alpha(\alpha^{g_N})$  and  $\beta$ ). This parameter is a function of the covariance parameter; hence, its estimate is computed as this function evaluated in the covariance parameter estimates. The standard errors for the estimated correlation parameters are obtained through the delta method using the sandwich estimator. Wald confidence intervals are obtained by using the delta method on Fisher’s Z scale and transforming the limits back to the original scale (which ensures confidence limits in the unit interval). If the estimate is larger than 0.999, we use the Wald confidence interval on the  $\rho$  scale (so without any transformation) because Fisher’s Z-transformation is not defined for values larger than 1 and may be unstable for values very close to 1. Another set of confidence intervals are obtained through the BCa confidence intervals based on the multiplier bootstrap where the weights are sampled from a unit-exponential distribution. Throughout, we aim for a nominal coverage of 95%.

<sup>22</sup>We had to limit the number of trials here to ensure that the simulations remain computationally feasible.

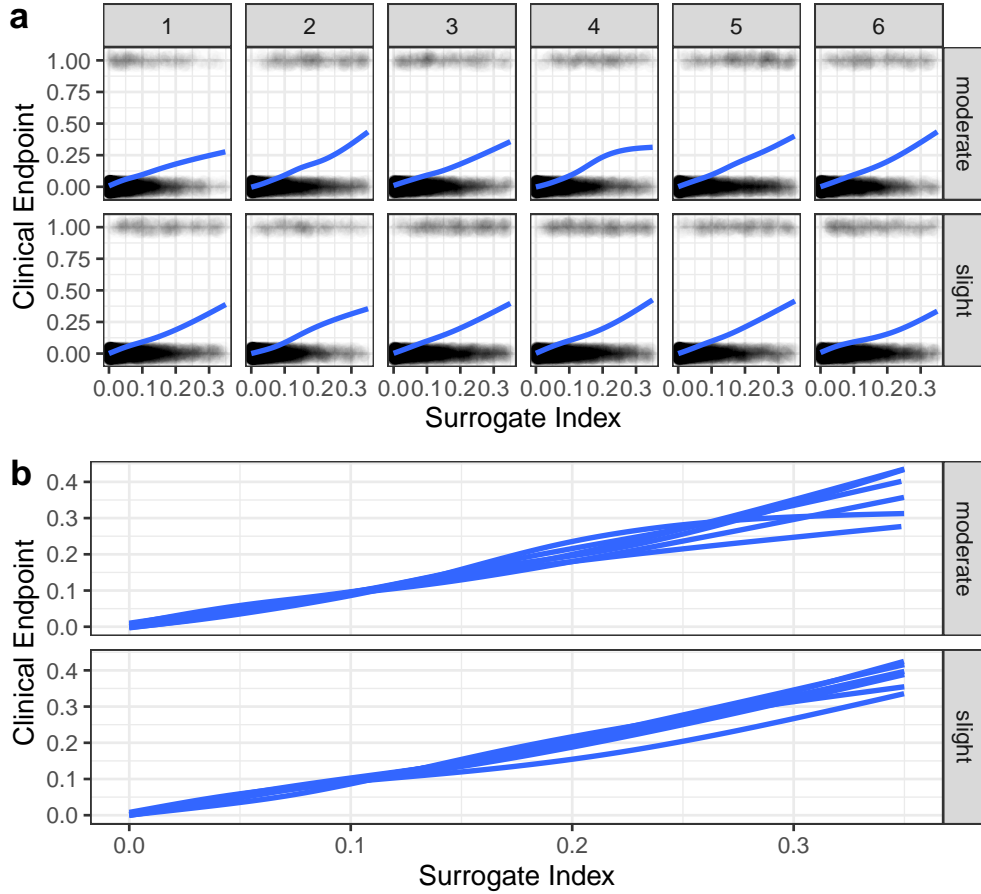


Figure 9: Vaccine scenario: simulated individual-patient data in six trials under slight and moderate violations of the surrogacy and comparability assumptions. Panel a shows scatter plots for the estimated surrogate index against the clinical endpoint, separately by trial (columns) and degree of violations of surrogacy and comparability (rows). Note that vertical jittering is used to avoid overplotting; in reality the clinical endpoint is either 0 or 1. Smooth regression curves are fitted to these data in each trial. Panel b shows the smooth curves from panel a in the same plot.

As mentioned in Section 6, two finite-sample adjustments are always used in the simulations. First, in the expression for the plug-in estimator (7), the variance of  $(\hat{\alpha}^g, \hat{\beta})'$  is estimated by dividing by  $N - 1$  instead of  $N$ . Second, the sandwich estimator in (9) is adjusted by multiplying it with  $(N - 1)/N$  and we use the  $t$  distribution with  $N - 1$  degrees of freedom for the Wald confidence intervals (instead of the standard normal distribution).

The covariance matrix estimator in (7) may yield estimates that are not positive definite due to the measurement error correction. As a result, the corresponding estimated trial-level correlation might fall outside the valid range of  $[-1, 1]$ . To address this, we consider an additional finite-sample correction: if the estimated covariance matrix is not positive definite, we replace it with the nearest positive definite matrix in the Frobenius norm. This is achieved using the `nearPD()` function from the *Matrix* R package.

The simulations also include coverage results for the Bayesian credible intervals based on the Bayesian model described in Section B.3. The Bayesian analyses were performed using the *rstan* with 1 chain and 10,000 iterations (Stan Development Team, 2025). the first 5,000 iterations were discarded as burn-in. As already noted before, this Bayesian approach is asymptotically invalid (i.e., the posterior distribution does not concentrate around  $\rho_{\text{trial}}^{gN}$  or  $\rho_{\text{trial}}^{g*}$  as  $N \rightarrow \infty$ ), but is included in the simulations because it is expected to be more stable for small  $N$  and may outperform the asymptotically valid (but finite-sample unstable) non-parametric estimator and corresponding confidence intervals.

**Data-Adaptive Estimands** The distributions of the data-adaptive estimands are shown in Figure 10. These figures show that there is little variability in the data-adaptive estimands in each setting. Furthermore, the data-adaptive estimands are close to 1 in the scenarios with only slight violations of the surrogacy and comparability assumptions. In

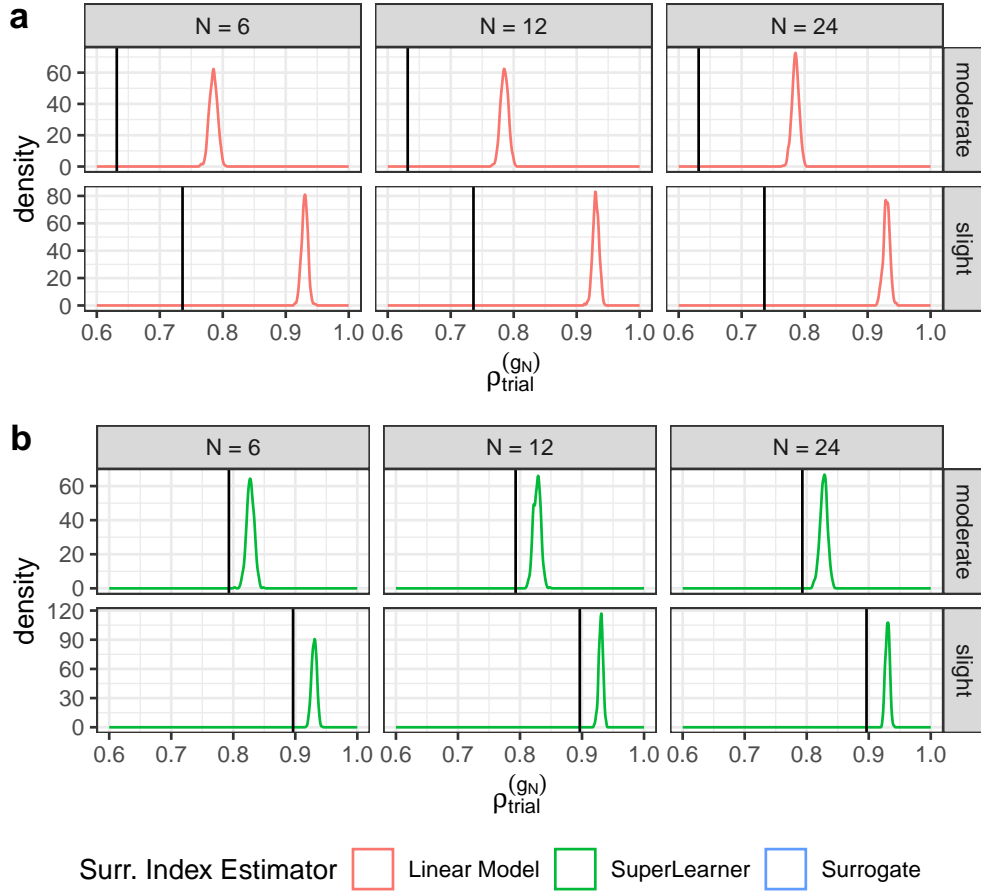


Figure 10: Distribution of the data-adaptive estimands  $\rho_{\text{trial}}^{gN}$  for (a) the proof-of-concept scenario and (b) the vaccine scenario. The vertical lines represent the values for the corresponding  $\rho_{\text{trial}}$  for the untransformed surrogate. The columns correspond to the different numbers of independent trials  $N$  and the rows correspond to the degree of violation of the surrogacy and comparability assumptions, moderate or slight violations. Note that some of the apparent variability in  $\rho_{\text{trial}}^{gN}$  in these plots is due to numerical noise in the Monte Carlo integration.

all scenarios, the data-adaptive estimands are also higher than their non-data-adaptive counterparts. This illustrates the potential advantage of using an estimated surrogate index over the surrogate endpoint itself.

**Bias and Estimation Error** Figure 11 (a) shows the median bias of the estimated trial-level correlation coefficients for the corresponding estimands (which are not data-adaptive for the untransformed surrogate and data-adaptive for the estimated surrogate indices). This figure shows that the estimator is median biased, but the bias decreases as  $N$  increases.

Figure 11 (b) shows the mean squared error (MSE) of the estimated trial-level correlation coefficients for the corresponding estimands. This figure shows that, as expected, the MSE decreases as  $N$  increases. Even for  $N = 6$  the MSE is small enough to consider the estimator as useful in practice. For a larger number of trials, the MSE is very small; hence,  $\rho_{\text{trial}}^{gN}$  can be estimated with high precision. Note, however, that this high precision is related to the true value being close to 1 in some scenarios. For instance, in the proof-of-concept scenario with moderate violations of the surrogacy and comparability assumptions, the MSE with the untransformed surrogate is considerably larger than the MSE in other settings where the estimand is closer to one.

Figure 11 (b) also shows that correcting the estimated covariance matrix to the closest positive definite matrix leads to a smaller MSE in some settings, but overall makes little difference.

**Coverage and Inference** Figure 12 (a) and (b) show the coverage of the confidence intervals for the estimated trial-level correlation coefficients for the corresponding estimands, respectively, for the Wald and BCa confidence

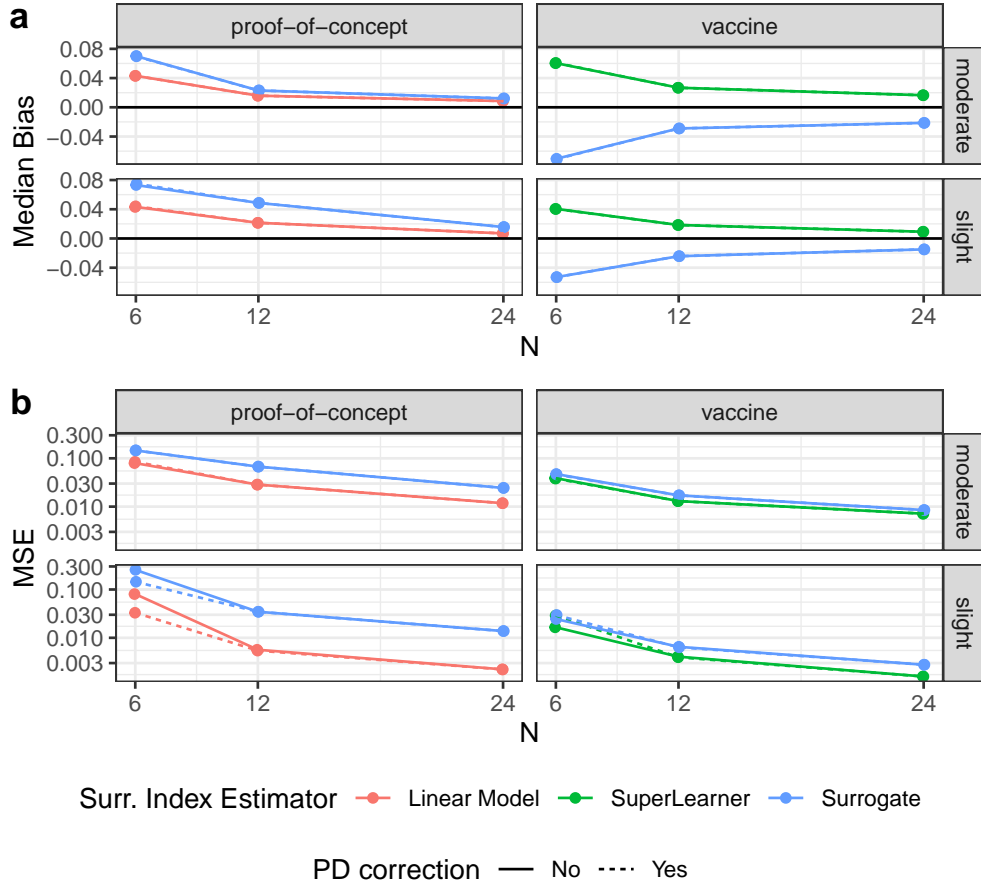


Figure 11: The median bias and mean squared error (MSE) of the estimated trial-level correlation coefficients for the corresponding data-adaptive or non-data-adaptive estimands as a function of the number of independent trials  $N$ . The columns correspond to the simulation scenario (proof of concept or vaccine) and the rows correspond to the degree of violation of the surrogacy and comparability assumptions, moderate or slight violations. PD: positive definite.

intervals. For  $N = 6$ , the empirical coverage is considerably lower than the nominal 95% for both the Wald and BCa intervals. Which one of these two has closer-to-nominal coverage for  $N = 6$  depends on the scenario. These deviations from nominal coverage are expected because (i)  $N = 6$  is a very small sample size, (ii) the estimator is non-parametric, and (iii) the correlation parameter is a non-linear function of the covariance parameters. As  $N$  increases to 24, the empirical coverage approaches the nominal 95% coverage for both the Wald intervals, but the BCa intervals still have some undercoverage.

Figure 12 (c) shows the empirical coverage of the Bayesian credible intervals. This figure shows that the Bayesian credible intervals have almost nominal coverage across all scenarios and sample sizes. As discussed before, the Bayesian approach is not asymptotically valid and the coverage will, therefore, converge to zero as  $N \rightarrow \infty$ . However, this does not preclude the Bayesian approach from being practically useful in small-sample size settings (e.g., for  $N = 6$ ) where non-parametric methods may be unstable.

### G.3 Verification of the Asymptotics and its Failure

To illustrate the alternative asymptotic framework of Appendix E and to verify the theoretical asymptotic results, we considered an additional simulation study where the number of independent trials  $N$  and the within-trial sample sizes  $n$  increase, at varying rates. We consider the same data-generating mechanism as in the proof-of-concept scenario (with moderate violations of surrogacy and comparability), but we set  $N$  and  $n$  to values in  $\{100, 500, 1000, 2000, 5000\}$ . We only consider the non-data-adaptive estimand here; so, the trial-level surrogacy for the untransformed surrogate. We use 100 MC replications for each setting.

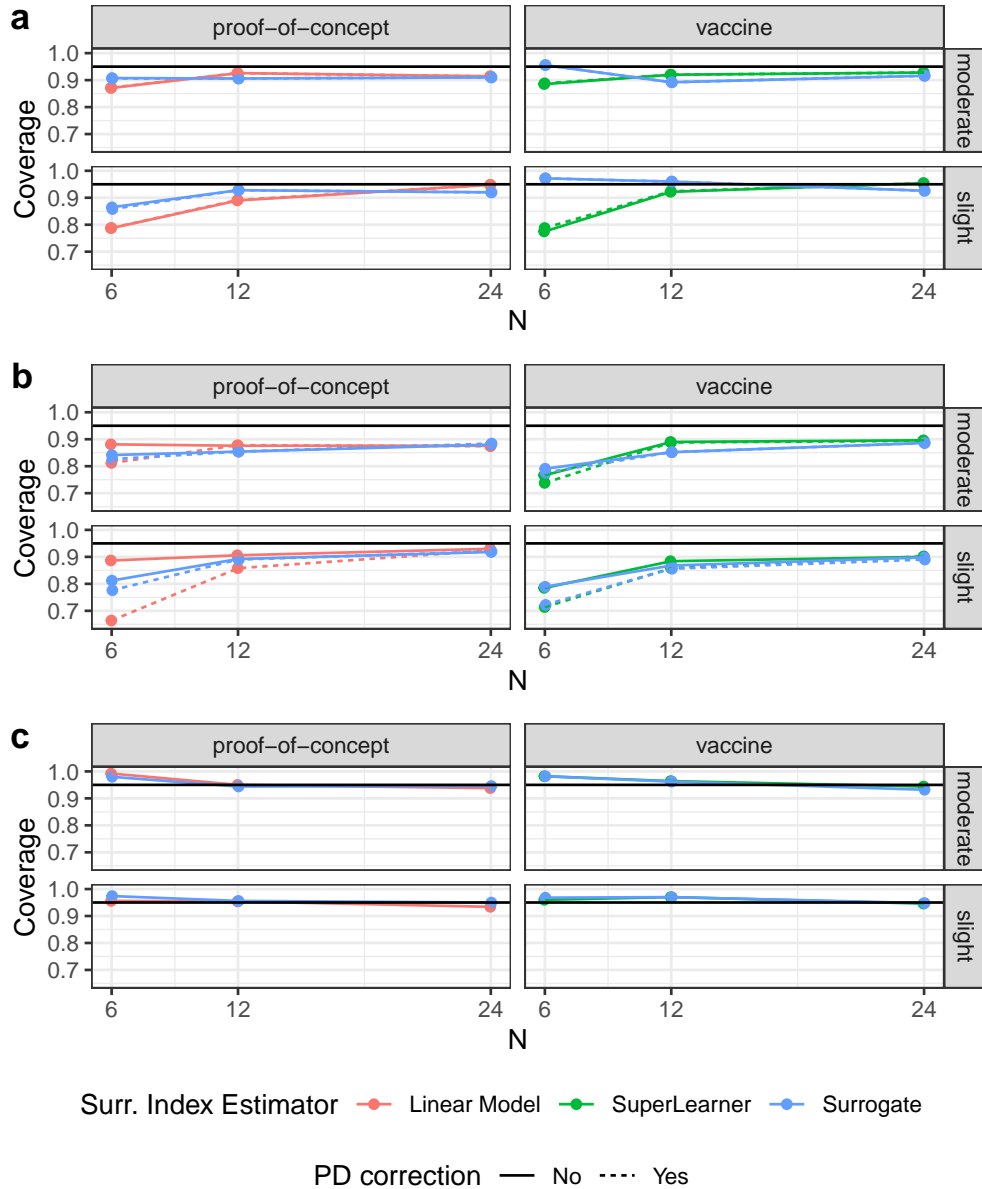


Figure 12: Empirical coverage of the confidence intervals for (a) the Wald, (b) BCa and (c) credible intervals, for the trial-level correlation coefficients as a function of the number of independent trials  $N$ . The horizontal line in each subfigure represents the nominal 95% coverage. The columns correspond to the simulation scenario (proof of concept or vaccine) and the rows correspond to the degree of violation of the surrogacy and comparability assumptions, moderate or slight violations. PD: positive definite.

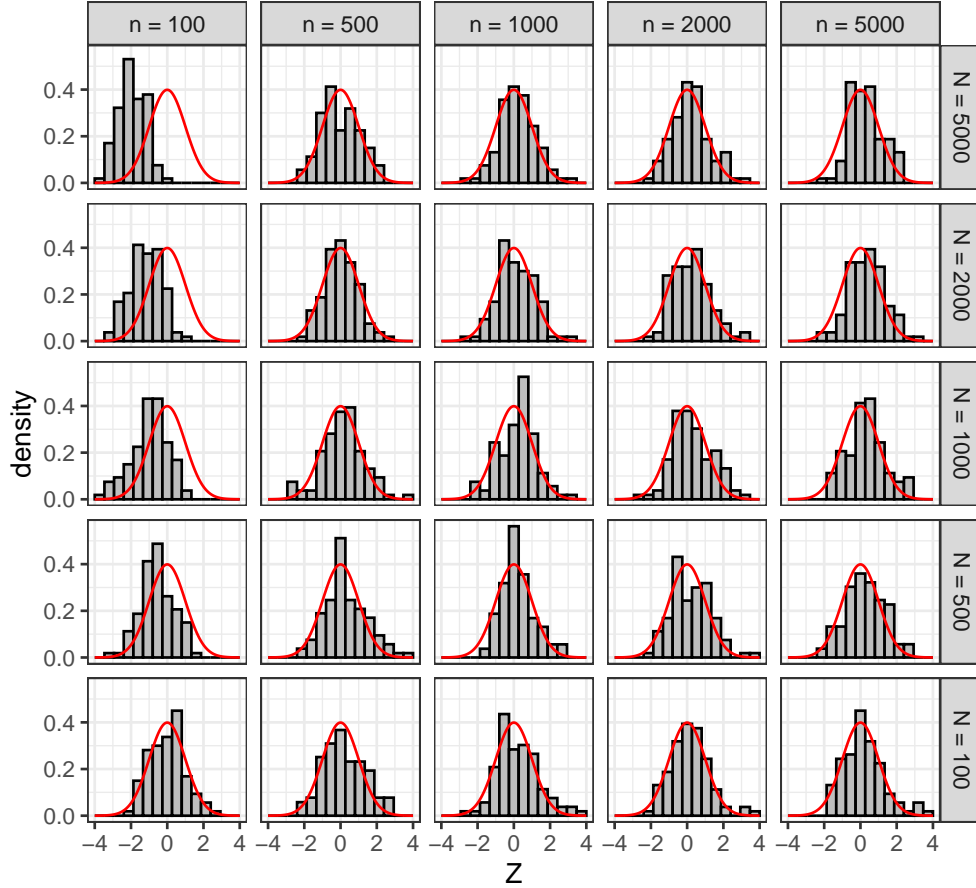


Figure 13: Distribution of the z-statistic for different combinations of the number of independent trials  $N$  and the within-trial sample sizes  $n$ . The red solid line represents the standard normal density.

The trial-level treatment effects on the surrogate and the clinical endpoint are estimated, as before, through fitting a linear regression model for  $S$  and  $Y$  with main effects for  $X$  and  $Z$ . However, we now add a flexible term for an extra random noise variable  $X_2$  to the linear regression model, where the noise is generated independently. More specifically, we add  $\text{bs}(X_2, \text{df} = 8)$  to the linear regression model for the surrogate and clinical endpoints. This introduces many additional parameters in the linear regression model, which are “not needed”. We further use the same unadjusted sandwich covariance estimator as before. By adjusting for additional noise, we expect this covariance estimator to be downwardly biased in finite samples, but it will still be consistent.

**Remark 16.** We have considered a bad covariance estimator to illustrate the “failure” of the asymptotic regime. This covariance estimator (i.e., the unadjusted sandwich covariance estimator) should not be used in practice for small sample sizes because there are many finite-sample adjustments readily available (Zeileis, 2004). With those finite-sample adjustments, the covariance estimators are almost unbiased, even in small samples, and inference “still works” in practice when  $N \gg n$ . This just shows that the rates derived in Appendix E are probably not relevant in most realistic scenarios because most reasonable estimators that are (only) asymptotically valid, tend to also have a small bias in finite samples.

To evaluate “failure” of the asymptotics, we first consider the z-statistic computed as  $z = (\hat{\rho}_{\text{trial}} - \rho_{\text{trial}}) / \hat{\text{SE}}$ , where  $\hat{\text{SE}}$  is the standard error of the estimated trial-level correlation coefficient. If the asymptotics work, then this statistic should follow a standard normal distribution. If the asymptotics fail, which we expect if the trial-level treatment effect estimators and their covariance estimators are biased, and the within-trial sample size  $n$  does not increase sufficiently fast as a function of the number of trials  $N$ , then the z-statistic should not follow a standard normal distribution. The estimated distribution of the z-statistic is shown in Figure 13 for all combinations of  $n$  and  $N$ . This figure shows that the z-statistic is approximately standard normal in all scenarios except when  $N \gg n$ .

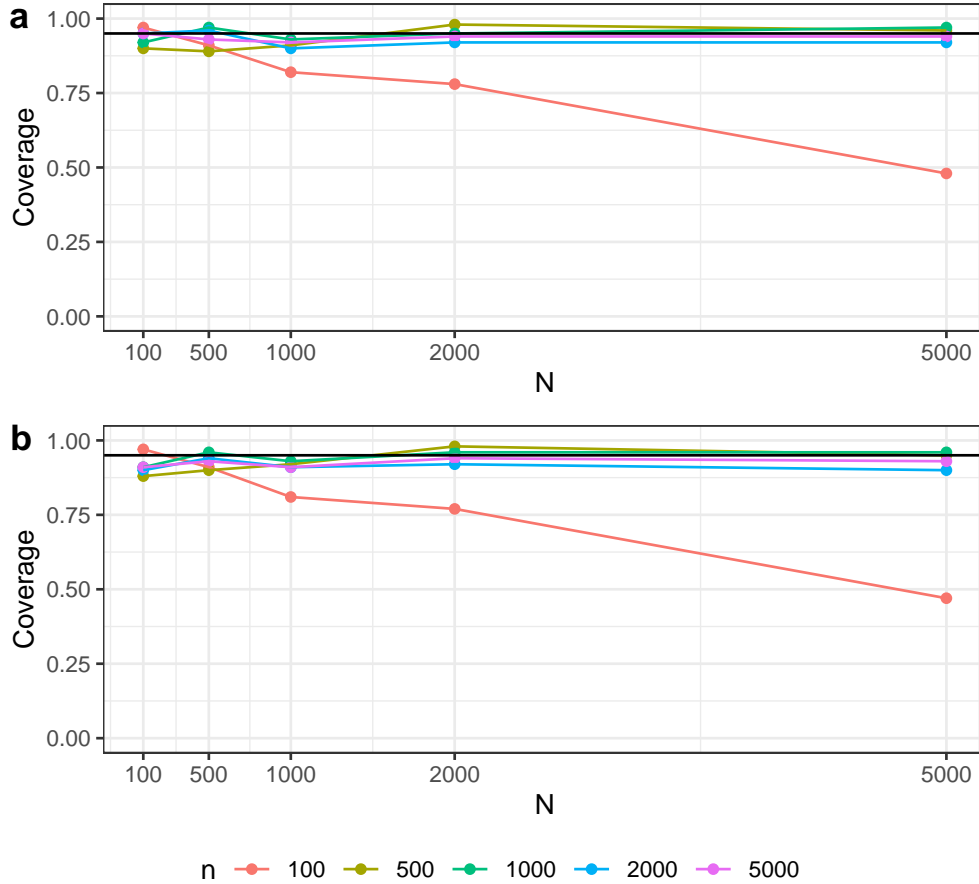


Figure 14: Empirical coverage of the confidence intervals for (a) the Wald and (b) BCa intervals, for the trial-level correlation coefficients as a function of the number of independent trials  $N$  for varying within-trial sample sizes  $n$ . The horizontal line in each subfigure represents the nominal 95% coverage.

The failure of the z-statistic to follow a standard normal distribution when  $N \gg n$  also leads to poor coverage of confidence intervals, whether they are indirectly based on the z-statistic (i.e., Wald confidence intervals) or constructed through the bootstrap. This is illustrated in Figure 14 (a) and (b) for the Wald and BCa bootstrap confidence intervals, respectively. For instance for  $n = 100$ , coverage is near nominal when  $N = 100$  but decreases as  $N$  increases to 5000. For  $n = 500$  and larger, the coverage is nominal from  $N = 100$  to  $N = 5000$ ; however, if we would increase  $N$  further, we expect the empirical coverage to decrease for any fixed  $n$ .

These results are of little practical relevance to the meta-analysis setting, however, as most meta-analyses have  $n \gg N$  and  $N$  is anyhow often very small. Still, these results may be useful beyond the meta-analysis setting where the observations are empirical distributions and the target parameters are related to the distribution of the “true” distributions (i.e.,  $P^T$ ) from which these empirical distributions (i.e.,  $P_n^T$ ) were obtained. See, for instance, Lin et al. (2023) for a discussion on causal inference with distributional outcomes.

## H Data Application

This section extends the results presented in the main text by providing additional analyses and further details on specific methodological choices. We begin by exploring the data. Next, we describe the adjustment of the neutralization titers to the circulating strains. We then detail how the surrogate indices were estimated and we evaluate their predictive performance. Finally, we provide additional results for the meta-analyses, including results from Bayesian meta-analyses.

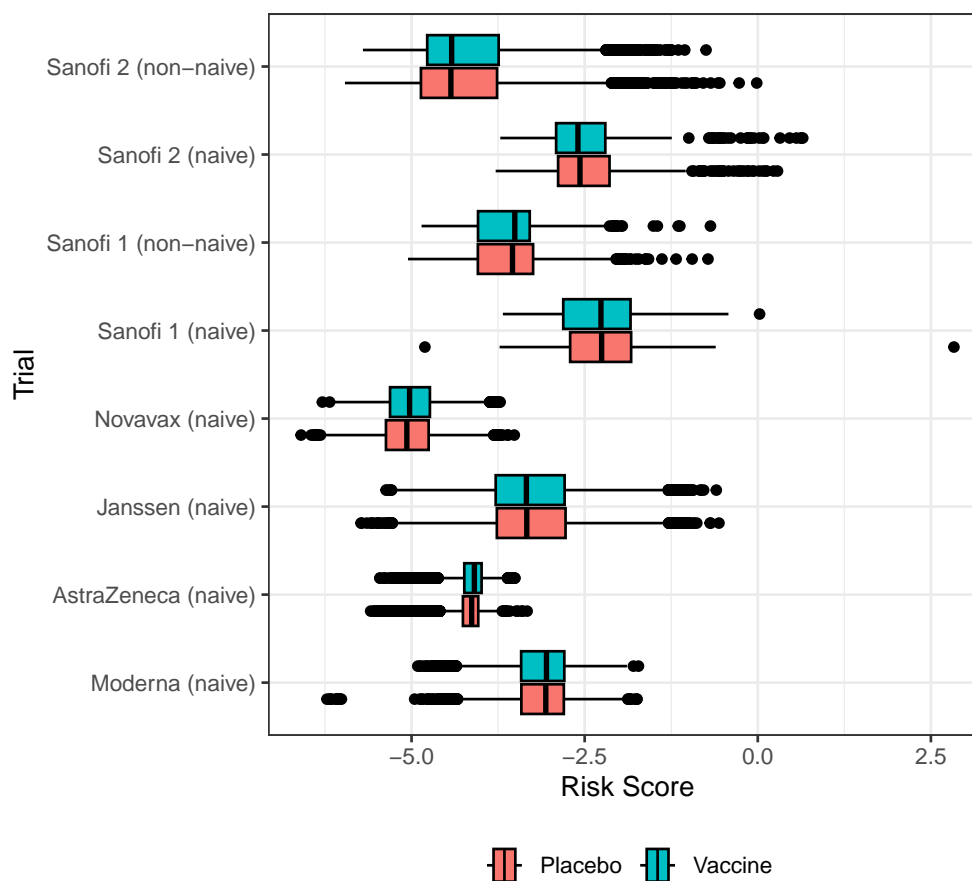


Figure 15: Distribution of the risk score by trial and treatment group. The risk score is defined as the logit of the predicted risk, based on an ensemble statistical learning algorithm trained on the placebo arm (USG COVID-19 Response Team / Coronavirus Prevention Network (CoVPN) Biostatistics Team et al., 2022).

## H.1 Data Exploration

Figure 15 displays the distribution of the risk score (defined in the figure caption) by trial and treatment group. This figure shows that there are substantial differences in the distribution of the risk score across trials which indicates that the probability of infection varies considerably between trials. These between-trial differences underscore the importance of accounting for trial-specific baseline risks when estimating the surrogate index. We initially included the risk score in the surrogate index estimation but later decided against it as this obscured the interpretation because the risk score is estimated from the placebo-arm data (including the clinical endpoint) in each trial separately and, hence, would only be known in new trials after observing the clinical endpoint.

Figure 16 displays the distribution of IgG Spike, nAb ID50, and adjusted nAb ID50 by trial and treatment group, revealing substantial differences in the distribution of the antibody markers across trials. Furthermore, the distributions of these markers do not completely overlap between trials. This lack of overlap makes trial-level overfitting more likely, as further discussed in Appendix D.3.

Figure 17 displays the estimated cumulative incidence functions of virologically confirmed symptomatic SARS-CoV-2 infection by trial and treatment group. This figure shows that there are substantial differences in cumulative incidence functions across trials and treatment groups. There also is substantial variability in the treatment effects (i.e., VE for infection by 80 days) between trials. This variability is desirable, as between-trial differences in treatment effects on the clinical endpoint are required for a meaningful trial-level surrogacy analysis. Indeed, the trial-level correlation quantifies the amount of variability in the trial-level treatment effects on the clinical endpoint that is explained by a linear regression on the treatment effects on the surrogate (index). If this variability is minimal, there is little variability

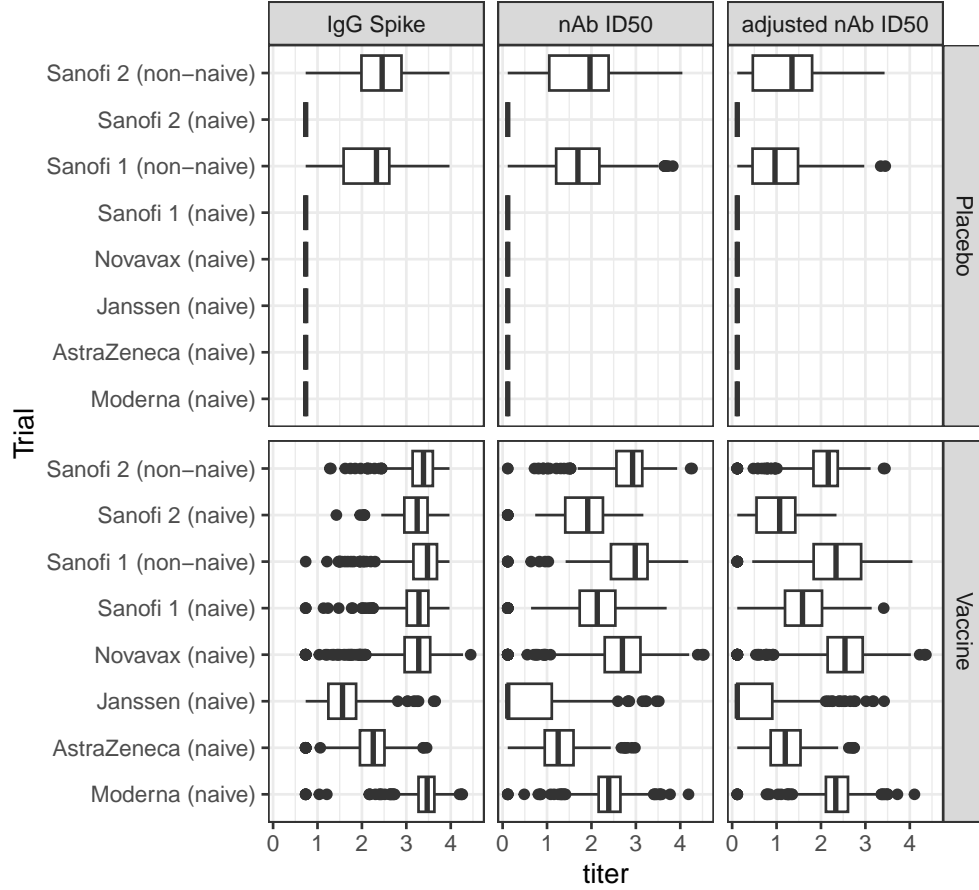


Figure 16: Distribution of IgG Spike, nAb ID50, and adjusted nAb ID50 by trial and treatment group. Antibody markers in the placebo groups of Moderna, AstraZeneca, Janssen, Novavax, and the naive Sanofi trials are set to the assay’s lower limit of detection divided by 2, as these participants are SARS-CoV-2 naive and are not expected to have antibodies against SARS-CoV-2. The boxplots are weighted by the case-cohort sampling weights.

to explain. In the limiting case where there is not variability in the trial-level treatment effects on the clinical endpoint, the trial-level correlation is ill defined.

## H.2 Adjustment of Neutralization Titer to Circulating Strains

The neutralization titer measured in the vaccine trials quantifies neutralization against the D614G reference strain. However, as detailed in Section 7.1, the D614G strain was not representative of the strain circulating during the trials. For example, during the Sanofi trials, the D614G strain was no longer circulating. When there is such a mismatch between the measured neutralization titer and the circulating strain, the practical relevance of trial-level surrogacy evaluation becomes questionable. To address this, we adjust the neutralization titer measured against the reference strain to approximate the neutralization titer against the circulating strains. This adjustment allows us to evaluate whether the neutralization titer against the circulating strains serves as a meaningful trial-level surrogate for infection with those strains.

In what follows, we describe the neutralization titer adjustment for data from a single trial. The same approach can be repeated for each trial separately. Let  $s_{\text{ref},i}$  be the neutralization titer (on the ID50 scale, so not log-transformed) against the reference strain for subject  $i$  and  $s_{v,i}$  the neutralization titer against strain  $v$  for subject  $i$ . We assume a vaccine- and variant-specific reduction in titer against non-reference strains, constant across subjects:

$$s_{v,i} = \frac{1}{c_v} \cdot s_{\text{ref},i} \quad (29)$$

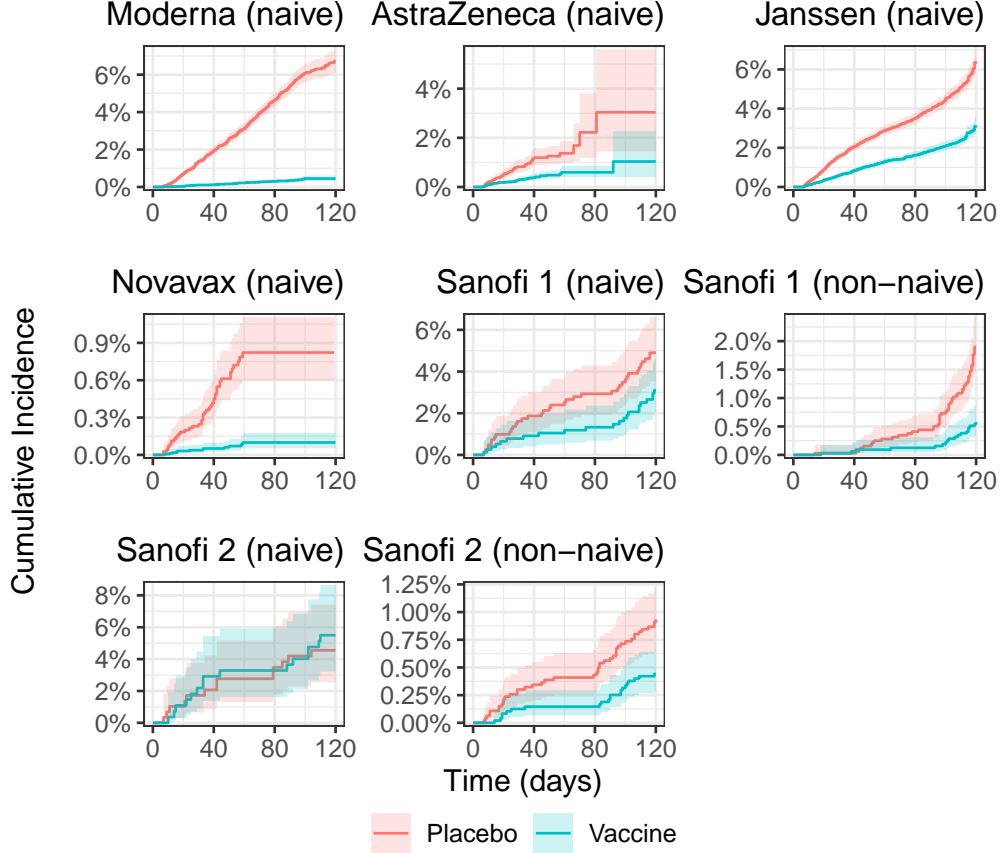


Figure 17: Estimated cumulative incidence functions (solid lines) of SARS-CoV-2 infection by trial and treatment group. The cumulative incidence functions are estimated using the Kaplan–Meier estimator. Shaded areas represent pointwise 95% confidence intervals. Note that the cumulative incidences are shown up to 120 days post marker measurement visit, even though some trials have substantially longer follow-up.

where  $c_v$  is the *abrogation coefficient*. Although  $c_v$  is unknown, it can be estimated using observations of  $s_{v,i}$  and  $s_{\text{ref},i'}$  as the geometric mean titer (GMT) ratio<sup>23</sup>:

$$\frac{\text{GMT}(s_{\text{ref}})}{\text{GMT}(s_v)} := \frac{e^{E(\log s_{\text{ref},i'})}}{e^{E(\log s_{v,i})}} = \frac{e^{E(\log s_{\text{ref},i'})}}{e^{E(\log s_{\text{ref},i} \cdot \frac{1}{c_v})}} = e^{E(\log s_{\text{ref},i'}) - E(\log s_{\text{ref},i}) + \log c_v} = e^{\log c_v} = c_v$$

We use the estimated GMT ratios reported in the literature, which are summarized in Table 4 for each trial. For the Sanofi trials, we consider the GMT ratios for naive and non-naive participants separately.

Since multiple strains circulated in each trial, computing  $s_v$  for a single strain is insufficient. Instead, we compute the weighted average neutralization titer against all circulating strains. The weights for each strain are subject-specific. Specifically, the weight for strain  $v$  and subject  $i$  is denoted by  $\pi_{v,i}$  and equals the proportion of the circulating strains that is strain  $v$  for individual  $i$ , averaged over the follow-up period for individual  $i$ <sup>24</sup>. These averaged proportions were obtained from GISAID for all subjects in the vaccine trials (GISAID Initiative, 2025; Shu & McCauley, 2017). The adjusted neutralization titer  $\tilde{s}_i$  can then be expressed as:

$$\tilde{s}_i = \sum_v \pi_{v,i} \cdot s_{v,i} = \sum_v \pi_{v,i} \cdot \frac{1}{c_v} \cdot s_{\text{ref},i} = s_{\text{ref},i} \cdot \sum_v \frac{\pi_{v,i}}{c_v}$$

<sup>23</sup>Note that we are using indices  $i$  and  $i'$  here because the GMT ratio can be estimated even if  $s_{v,i}$  and  $s_{\text{ref},i'}$  are not measured on the same subjects.

<sup>24</sup>Suppose that there are only two strains  $v_1$  and  $v_2$ , and patient  $i$  is followed for three days where 30%, 40%, and 50% of the infections were due to strain  $v_1$  on day 1, 2, and 3, respectively. Then  $\pi_{v_1,i} = \frac{1}{3} (0.3 + 0.4 + 0.45)$ .

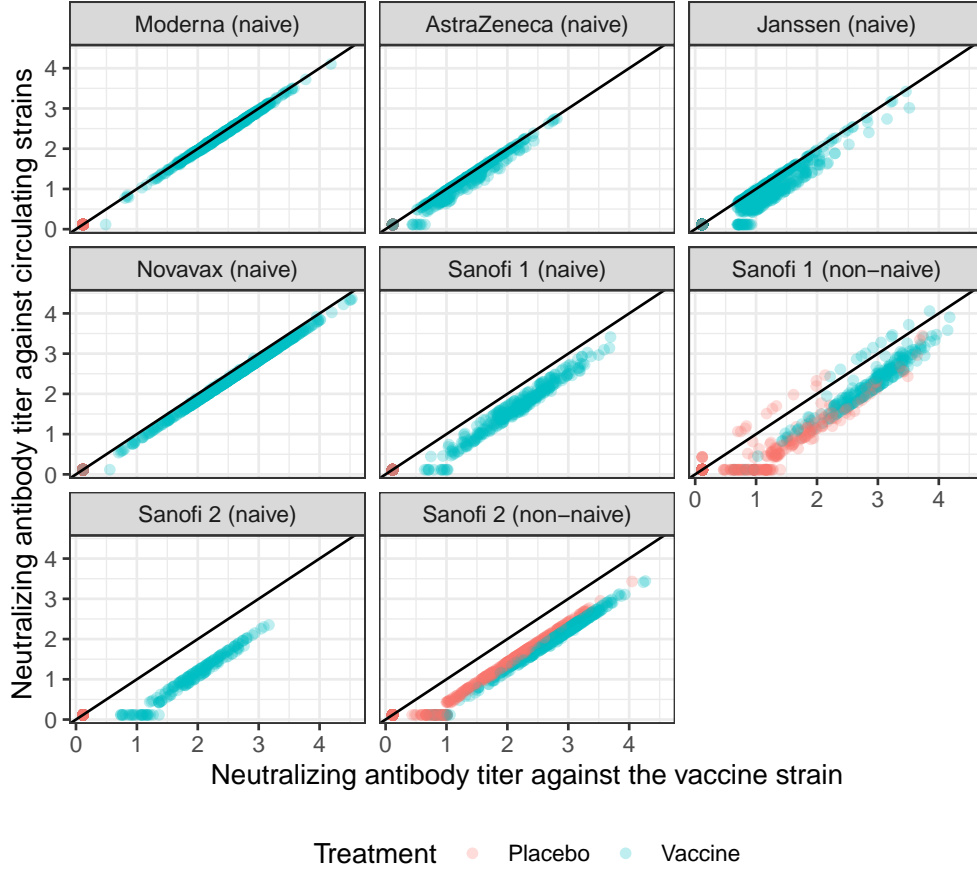


Figure 18: nAb ID50 titers against the adjusted nAb ID50 titers.

Thus, for each individual  $i$ , the adjustment factor  $\sum_v \frac{\pi_{v,i}}{c_v}$  is computed and multiplied by the original titer  $s_{\text{ref},i}$  to obtain  $\tilde{s}_i$ , the titer adjusted to the circulating strains.

**Remark 17** (Missing GMT ratios). The estimated GMT ratios in Table 4 cover the most prevalent strains in each trial. However, for some strains that circulated in some of the trials, we do not have estimated GMT ratios. This is only a minor practical issue because the missing strains were not very prevalent. To avoid any further problems caused by the missing estimated GMT ratios, we set the variant-specific weights  $\pi_{v,i}$  to zero for the missing strains.

The nAb ID50 titers are plotted against the adjusted nAb ID50 titers in Figure 18. This figure shows that, as expected, the adjustment is larger for the Sanofi trials because the circulating strains in these trials were more distant from the reference strain than in the other trials.

**Limitations** The adjustment described above has important limitations. We highlight a few of them here.

First, the adjustment is based on the assumption that there is a constant multiplicative reduction in neutralization titer against the non-reference strains across subjects (i.e., the constant  $c_v$  is the same for all subjects from the same trial). This assumption may not hold in practice, as the reduction in neutralization titer may vary across individuals. Still, we expect this assumption to hold approximately in practice because neutralization titers against different strains are often strongly correlated.

Second, the adjustment is based on estimated GMT ratios. We do not take the sampling variability of these estimates into account; so, if the GMT ratio estimates are imprecise, the adjustment may not be accurate.

Third, we use a weighted average of the neutralization titers against the circulating strains. This summary loses information. For example, a given subject may have a high neutralization titer against all circulating strains except one. In this case, the subject is still at risk of infection with the strain against which they have a low neutralization titer, even

though their weighted average neutralization titer is high (and thus suggests that the subject is at low risk of infection by the circulating strains). However, we expect this to be a minor issue because neutralization titers against different strains are often strongly correlated.

### H.3 Surrogate Index Estimators

To estimate the surrogate index, we consider the following baseline covariates:

- **age.** Age in years measured at the time of enrollment in the trial.
- **BMI.** Body mass index (BMI) divided into four categories: underweight ( $\text{BMI} < 18.5$ ), normal weight ( $18.5 \leq \text{BMI} < 25$ ), overweight ( $25 \leq \text{BMI} < 30$ ), and obese ( $\text{BMI} \geq 30$ ).
- **sex.** Biological sex.
- **high\_risk.** A binary variable indicating whether the subject is at high risk of severe COVID-19 (Polack et al., 2020)
- **logit\_prob\_infection.** The logit of the estimated cumulative incidence of the infection endpoint 80 days post-marker measurement visit in the placebo arm of the participant’s trial.

We further let `time_to_event` be the time from six days post marker-measurement visit to the time of the infection event or censoring, and `event` be the event indicator. `infection_80d` denotes whether the infection event was observed within 80 days post marker measurement visit. Subjects censored before 80 days have `infection_80d = NA`. We let `marker` refer to the base-10 logarithm of IgG Spike, nAb ID50, or adjusted nAb ID50.

We consider the following two approaches to estimate the surrogate index:

- **Cox proportional hazards model.** The surrogate index is estimated using a Cox proportional hazards model with the following form:  $\text{Surv}(\text{time\_to\_event}, \text{event}) \sim \text{sex} + \text{high\_risk} + \text{BMI} + \text{bs}(\text{age}) + \text{strata}(\text{trial}) + \text{ns}(\text{titer}, \text{knots} = \text{c}(1.5, 2.5), \text{Boundary.knots} = \text{c}(0, 4))$ . We have truncated the follow-up time to 120 days post marker measurement visit. Hence, all observations are censored at 120 days (even though we have longer follow-up for some subjects). The observations are weighted by the case-cohort weights.
- **SuperLearner.** The surrogate index is estimated using the SuperLearner algorithm implemented in the *s3* R package (Coyle et al., 2021; van der Laan et al., 2007) using `infection_80d` as outcome. We use the following library of candidate algorithms:
  1. Logistic regression with main effects for all covariates and the surrogate.
  2. Logistic regression with main effects for only `logit_prob_infection` and the surrogate.
  3. Logistic regression with main effects for all covariates and the following natural cubic splines for the surrogate:  $\text{ns}(\text{marker}, \text{knots} = \text{c}(1.5, 2.5), \text{Boundary.knots} = \text{c}(0, 4))$ .
  4. Logistic regression with main effects for all covariates and the surrogate, and an interaction term between the `marker` and `sex`.
  5. Logistic regression combining all terms from the previous two models.
  6. Generalized additive model (GAM) with smooth terms for all continuous covariates and the surrogate. We used the defaults of `Lrn_r_gam`.

We use the meta-learner as implemented in `Lrn_r_solnp` with binomial loglikelihood loss function and use leave-one-trial-out cross-validation instead of the default. The observations with a missing `infection_80d` or `marker` are excluded; the remaining observations are weighted by the product of the inverse probability of censoring weights (IPCWs) and the case-cohort weights. The IPCWs are estimated using the Kaplan–Meier estimator stratified by trial and treatment arm.

We have estimated the surrogate index by pooling the individual-level data from all trials except the non-naive Sanofi trials. The estimated receiver operating characteristic (ROC) curves for predicting `infection_80d` with the estimated surrogate indices are shown in Figures 19–21, stratified by trial. The ROC curves for trials whose data were not used for estimating the surrogate index (Sanofi 1 (non-naive) and Sanofi 2 (non-naive)) can be viewed as an external validation of the predictive performance of the estimated surrogate index. Note that the ROC curves are based on the subjects with an observed `infection_80d` and `marker`, weighted by the product of the IPCWs and the case-cohort weights.

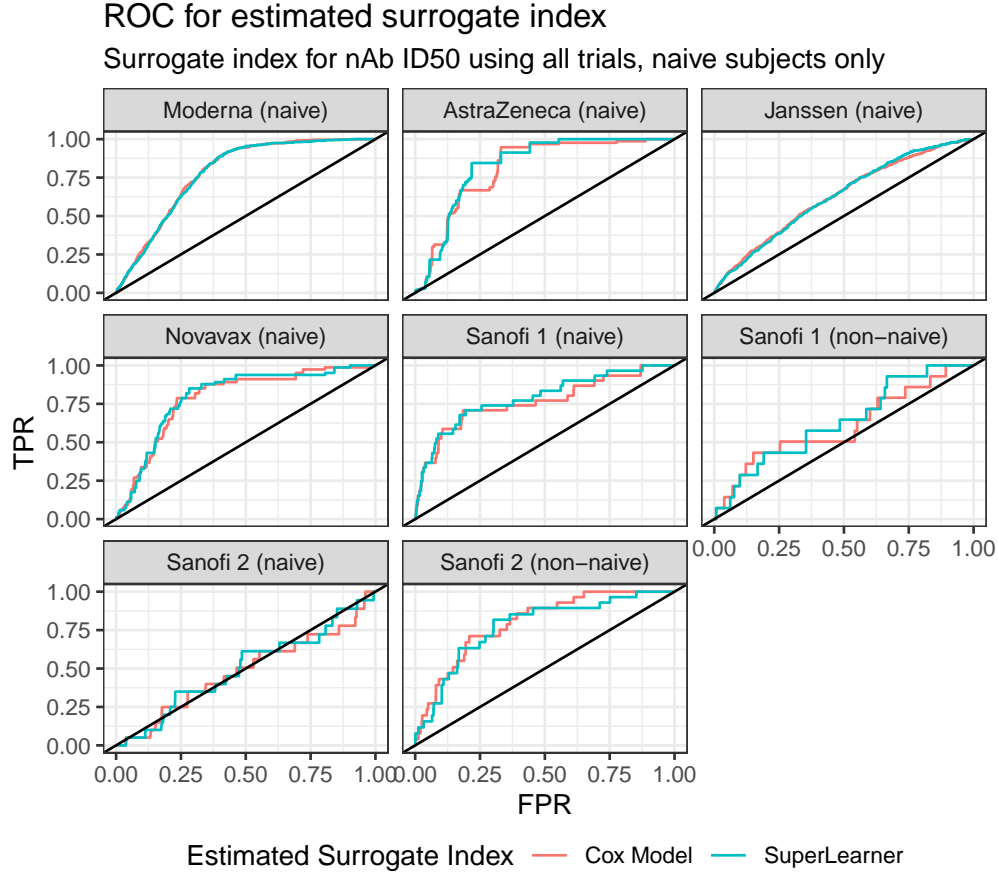


Figure 19: Receiver operating characteristic (ROC) curves for predicting `infection_80d` with the estimated surrogate index based on nAb ID50. The surrogate index was estimated using all trials with only naive subjects.

## H.4 Additional Results

### H.4.1 Additional Non-Parametric Meta-Analysis Results

Tables 5 and 6 present the same results as in Tables 2 and 3 of the main text, but using Wald-type confidence intervals based on the sandwich covariance estimator and a  $t$  distribution with  $N - 1$  degrees of freedom (instead of the BCa bootstrap confidence intervals). These confidence intervals are narrower than the BCa bootstrap confidence intervals, but as indicated in the simulations, they may undercover.

### H.4.2 Bayesian Meta-Analysis

We consider a Bayesian analysis based on the bivariate normal model as described in Appendix B.3 and also studied in the simulations. We use the same estimated surrogate indices as in the non-parametric frequentist analysis and ignore that fact that  $g_N$  depends on the observed data. The Bayesian analyses were performed using *rstan* with 4 chains and 20,000 iterations per chain (Stan Development Team, 2025). The first 5000 iterations were discarded as burn-in. The posterior distributions for  $\rho_{\text{trial}}^{g_N}$  are shown in Figures 22 and 23.

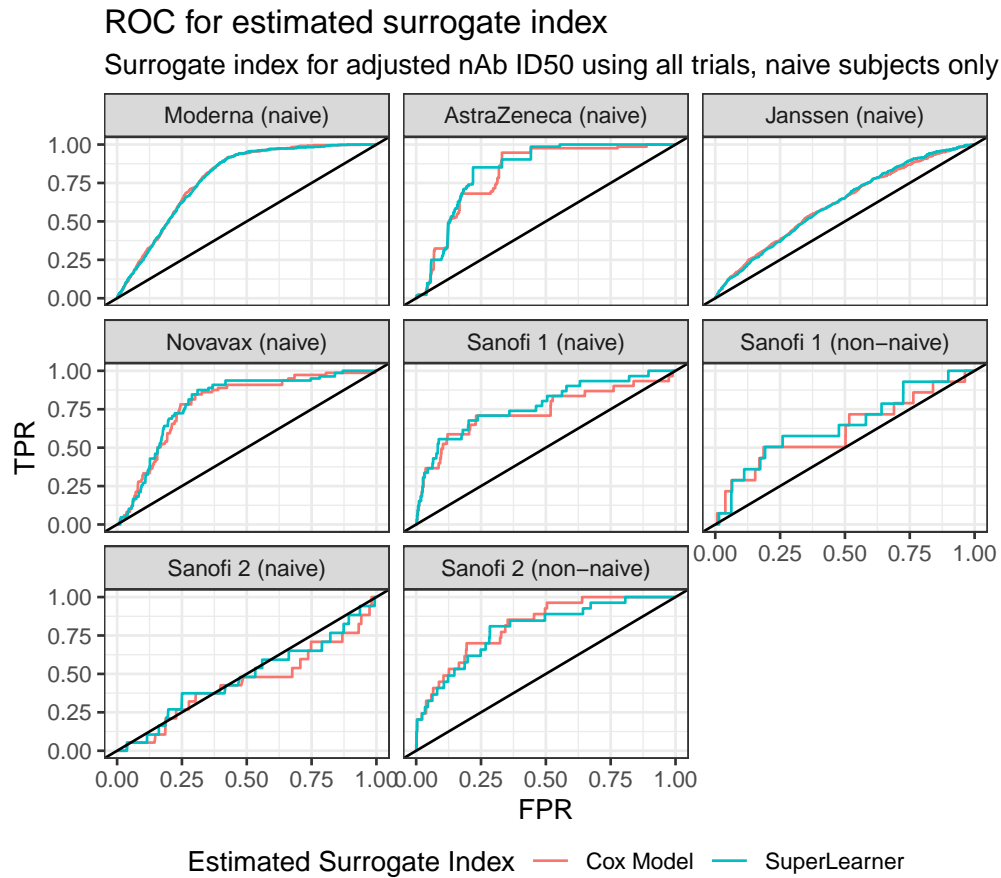


Figure 20: Receiver operating characteristic (ROC) curves for predicting `infection_80d` with the estimated surrogate index based on the adjusted nAb ID50. The surrogate index was estimated using all trials with only naive subjects.

Table 4: Estimated GMT ratios for the neutralization titer against the reference strain and the circulating strains.

Trial	Ref.	Epsilon	Gamma	Zeta	Alpha	Delta	Lambda	Iota	Beta	Mu	Omicron	BA.1	BA.2	BA.4.5
Moderna	1	2.1	3.2	3.2	-	-	-	-	-	-	-	-	-	-
AstraZeneca	1	1.55	3.4	-	0.9	1.55	1.55	-	-	-	-	-	-	-
Janssen	1	1.55	3.4	2.2	0.9	1.55	1.55	0.9	3.6	3.6	-	-	-	-
Novavax	1	2.1	3.2	-	1.2	-	-	2.3	7.4	-	-	-	-	-
Sanofi 1 Naive	1	-	-	-	-	2	-	-	-	-	4.2	4.9	3.3	4
Sanofi 1 Non-Naive Vaccine	1	-	-	-	-	0.59	-	-	-	-	4.7	7.3	4.3	6.5
Sanofi 1 Non-Naive Placebo	1	-	-	-	-	0.43	-	-	-	-	5.2	11.8	9.1	11.4
Sanofi 2 Naive	1	-	-	-	-	1.4	-	-	-	-	3.3	6.3	5.8	9.1
Sanofi 2 Non-Naive Vaccine	1	-	-	-	-	1.1	-	-	-	-	4	7.7	5.2	6.6
Sanofi 2 Non-Naive Placebo	1	-	-	-	-	1.1	-	-	-	-	4.4	4.6	3.7	4.3

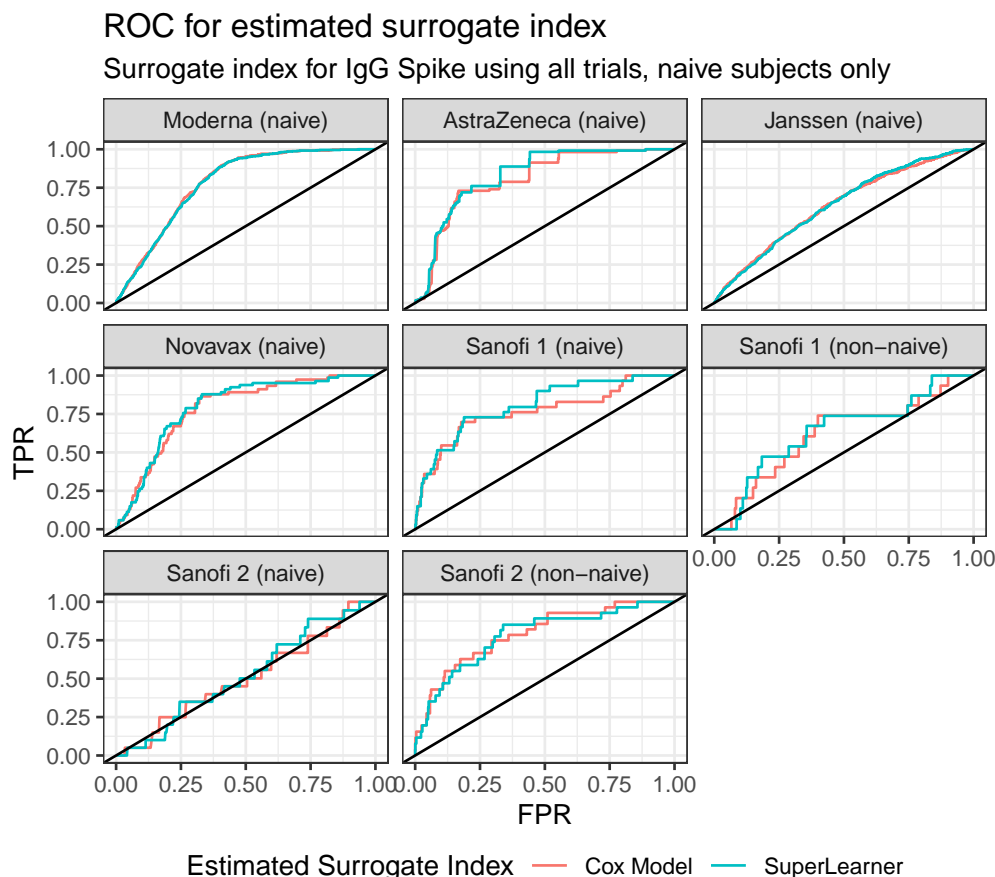


Figure 21: Receiver operating characteristic (ROC) curves for predicting `infection_80d` with the estimated surrogate index based on IgG Spike. The surrogate index was estimated using all trials with only naive subjects.

Table 5: Estimated trial-level correlations with 95% Wald confidence intervals based on the sandwich estimator for the standard error for the meta-analysis that includes all naive trials. The Antibody Marker column indicates the meta-analyses where the antibody marker (without any transformation) is evaluated as a trial-level surrogate endpoint.

Surrogate	Antibody Marker	Est. Surrogate Index	
		Cox Model	SuperLearner
IgG Spike	0.33 (-0.50, 0.84)	0.34 (-0.56, 0.87)	0.33 (-0.53, 0.86)
nAb ID50	0.47 (-0.21, 0.84)	0.56 (-0.10, 0.88)	0.57 (-0.07, 0.88)
Adjusted nAb ID50	0.77 (0.34, 0.93)	0.88 (0.66, 0.96)	0.87 (0.60, 0.96)

Table 6: Estimated trial-level correlations with 95% Wald confidence intervals based on the sandwich estimator for the standard error for the meta-analysis with the pseudo-real data. The Antibody Marker column indicates the meta-analyses where the antibody marker (without any transformation) is evaluated as a trial-level surrogate endpoint.

Pseudo-Real Data	Surrogate	Antibody Marker	Est. Surrogate Index	
			Cox Model	SuperLearner
Increased Precision	IgG Spike	0.32 (-0.48, 0.83)	0.33 (-0.54, 0.86)	0.31 (-0.51, 0.84)
	nAb ID50	0.44 (-0.21, 0.82)	0.54 (-0.11, 0.86)	0.54 (-0.08, 0.86)
	Adjusted nAb ID50	0.73 (0.31, 0.91)	0.84 (0.58, 0.94)	0.84 (0.54, 0.94)
Increased Number of Trials	IgG Spike	0.34 (0.01, 0.60)	0.35 (-0.01, 0.63)	0.33 (-0.01, 0.61)
	nAb ID50	0.47 (0.23, 0.65)	0.57 (0.35, 0.73)	0.58 (0.37, 0.73)
	Adjusted nAb ID50	0.77 (0.65, 0.86)	0.89 (0.83, 0.93)	0.88 (0.81, 0.92)

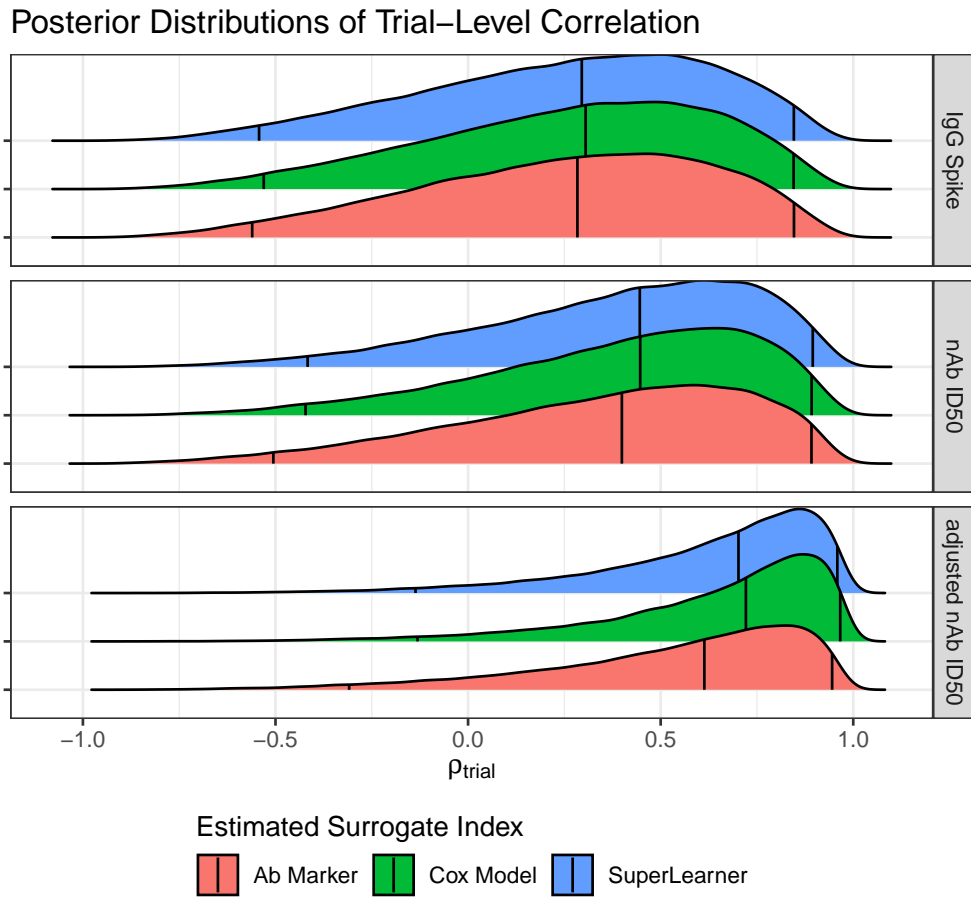


Figure 22: Posterior distributions for  $\rho_{\text{trial}}^{gN}$  from the Bayesian analysis assuming a bivariate normal model. The posterior distributions are shown for the untransformed surrogate and the estimated surrogate indices. The first and third vertical lines represent the 95% equal-tailed credible intervals and the middle vertical line represents the posterior median.

Posterior Distributions of Trial-Level Correlation

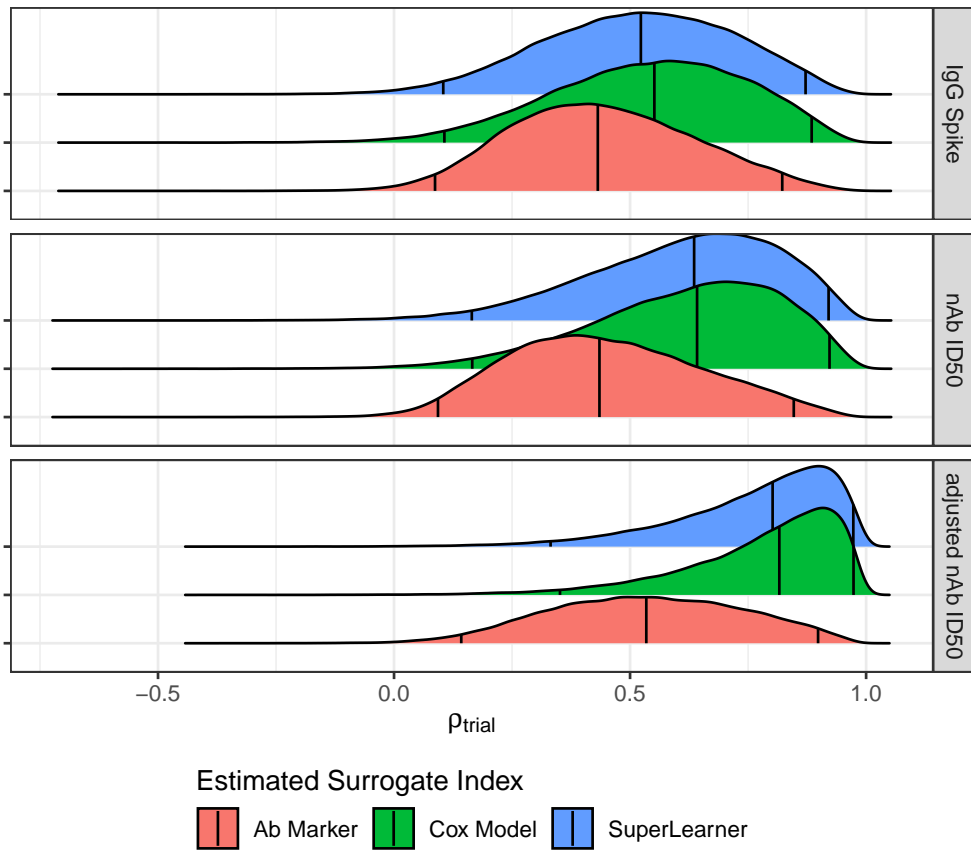


Figure 23: Posterior distributions for  $\rho_{\text{trial}}^{\alpha^g N}$  from the Bayesian analysis assuming a bivariate normal model with proportional regression of  $\beta$  on  $\alpha^g$  as described in Appendix B.3. The posterior distributions are shown for the untransformed surrogate and the estimated surrogate indices. The first and third vertical lines represent the 95% equal-tailed credible intervals and the middle vertical line represents the posterior median.